AD NUMBER

AD837647

NEW LIMITATION CHANGE

TO

Approved for public release, distribution unlimited

FROM

Distribution authorized to U.S. Gov't. agencies only; Administrative/Operational Use; Jun 1968. Other requests shall be referred to Commander, Naval Civil Engineering Lab, Port Hueneme, CA 93041.

AUTHORITY

USNCEL ltr, 10 Oct 1968

R 591

Technical Report

OCEAN BOTTOM BREAKOUT FORCES

Including Field Test Data and the Development of an Analytical Method

June 1968

NAVAL FACILITIES ENGINEERING COMMAND

NAVAL CIVIL ENGINEERING LABORATORY

Port Hueneme, California 93041

OCEAN BOTTOM BREAKOUT FORCES

Including Field Test Data and the Development of an Analytical Method

Technical Report R-591

by

Bruce J. Muga

ABSTRACT

Theoretical and experimental studies were conducted in order to arrive at some appropriate engineering estimates of the force required to extract bodies of various sizes and shapes from the ocean bottom sediments. A review of the literature concerned with breakout forces is presented.

From tests conducted in San Francisco Bay on variously shaped objects having submerged weights of up to 22,200 pounds, it was found that the following empirical formula described well the breakout force requirement:

$$F = 0.20\, A_{max}\, q_d\, e^{-0.00540\,(t\,-\,280)}$$

where F = breakout force, lb

A_{max} = horizontal projection of the maximum contact area, in.^{2}

q_d = average supporting pressure provided by the soil to maintain the embedded object in static equilibrium, lb/in.^{2}

t = time allowed for breakout, min

Results yielded by the empirical formula agreed very well with a complicated theoretical procedure based on an iterative solution of a lumped parameter model of the ocean bottom. Solutions were obtained for various load conditions and bottom (object) geometries.

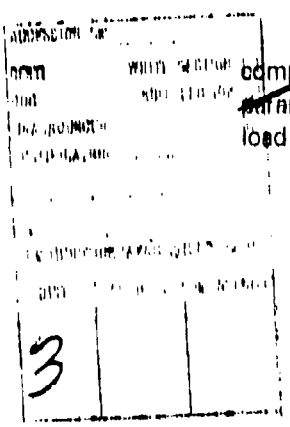

EVALUATION SHEET

Technical Report TR-591

Title OCEAN BOTTOM BREAKOUT FORCES. Including Field Test Data and the Development of an Analytical Method

Author Bruce J. Muga

Task No. _____

The following questions are designed to elicit comments that will help NCEL improve the quality of its reports. Specific and detailed answers will be most appreciated.

1. Was the technical material worth publishing?

2. Was the technical material organized in a coherent manner?

3. Were the title, abstract, and introduction indicative of the reports' contents?

4. Did the report contain any unnecessary or irrelevant material, or did it lack essential material?

5. Do you have any comments about the typography used, the layout of the report, or its general readability?

(additional space on back)

CONTENTS

INTRODUCTION

There is an increasing interest being shown in deep sea operations. This interest, having scientific origins, has been augmented by the need to enhance the national security and to prevent catastrophes. As a result, the engineering aspects of certain practical problems of immediate interest have tended to dwarf the longer term scientific aspects. The study reported herein, which was set into motion following the loss of the USS THRESHER, is concerned with one of these practical problems.

Briefly, the objectives of the study, appropriately described as the "breakout force" problem, are threefold. First, some appropriate engineering estimates must be made of the force required to extract bodies of various shapes, sizes, and skin surface compositions from the ocean bottom sediments. Second, it must be determined how far the estimates may be in error. Third, the effectiveness of various schemes for reducing the required force must be evaluated.

The study is a continuing 3-year effort of which this report is intended to describe the progress made in the first 2 years. Thus, although this report is not considered to be a complete treatment of the subject matter, it makes it possible to estimate the force requirements with some degree of confidence. In addition, the theoretical treatment has been substantially verified by field tests and is believed to be a significant contribution to analytical methods which heretofore have not been widely used. It appears that many practical problems exist for which such methods have application.

BACKGROUND

Documented experience relative to the problem of freeing objects from the ocean bottom is limited. The reports referenced in Table 1 mention the "mud suction" force; however, no measurements of such a force seem to have been made. A description of the nature of the problem may be provided by brief reviews of the salvage operations listed in Table 1.

Table 1. Selected Marine Salvage Operations

Sunken Objects	Date of Salvage Operations	Reference
SÖDRA SVERIGE	1896-97	Anonymous (1956)
LIBERTÉ	1911-25	J. Crapaud (1925)
S-51	1925-26	U. S. Navy (1927)
S-4	1927-28	U. S. Navy (1929)
USS SQUALUS	1939	(a) R. A. Tusler (1940) (b) C. E. Momsen (1964)
USS LAFAYETTE (ex SS NORMANDIE)	1942-43	U. S. Navy (1946)
PHOENIXES	1944	E. Ellsberg (1960)

SÖDRA SVERIGE. The SÖDRA SVERIGE, a cargo-passenger steamship with an 800-ton displacement, sank in the Baltic Sea in 1895 in a depth of 185 feet. The ship came to rest at a sharp angle from the vertical and during the course of a year sank about 10 feet into the clay bottom. Calculations indicated that the ship had a submerged weight of 600 tons and that a force of 960 tons would be sufficient to break it loose from the bottom. Sixteen wooden pontoons, each having a lifting force of 60 tons, were attached to the ship and pumped out. This was sufficient to righten the ship and raise it off the bottom.

LIBERTÉ. The French battleship LIBERTÉ, with an 8,000-ton displacement, sank in the harbor at Toulon in 1911. The salvage effort extended over a period of 14 years. During the long period of submergence, the wreck settled into the mud and Crapaud (1925) reports that "a considerable part of the task of the salvors consisted in breaking this contact and freeing the bulk so that it could be lifted and towed away." No information was given to permit an estimation of the breakout force.

S-51. The S-51 was a 1,230-ton submarine which sank in 1925 approximately 14 miles east of Block Island. The depth at the site was 132 feet and the submerged weight was estimated to be 1,000 tons. The boat came to rest on a clay bottom with an 11-degree port list. Ellsberg (1927) estimated that the breakout force was about 8,000 tons. "a force so large we could never hope to overcome it by direct lift." His plan, which

was executed successfully, was to "break the suction by letting water in between hull and clay in two ways—first, by rolling the boat to starboard, and second by lifting her one end (stern) first."

S-4. The S-4 was an 830-ton boat which sank in 1927 in 102 feet of water off Provincetown. It was initially and intermittently buried in a very permeable mud to a depth of 7 or 8 feet. The boat, whose submerged weight amounted to 722 tons, was raised by lifting the stern first. Saunders (1929) states that "the bottom had an upper layer of very soft silt or mud not more than one foot deep. Underneath this, the bottom was more soft than hard, of a decidedly sand character, mixed with minute shells. The texture of the bottom was sufficiently coarse to permit the passage of water through it...yet sufficiently firm to hold its position when excavating tunnels underneath the vessel. Due to the permeable characteristic of the bottom it is estimated that the so-called 'suction effect' on the S-4 was practically nil." As a matter of fact, there are no indications that breakout was a problem.

USS SQUALUS. The salvage of the USS SQUALUS is perhaps the most widely reported and documented of all marine salvage operations. The USS SQUALUS, which sank in 1939 about 5 miles south of the Isles of Shoals off Portsmouth Harbor, was a 1,450-ton-displacement boat having a submerged weight of 1,100 tons. The boat came to rest with a 10-degree-up angle in 240 feet of water on a mud bottom in which the stern was buried up to the superstructure deck. The entire operation consisted of five separate attempted lifts, three of which were from a mud bottom. Only the first lift is pertinent to this report. No estimate of the breakout force is reported; however, in a review of the events describing the unsuccessful lift of 13 July, Tusler (1940) indicates that the "unknown amount of mud suction tending to hold the bow down" was one of the main factors contributing to the failure. Previous to the attempted lift, Tusler states that "the bow had sunk down an unknown amount into the soft mud of the bottom, but due to the shape of the bow, it was thought that the mud suction would be relatively insignificant." In any event during each attempted lift, the USS SQUALUS was raised by lifting one end first.

USS LAFAYETTE (ex SS NORMANDIE). The SS NORMANDIE was a 65,000-ton passenger vessel which sank in 49 feet of water adjacent to Pier 88, New York City Harbor. The submerged weight was estimated to be 50,000 tons. The vessel came to rest lying on one side in an organic river mud which was about 25 feet thick and which was underlain by a gray organic silty clay having a compressive strength of from 0.3 to 0.6 ton/ft^2. (This operation is of interest since it appears to have been the first time the principles of soil mechanics were considered in a salvage operation of this

type. The fact that Professor K. Terzaghi served as consultant is a historical note of some importance. He was not concerned with breakout but rather with determining if the soil had sufficient strength to support the vessel without serious movement during the year and a half of preparation for righting, with the effect dredging would have on the settlement of the ship, and with the probable effective soil bearing plane.) It was anticipated that breaking contact between the ship's hull and the mud would be a serious problem. Accordingly, in addition to pumping out some 15,000 tons of mud which had entered the hull through the cargo doors and portholes, numerous porthole patches were fitted with pipes through which water and compressed air could be jetted to disintegrate the mud. The flotation of the vessel was preceded by a rotation or turning operation. Masters (1954) notes that during the rotation operation, the air and water jets were set to work, although the vessel did not stick as expected.

PHOENIXES. The PHOENIXES were 200-foot-long floating blocks of reinforced concrete which were to be sunk in a line off the Normandy beaches to provide a breakwater during the European invasion. Each unit was 60 feet wide, 60 feet high, and displaced 6,000 tons. They were divided into watertight compartments and fitted with valves for controllable flooding. Approximately 100 of these PHOENIXES were purposely sunk in staging areas off the south coast of England prior to invasion. The first attempt to refloat a PHOENIX by pumping failed. It was determined that the mud bottom suction was holding the PHOENIX down. The traditional method of breaking this contact is to apply buoyancy to one end and to use the ship as a lever. In this manner the contact is broken along the bottom, eventually freeing the vessel from the mud. However, in the case of the PHOENIXES there was not enough time to allow this system to work, because the rising tides would submerge the pump platforms before the lever action could be made effective. A second alternative is to jet air or water underneath the sunken vessel to partially reduce the contact and lessen the holding force. In the case of the PHOENIXES, compressed air was employed (all pumps were being used to empty the flooded compartments) to reduce the holding force to allow the excess buoyancy to float the PHOENIXES.

In addition to the case histories cited above, there are many other records of maritime salvage operations in which a ship has been raised from a mud bottom under very unfavorable circumstances. The background provided herein is not intended to be an all-inclusive treatment of salvage. Only those cases in which the breakout force was alluded to in the published literature were selected. It is worthy of note, however, that the published record (Bowman, 1964) of the salvage of the entire German High Seas fleet, which was scuttled at Scapa Flow, does not mention that breakout was a

problem. Further, the U. S. Navy's experience with the ex-German submarine 1105 did not disclose the breakout problem, although the tests were carried out with the submarine eventually lying on a mud bottom (letter from Commander Task Unit 49.4.3).

In summary, the problem of freeing vessels from the ocean bottom has been recognized for a long time. However, a number of factors in combination with each other have tended to prevent the synthesis of the basic principles of naval architecture and those of soil mechanics. The development of modern soil mechanics dates from the work of K. Terzaghi during the 1920s and is a relatively recent event in terms of man's experience with sea-going vessels. Moreover, when the unknown behavior of ocean bottom sediments is considered, one can appreciate why the marine salvor attaches more importance to hydrostatic calculations than to gross estimates of the mud suction effect.

FIELD TESTS

A field test program was designed to correlate the breakout force with the breakout time, object size, object shape, and soil strength. The breakout force calculated from the resulting empirical formula was compared with the analytical value. A detailed description of the site selection and soil borings is given in Appendix A. A detailed description of the selection of body shapes and dimensions is given in Appendix B.

Limitations

A number of factors disclosed by a preliminary survey and recent experience imposed some limitations on the conduct of the field tests. These factors were:

1. The tests could not be conducted near any existing pier, wharf, or other fixed structure due to the presence of shell fragments and other debris in the soil.

2. Each test was required to be conducted in an essentially undisturbed deposit, even though local remolding of the soil was known to take place.

3. Since breakout is essentially a time-dependent process, it is necessary to apply relatively constant force levels over long periods and to measure the movement of the object with respect to the undisturbed deposit in which it is embedded.

Apparatus

The use of a mobile bottom-resting platform, even if one had been available, was determined to be uneconomical. A proposal to drive groups of piles at various locations within San Francisco Bay also proved to be uneconomical. It was intended that the piles would support fixed decks from which the tests could be conducted.

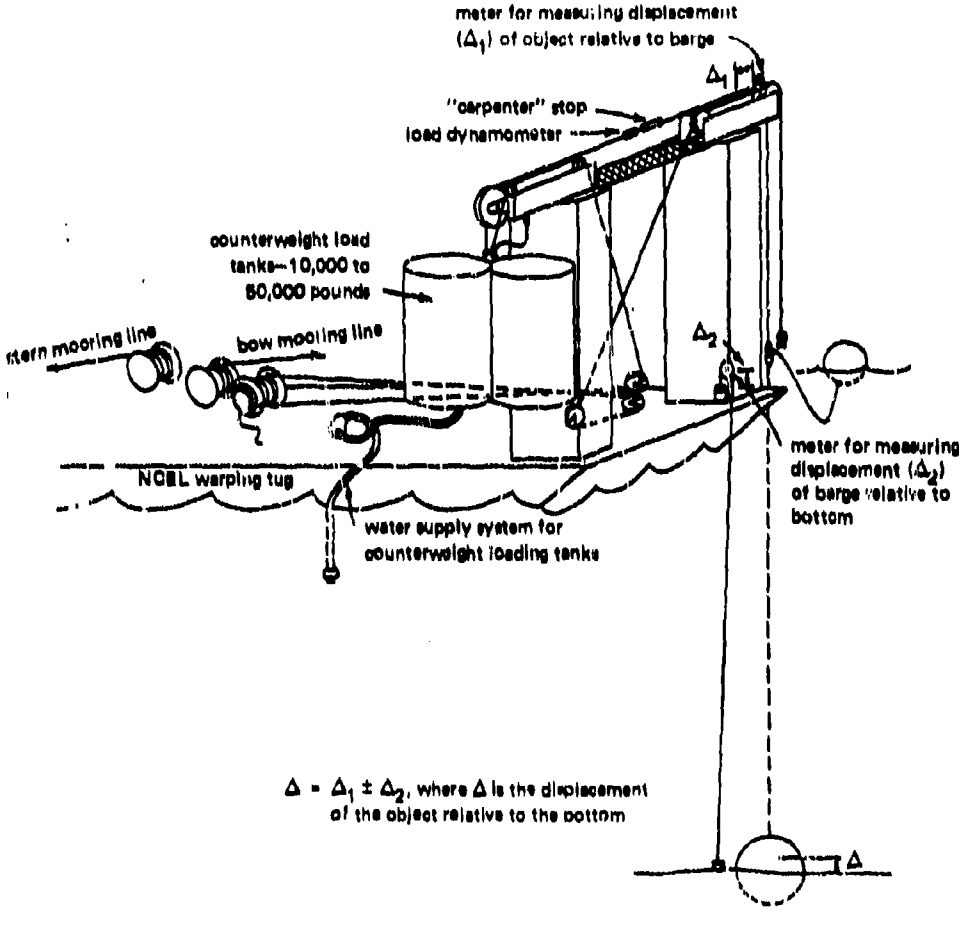

Figure 1. Schematic of test apparatus.

A 35-foot x 88-foot floating barge, called the NCEL warping tug, was selected, largely because of its availability. The warping tug was modified to accommodate a counterweight loading system, a schematic of which is shown in Figure 1. The counterweight system permits the application of relatively constant loads over long periods of time, since it compensates for tide changes, varying freeboard, and the short-term heave, pitch, and roll of the barge. The system consists of a frame composed of pontoons (5 x 5 x 7 feet) which provide an elevated support for the counterweight. The counterweight proper consists of twin 6-foot-diameter by 12-foot-long tanks. These tanks when filled with varying amounts of water are capable of providing from 9,000 to 49,000 pounds of force. The force levels can be carefully controlled. A photograph of the system is shown in Figure 2.

The "carpenter stopper," shown in Figure 3, allows an adjustment of the length of the line from the counterweight to the test object. It is a critical piece of equipment since it can be used to connect one line anywhere along the length of another line without damaging either line. It develops the full strength of the lines and does not disengage when the lines are slacked.

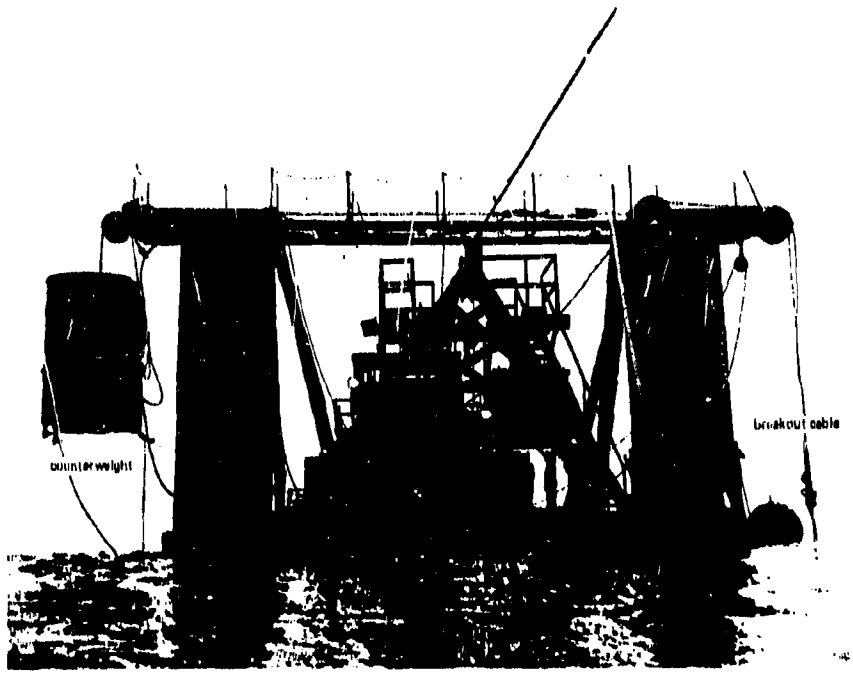

Figure 2. Photograph of test apparatus.

The warping tug was secured in position with a two-point moor, fore and aft. The stern line was anchored with a 9,000-pound STATO* anchor and the bow line was made fast to the end of a pier. Sufficient tension was developed in the mooring lines to resist significant transverse movements of the barge. Position was checked by measuring (with a transit) the angle of the moor relative to the pier and by metering the bow line.

Force was measured and recorded by an in-line calibrated strain-gage dynamometer. Displacement of the test specimen relative to the barge was measured by a potentiometer-backed wheel driven by the sheave over which the lifting line was reeved. Displacements of the barge relative to the bottom were also measured by a potentiometer-backed wheel over which a small counterweight and a mud float were suspended (see Figure 1). Some difficulty was experienced from floating debris, which tended to become entangled in the wire line. A facsimile of an oscillogram for one of the tests is shown in Figure 4.

Figure 3. Load dynamometer and carpenter stopper.

RESULTS OF FIELD TESTS

Presentation of Data

The data as reduced from the oscillograms are portrayed graphically in Figures 5 through 10. It is to be

* A mooring anchor named after the two NCEL employees (Stalcup and Towne) who designed and developed it.

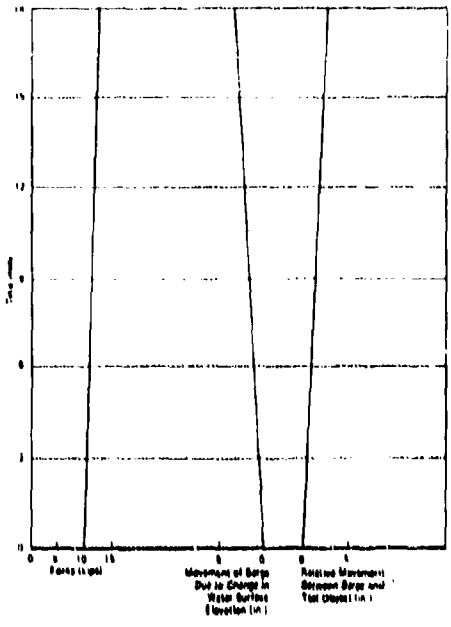

Figure 4. Facsimile of test data.

emphasized that these are essentially raw data which have not been corrected for obvious errors, although some test data were discarded primarily for reasons of incompleteness. The data are presented in the form of depth of embedment in inches versus time in minutes from the beginning of each test. The beginning of each test was taken to be the time at which the counterweight tanks began to be filled with water. For each of the tests, unless so indicated, the rate of load application (that is, the filling of the tanks) was uniform, although it varied from test to test. For each test, the applied load over and above the submerged weight of the test specimen (in salt water) is indicated. In addition, certain other information is presented for each test. This includes (1) the time elapsed from the placement of the object to the start of the test; (2) the location of the test object relative to the pier in bearing and distance; and (3) the local shear strength at a depth equivalent to the depth of settlement of the object. The latter was obtained by divers using a vane device. To aid in interpreting the figures, the following example is described in detail.

Example (Test No. 38, Figure 5). The test object was a cube which was placed in position 240 feet from the pier at an angle of 90 degrees measured clockwise from an imaginary line perpendicular to the longitudinal axis of the pier and having its origin at the southeast corner of the pier. The object settled a distance of 36 inches into the bottom sediments and was allowed to remain in place undisturbed for 68 hours. In-situ vane shear strength at a depth of 36 inches was measured to be 0.83 psi. The submerged weight (in salt water) of the cube was 20,000 pounds. At the beginning of the test a load of 9,000 pounds was applied to the object, which corresponds to the dead weight of the counterweight tanks. Water was added at about the rate of 215 lb/min. After approximately 100 minutes, the total applied force was 30,500 and the object moved noticeably and broke free of the bottom.

The data from all of the tests are conveniently displayed in Table 2. To bring some order out of the large number of parameters required to describe the breakout phenomenon, the original raw data presented in

Figures 6 through 8 have been replotted and appear in Figures 11 through 14. The ordinate has been normalized by dividing the instantaneous embedded depth by the original embedded depth. It was expected that the freeing of the object or alternatively the failure of the soil medium could be clearly identified and correlated both for similar and dissimilar objects. However, this hope did not materialize.

Formulation of Empirical Equation

Unfortunately, the various classical theories of failure which have been widely employed in the practice of soil mechanics and foundation engineering, such as the Mohr-Coulomb theory, assume that the stress conditions alone determine the state of failure of a material, irrespective of the load duration and the stress history. However, it has become increasingly clear that the load duration is a major factor in the breakout process. Schmid and Kitago (1965) stated:

"That clay soils have time-dependent shear properties has been recognized for a long time, but the profession still frequently approaches problems of time-dependent stress-strain behavior of clay soils as if they could be analysed completely on the basis of the theory of elasticity or plasticity without regard to the actual rheological properties. Time effects are often discussed, if at all, merely on a qualitative basis. One reason for this may be the complexity resulting when time is considered an additional variable in any problem. Another reason may be the difficulty of abandoning old and familiar concepts that usually are sufficient for most structural materials, and another the lack of familiarity of most soil engineers with rheological theory, since its application to problems of soil mechanics is still developing.

"There appears to be general agreement, however, that saturated clay soils do behave like viscoelastic or viscoplastic materials. As a consequence, the classical failure theories...cannot and do not completely describe the material behavior of clay soils. Either they have to be modified to permit a quantitative assessment of stress history, temperature, and rate of loading or they have to be replaced by theories that include these effects."

In the classical theories, one or two of such material parameters as yield stress, Young's modulus, or Poisson's ratio are sufficient to describe the behavior of an isotropic material. Such simplifications are inadequate to predict breakout behavior.

To keep the problem as simple as possible and yet retain all of the essential features, the breakout test data will be analyzed stepwise in the following paragraphs.

BLANK PAGE

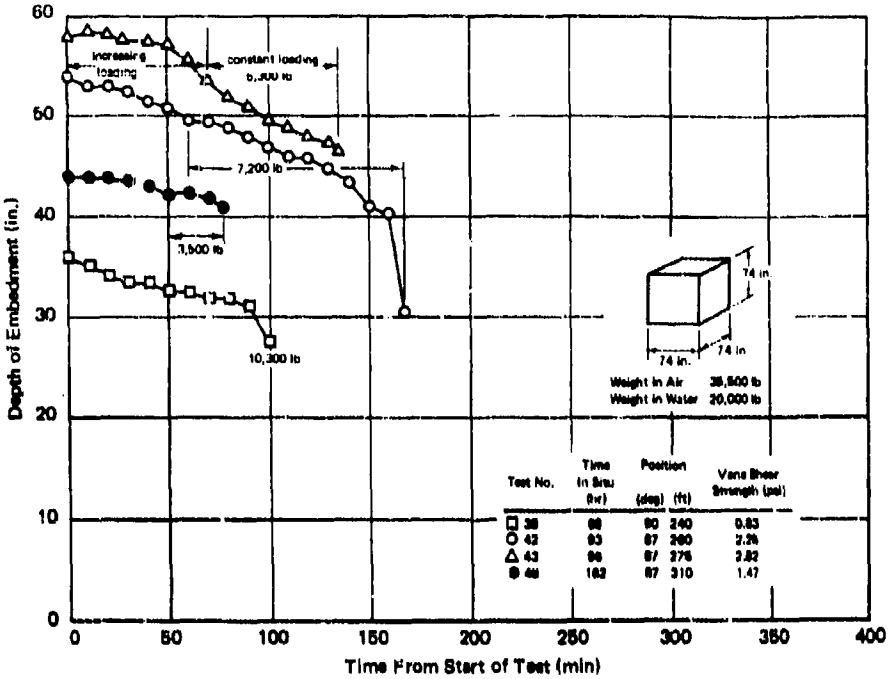

Figure 5. Displacement history curves of cube.

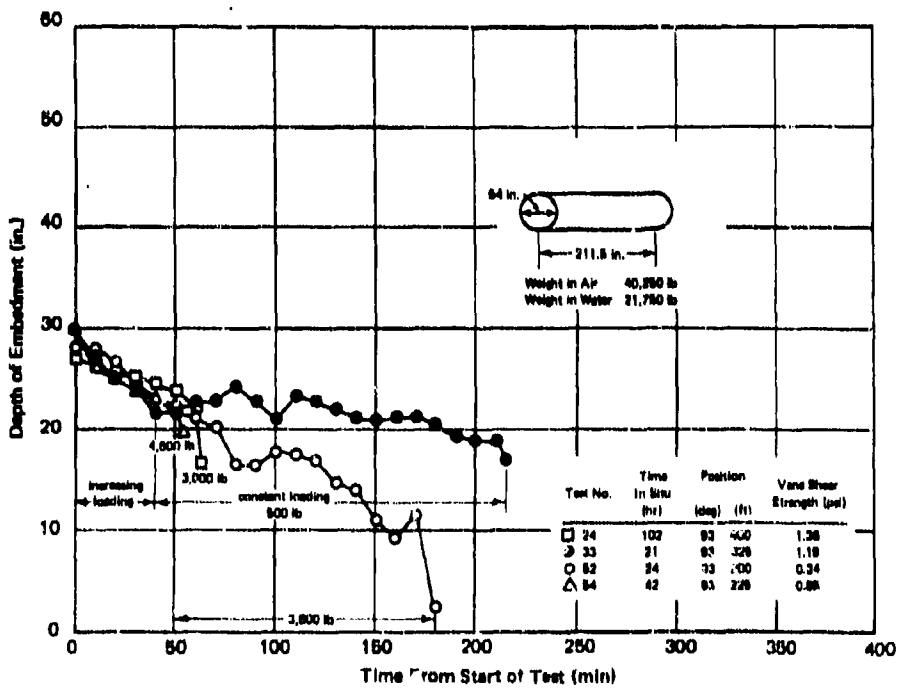

Figure 8. Displacement history curves of cylinder.

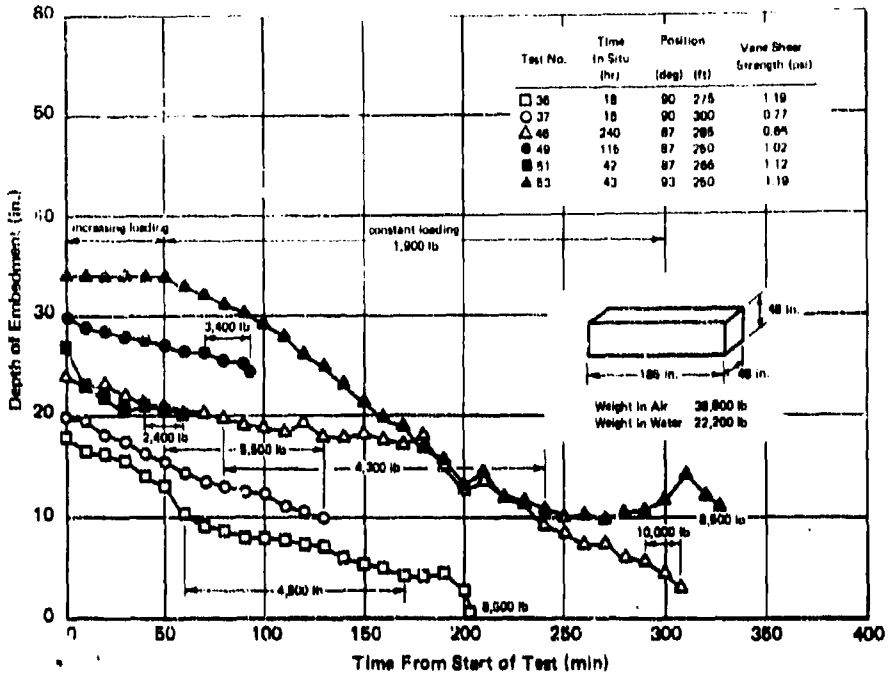

Figure 8. Displacement history curves of prism.

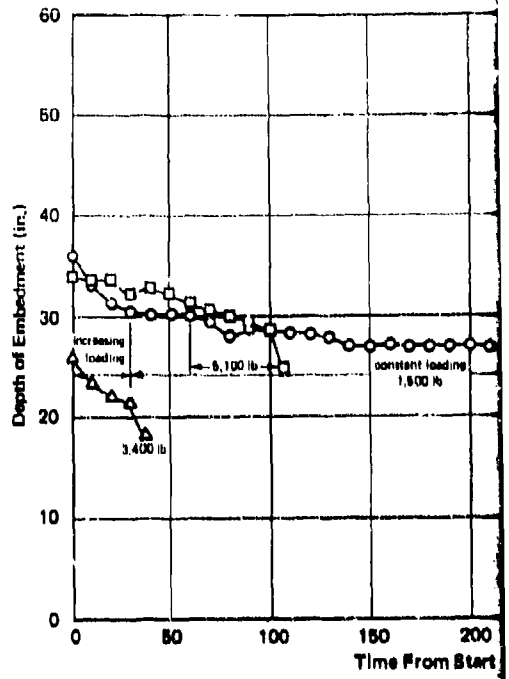

Figure 7. Displacement his

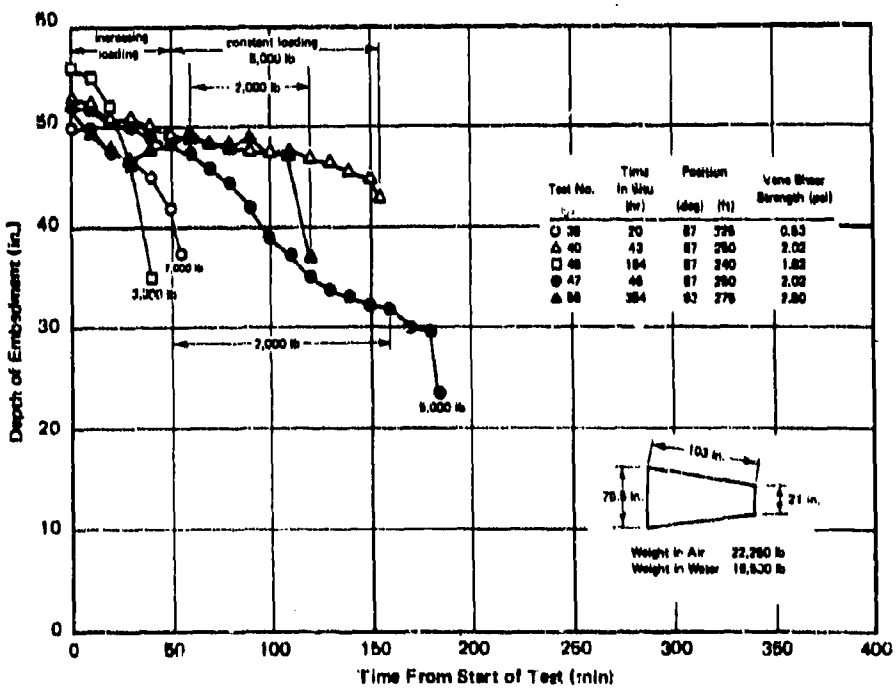

Figure 9. Displacement history curves of cone.

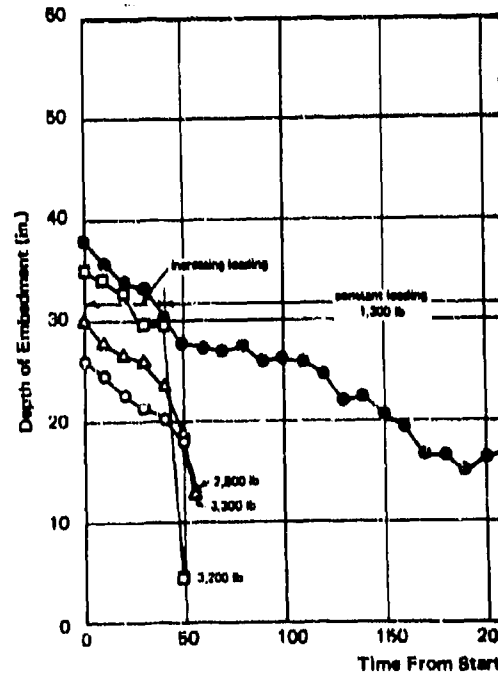

Figure 10. Results of field

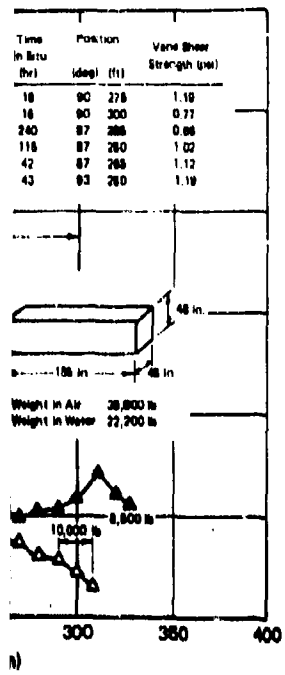

n)

is of prism.

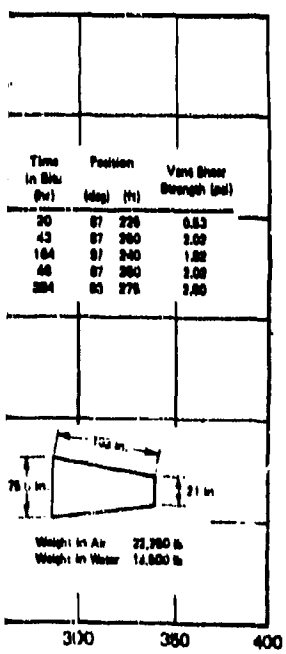

n)

is of cone.

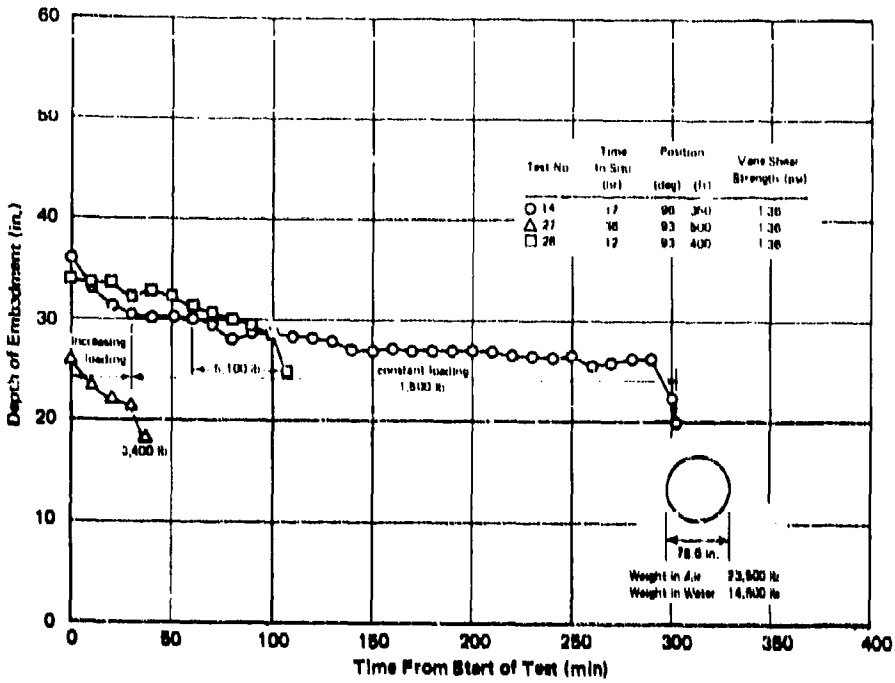

Figure 7. Displacement history curves of sphere.

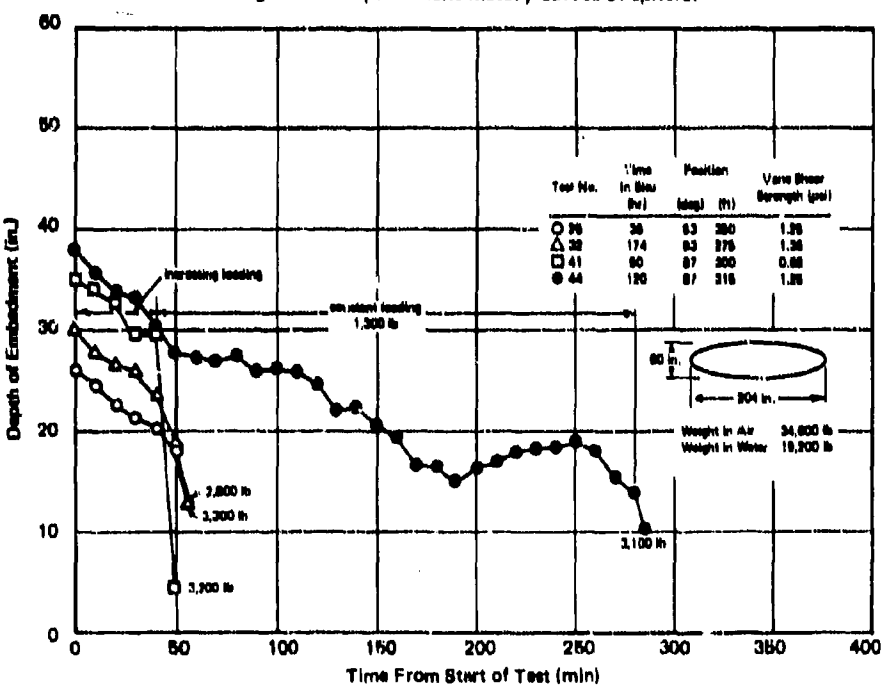

Figure 10. Results of field test data with ellipsoid.

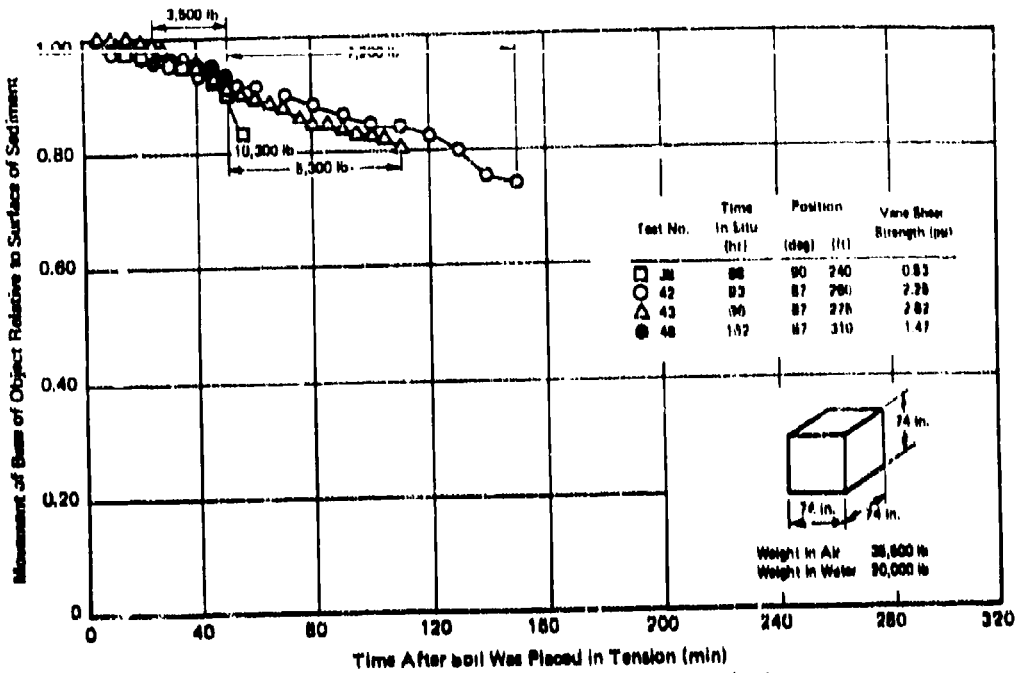

Figure 11. Normalized displacement history of cube.

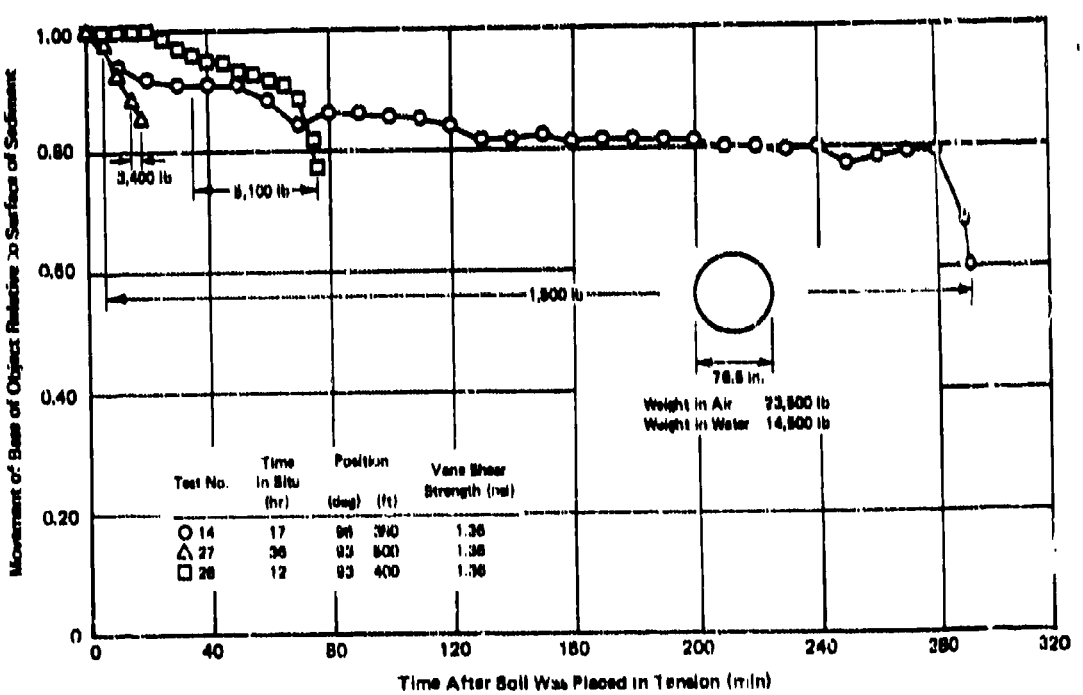

Figure 13. Normalized displacement history of sphere.

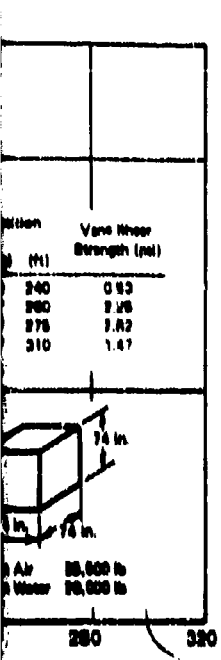

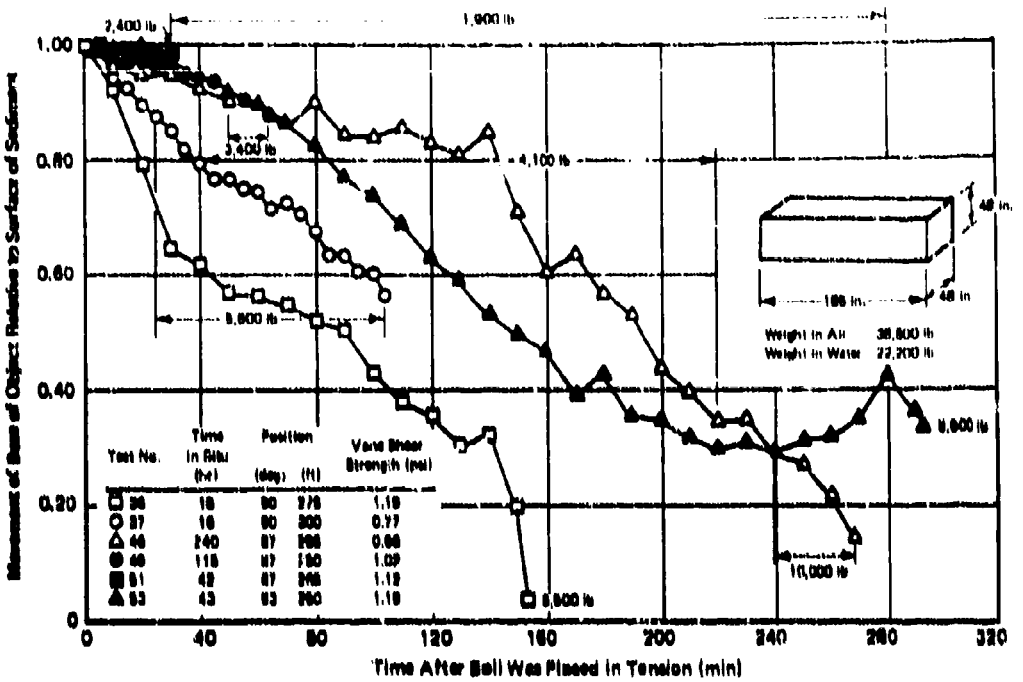

Figure 12. Normalized displacement history of prism.

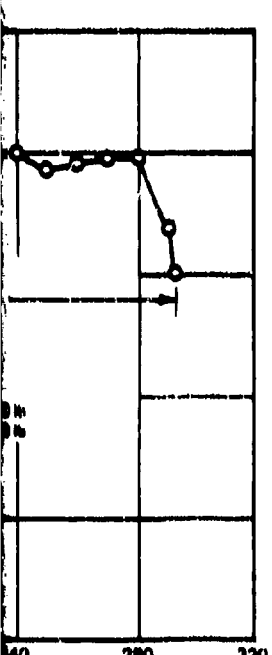

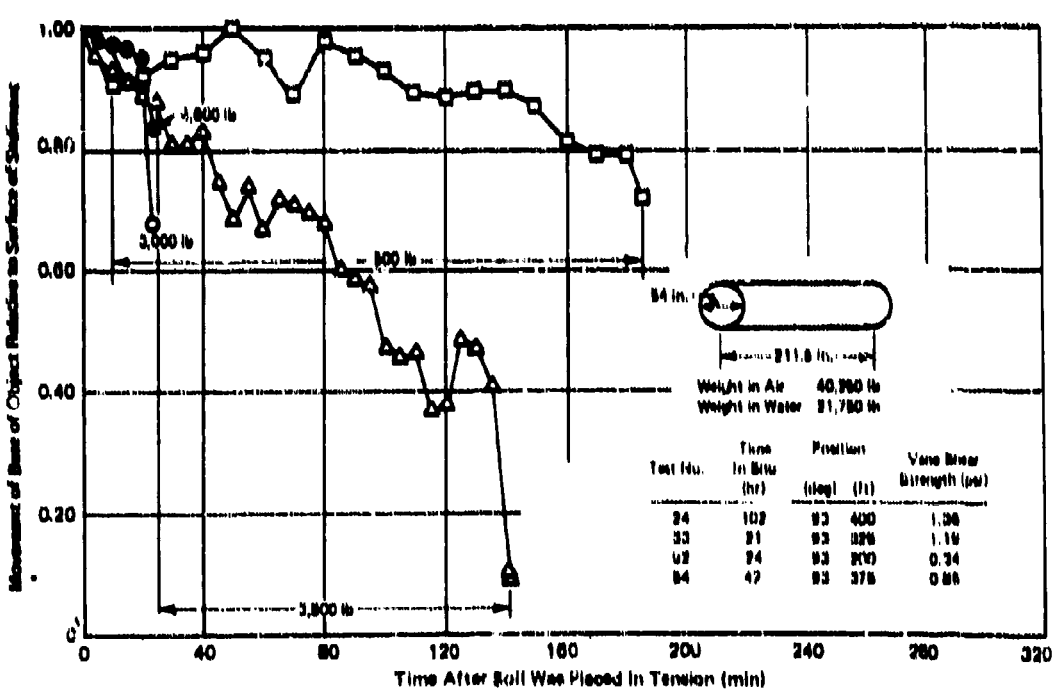

Figure 14. Normalized displacement history of cylinder.

13

Test Object	Test Number	Position Bearing (deg)	Position Distance (ft)	Depth of Embedment (in.)	Cohesion of Soil at Position and Depth of Embedment (psf)	Time In Situ (hr)	Weight of Test Object in Air (lb)	Weight of Test Object in Water (lb)
Cube	34	90	225	48	0.65	19	36,500	20,000
Cube	38	90	240	36	0.83	68	↓	↓
Cube	42	87	260	54	2.25	93		
Cube	43	87	275	58	2.82	96		
Cube	48	87	310	44	1.47	162		
Cube	50	87	300	40	0.83	44		
Prism	36	90	250	20	1.11	26	38,800	22,200
Prism	38	90	275	18	1.19	18	↓	↓
Prism	37	90	300	20	0.77	16		
Prism	46	87	285	36-12	0.66	240		
Prism	49	87	250	30	1.02	116		
Prism	51	87	265	27	1.12	42		
Prism	53	93	250	34	1.10	43		
Sphere	10	90	300	"	"	67	23,500	14,500
Sphere	11	90	300	"	"	19	↓	↓
Sphere	13	90	325	"	"	18		
Sphere	14	90	350	90	"	17		
Sphere	23	93	600	"	"	15		
Sphere	27	93	500	34	"	30		
Sphere	28	93	400	26	"	12		
Sphere	29	93	350	60	2.28	70		
Sphere	30	93	375	30	"	13		
Cylinder	19	93	400	40	"	24	40,250	21,750
Cylinder	20	↓	425	40	"	16	↓	↓
Cylinder	24		400	27	1.36	102		
Cylinder	31		300	32	1.36	168		
Cylinder	33		325	30	1.19	21		
Cylinder	52		200	28	0.34	24		
Cylinder	54		225	30	0.68	42		
Cylinder	26		375	28	"	24		
Cylinder	22		600	"	"	"		
Cone	39	87	225	50	0.53	20	22,250	16,500
Cone	40	87	250	53	2.02	43	↓	↓
Cone	45	87	240	56	1.82	164		
Cone	47	87	250	52	2.02	40		
Cone	55	93	275	52	2.80	314		
Ellipsoid	25	93	350	28	1.25	36	34,000	19,200
Ellipsoid	32	93	275	30	1.30	174	↓	↓
Ellipsoid	41	87	300	35	0.90	90		
Ellipsoid	44	87	315	31	1.25	120		

Table 2 Summary of Field Test Results

Time in Situ (hr)	Weight of Test Object in Air (lb)	Weight of Test Object in Water (lb)	Buoyant Force of Water (lb)	Volume of Soil Displaced by Embedded Object (ft^3)	Submerged Weight of Soil Displaced by Embedded Object (lb)	Weight Supported by Soil (lb)	Cross Sectional Area ($in.^2$)	Force/Area Supported by Soil (psi)	Depth of Embedment at Breakout (in.)	Applied Force Greater Than Weight of Object in Water (lb)	Volum Soil Disp at Tim Breake (ft^3
19	35,600	20,000	15,600	158	4,740	15,260	6,476	2.79	--	9,000	--
68				116	3,480	16,520		3.03	27.6	10,300	87.5
9				175	5,250	14,760		2.69	30.6	7,200	66.7
9.5				188	5,640	14,360		2.62	46.4	5,300	147.0
162				142	4,260	16,740		2.87	40.9	3,600	129.6
44				129	3,870	16,130		2.95	3.6	2,000	0
26	38,800	22,200	16,600	108	3,240	18,960	8,880	2.14	--	6,400	--
18				97	2,910	19,290		2.17	0.5	8,500	2.5
16				108	3,240	18,960		2.14	0.9	5,500	50.0
240				130	3,900	18,300		2.06	3.1	10,000	15.9
115				162	4,860	17,340		1.95	24.6	3,400	120.4
42				146	4,380	17,820		2.01	20.6	2,400	105.8
43				184	5,520	16,680		1.88	11.4	8,500	58.5
67	23,600	14,600	9,000	--	--	--	--	--	--	4,500	--
19				--	--	--	--	--	--	2,500	--
18				--	--	--	--	--	--	4,000	--
17				81.9	1,857	12,043	4,604	2.76	10.7	1,500	22.4
15				--	--	--	--	--	--	1,500	--
36				56.8	1,698	12,902	4,648	2.81	25.0	5,100	34.6
12				36.4	1,092	13,408	4,137	3.24	18.3	3,400	19.6
70				123.0	3,690	10,810	4,599	2.36	--	1,500	--
13				81.9	1,857	12,043	4,604	2.76	--	1,000	--
24	40,260	21,760	18,500	222	6,660	15,000	11,421	1.32	--	2,000	--
16				222	6,660	15,000		1.32	--	2,000	--
102				140	4,200	17,560		1.54	16.5	3,000	72.2
168				172	5,160	16,890		1.48	--	3,250	--
21				160	4,980	16,770		1.47	17.0	900	76.1
24				146	4,380	17,370		1.52	2.1	3,900	3.5
42				160	4,980	16 770		1.47	10.7	4,800	91.5
24				146	4,380	17,570		1.52	--	1,300	--
										6,000	--
20	22,260	10,500	6,760	120	3,780	12,720	5,600	2.27	37.4	7,000	98
43				128	3,840	12,660		2.26	42.0	5,000	100
164				132	3,960	12,540		2.24	36.0	3,300	92
46				127	3,810	12,690		2.26	23.4	6,000	60
384				127	3,810	12,690		2.26	30.8	2,000	95
30	34,600	10,200	15,400	92	2,760	16,440	9,300	1.77	13.1	2,900	30
174				115	3,430	15 770	9,400	1.68	12.6	3,300	27
90				114	4,320	14,880	9,400	1.58	4.3	3,200	6
120				160	4,800	14,400	9,400	1.53	10.3	3,100	20

Applied Force Greater Than Weight of Object in Water (lb)	Volume of Soil Displaced at Time of Breakout (ft^3)	Submerged Weight of Soil Displaced at Time of Breakout (lb)	Resistance of Soil to Breakout (lb)	Cross-Sectional Area at Time of Breakout ($in.^2$)	Resistance of Soil to Breakout in Force/Area (psi)	Total Time of Test (min)	Time Force Equals Submerged Weight of Object (min)	Total Time of Duration of Maximum Force (min)
9,000	--	--	--	5,476	--	125	67	20
10,300	87.5	2,625	12,925	↓	2.36	100	53	0
7,200	96.7	2,901	10,101	↓	1.84	166	30	110
6,300	147.0	4,410	9,710	↓	1.77	136	95	0
3,500	129.6	3,888	7,388	↓	1.35	76	37.5	31
2,000	0	0	2,000	↓	0.37	410	44	360
6,400	--	--	--	--	--	--	--	0
8,500	2.5	75	8,575	8,880	0.97	203	45	10
5,500	50.9	1,527	7,027	↓	0.79	129	33	85
10,000	15.9	477	10,477	↓	1.19	308	64	20
3,400	126.4	3,792	7,192	↓	0.81	92	47.5	35
2,400	105.8	3,174	5,574	↓	0.63	62	45	5
8,500	58.6	1,758	10,258	↓	1.16	327	47	0
4,500	--	--	--	--	--	44	16.5	17
2,500	--	--	--	--	--	69	22	37
4,000	--	--	--	--	--	357	12.5	0
1,500	22.4	672	2,172	3,520	0.62	305	11	290
1,500	--	--	--	--	--	39	34	0
5,100	34.0	1,020	6,120	4,061	1.51	106	39	43
3,400	19.6	588	3,988	3,360	1.19	48	31	3
1,500	--	--	--	--	--	480	35	437
1,000	--	--	--	--	--	469	34	432
2,000	--	--	--	--	--	--	--	--
2,000	--	--	--	--	--	196	12	120
3,000	72.6	2,178	5,178	10,490	0.49	63	52	2
3,250	--	--	--	--	--	--	--	--
600	76.7	2,301	2,901	10,017	0.26	215	12	176
3,800	3.3	99	3,899	4,316	0.90	181	46	131
4,000	91.1	2,733	7,333	10,998	0.67	64	25	0
1,300	--	--	--	--	--	--	--	--
5,000	--	--	--	--	--	60	33.5	7
7,000	98	286	7,286	9,400	0.78	55	35	0
5,000	100	327	5,327	↓	0.57	155	30	110
3,300	92	276	3,576	↓	0.38	39	20	3
5,000	60	180	5,180	↓	0.55	185	30	0
2,000	95	285	2,285	↓	0.24	120	55	0
2,800	30	900	3,700	6,700	0.55	55	43	0
3,300	27	810	4,110	6,400	0.64	58	44	0
3,200	6	180	3,380	2,800	1.21	40	33	0
3,100	20	600	3,700	5,400	0.69	285	36	0

BLANK PAGE

Beginning with a very simple formulation of the mechanics of breakout, one may set*

$$F = kCA \tag{1}$$

where F = breakout force

C = cohesion, or alternatively a measure of the vane shear strength

A = horizontal projection of the contact area

k = constant which is a function of object size, object shape, time duration of applied force, rate force is applied, soil sensitivity,** and the elapsed time which the object has been in place after the initial disturbance

Thus, we may write

$$\frac{F}{CA} = k$$

or

$$\log \frac{F}{CA} = \log k \tag{2}$$

Letting C and k take on slightly different meanings, we may write

$$\frac{F}{\underline{C}A} = Qe^{-R(t - t_o)} \tag{3}$$

where $\underline{C}$ = effective average cohesion along the failure surface at the instant of breakout

Q = constant

R = slope of the "failure line" when $\log (F/\underline{C}A)$ is plotted versus time, t

t = time allowed for breakout, or alternatively the elapsed time during which the breakout force is applied

t_o = reference time in minutes

---

* The reader is referred to the nomenclature on page 31.

** Ratio of cohesion of undisturbed soil to cohesion of disturbed soil at constant water content.

The constants Q and R are functions of the load duration or strain rate. In Equation 3, when $t = \infty$, the force required for breakout is a minimum. Conversely, as t is allowed to approach zero, that is, as the time allowed for breakout becomes increasingly short, the force requirement reaches a maximum constant value.

The quantity $\underline{C}$ requires some comment, since it is also a time-dependent function which is related to the soil sensitivity. It may be estimated by an equation of the type

$$\underline{C} = \frac{C}{s} + \left(C - \frac{C}{s}\right)\left[1 - e^{-b\,t/(t - t_1)}\right] \qquad (4)$$

where s = degree of soil sensitivity

b = numerical constant used to force $\underline{C} = C$ for very large t, in keeping with our knowledge of thixotropic material behavior

t_1 = reference time related to the thixotropic behavior of a material in regaining a stated percentage of its strength after initial disturbance

To illustrate that Equation 4 is approximately correct, we note that (1) for $t = 0$, then $\underline{C} = C/s$, (2) for $t = t_1$, $\underline{C} = C$, and (3) for very large t, $\underline{C} = C$ even for relatively small values of b. Dimensionless graphs of Equation 4 are shown in Figures 15 and 16 for values of $b = 1.0$ and $s = 5.0$ and 8.0, respectively. Experimental information on the validity of Equation 4 seems to be nonexistent. In addition, the reference time t_1 seems to be highly variable, being very short (that is, on the order of minutes) for such thixotropic materials as drilling muds and perhaps very long (that is, measured by geologic time) for many deep marine sediments.

On the basis of experimental test results we may estimate s, C, t_1, t_o, and the constants Q and R, and then compute the force F required to extract the specimen as a function of time, t. For example

$$F = \underline{C} A Q e^{-R(t - t_o)} \qquad (5)$$

or for maximum C

$$F = C A Q e^{-R(t - t_o)} \qquad (6)$$

It is to be emphasized that the reference times are those determined from large-scale field tests.

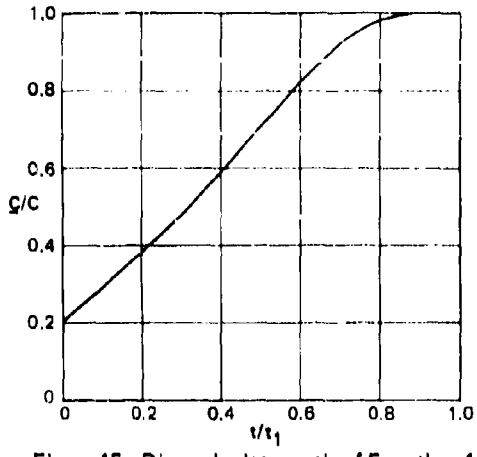

Figure 15. Dimensionless graph of Equation 4 for b = 1.0, s = 5.0.

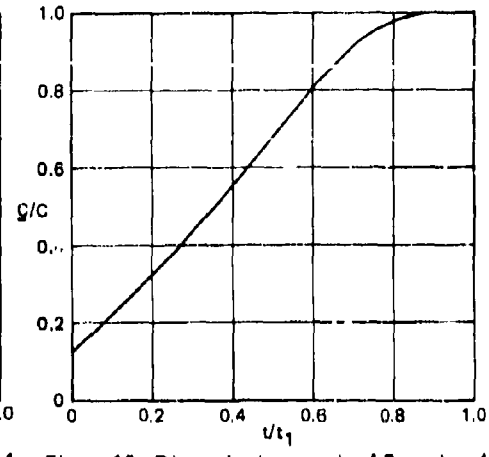

Figure 16. Dimensionless graph of Equation 4 for b = 1.0, s = 8.0.

The foregoing illustrates how the field data may be analyzed and used for predicting breakout, assuming that scale effect is negligible. In connection with the data reduction it was found that the cohesion, C, as obtained by vane shear tests, showed marked variability. Thus, as an alternative measure of the sediment strength, it was expedient to use the quantity q_d, which is defined as the average supporting pressure provided by the soil to maintain the embedded object in static equilibrium, in all of the data reduction since it exhibited very consistent trends. In a sense this is fortunate since the problem then becomes completely determinate, being no longer dependent on external measurements.

Some of the data summarized in Table 2 are presented in Figures 17 and 18. Figures 18a, 18b, and 18c are semilogarithmic graphs of the data appearing in Figures 17a, 17b, and 17c, respectively. The elapsed time over which the maximum force was applied appears as the ordinate in all figures. In Figures 17a and 17b the abscissa is the dimensionless quantity, $F/(A_{max}\, q_d)$; in Figure 17c the abscissa is $F/(Aq_d)$. In Figures 17b, 17c, 18b, and 18c the force F represents the net breakout force, which is the applied force minus the submerged weight of the object, not only that portion submerged in salt water, but also that portion of the object embedded in the bottom sediment.

Figure 18a indicates some of the trends in selected data from Table 2. The coefficients Q, R, and t_o used in Equation 5 are also shown on the figure. Although the data are extremely limited, the figure indicates that the forces required to extract the cube and the prism are higher than those for the cylinder and sphere. This seems to be in agreement with previous field experience.

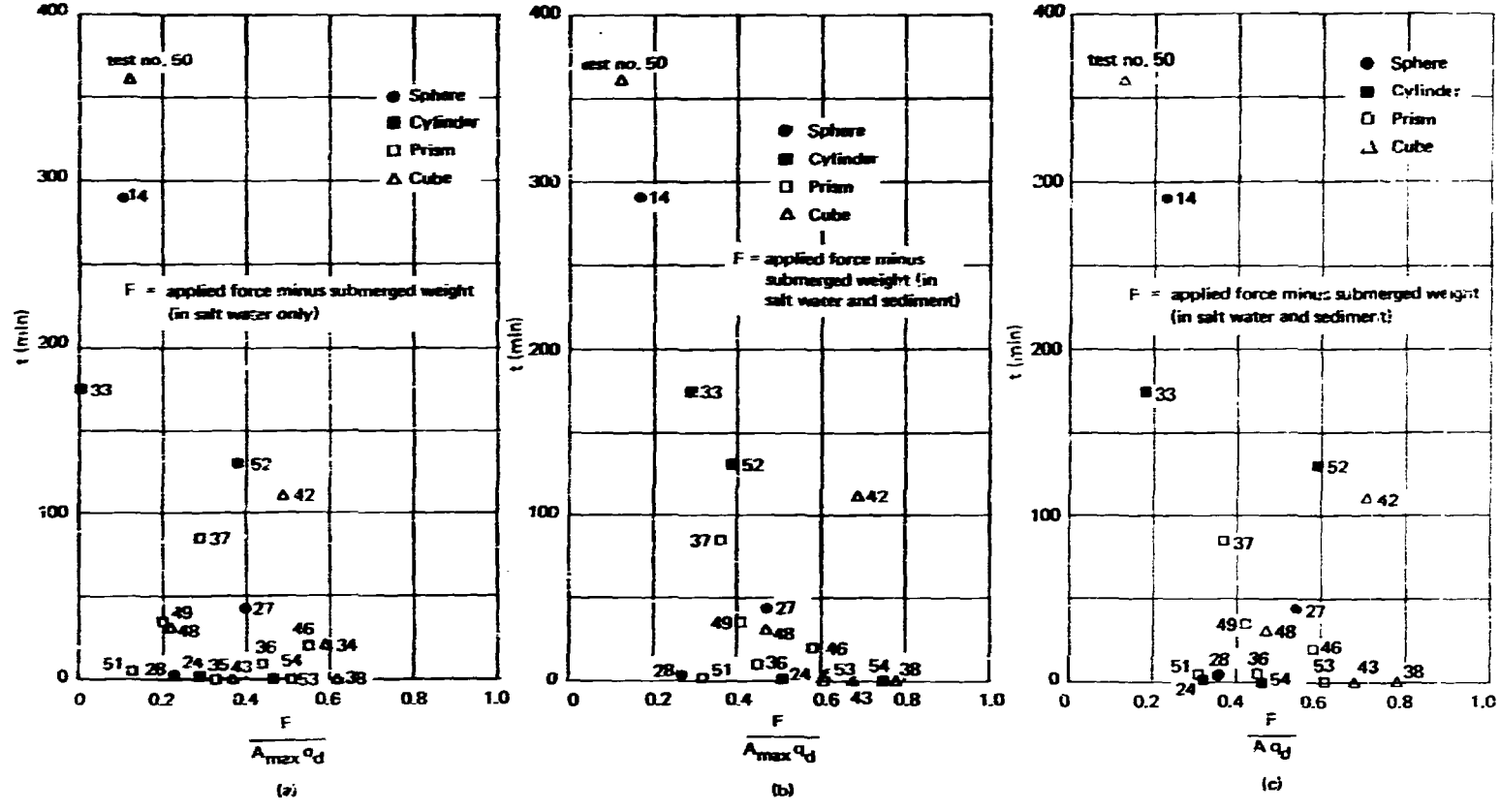

Figure 17. Selected data from Table 2.

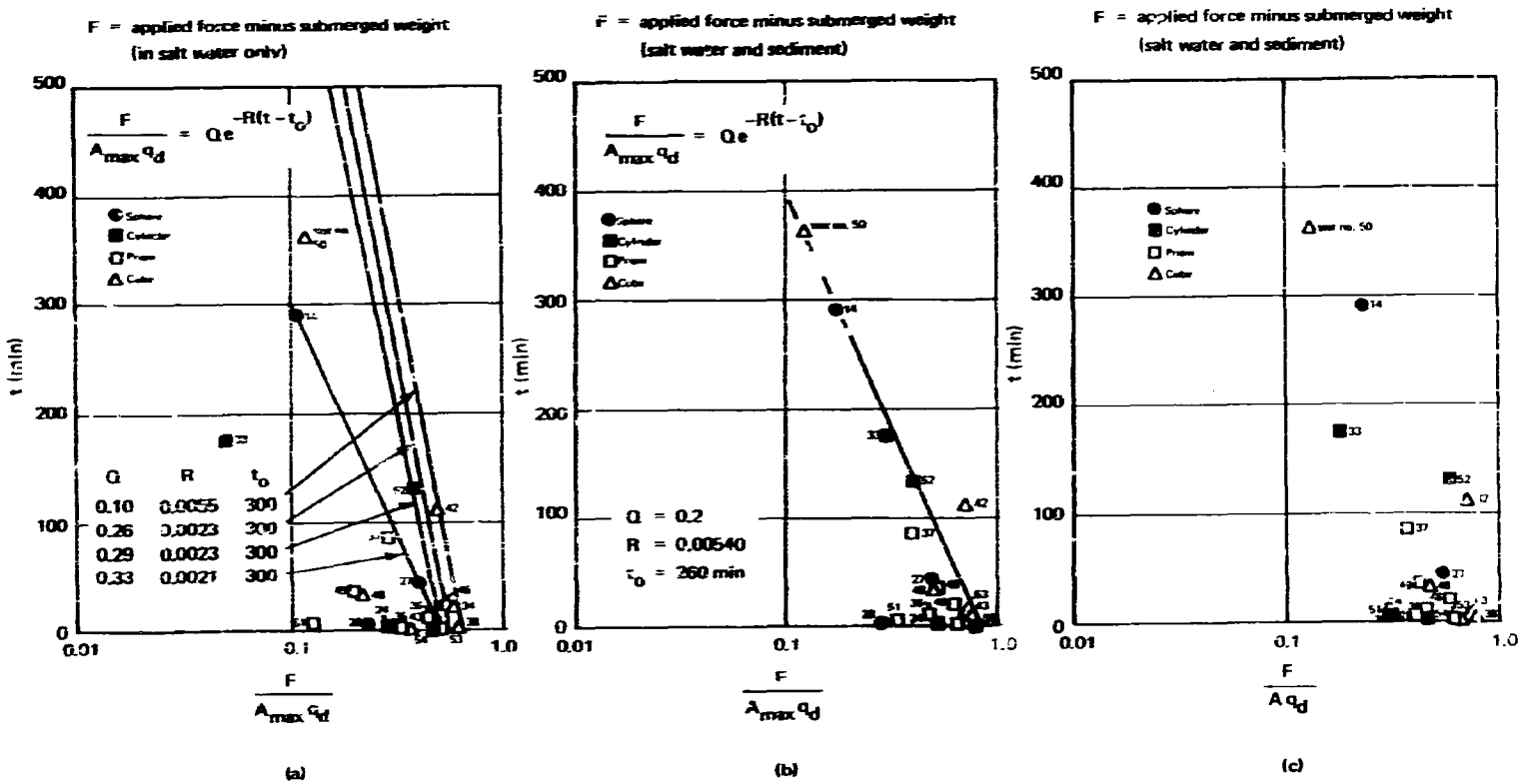

Figure 18. Selected data from Table 2 on semilogarithmic graphs.

Figure 18b exhibits the clearest consistent relationships for all of the included data. That is, the trends shown in Figure 18a for the various shaped objects appear to be almost entirely obscured when the numerator in the abscissa is reduced by an amount equal to the submerged weight of the volume of sediment displaced by the embedded object.

From these data, the equation for computing breakout has been determined to be:

$$F = 0.20\, q_d\, A_{max}\, e^{-0.00540(t-260)} \qquad (7)$$

where A_{max} = horizontal projection of the maximum contact area

For t = 0, Equation 7 reduces to

$$F = 0.81\, q_d\, A_{max} \qquad (8)$$

For t = 260 minutes, the breakout force requirement becomes

$$F = 0.20\, q_d\, A_{max} \qquad (9)$$

It is to be emphasized that relationships such as appear in Figures 18a, 18b, and 18c, of which Equation 7 is typical, are based on only one type of sediment (that is, that found in San Francisco Bay) and one size of test objects, all of which were similar both from characteristic length and bearing load.

THEORETICAL ANALYSIS

To introduce the theoretical procedure employed in this study it seems useful to pause and ask why and in what way is it worthwhile to proceed with the development of complicated models and procedures. That question is best answered by the following quotation from Whitman (1984):

"Highly complex theories should seldom be used in soil engineering practice. The advent of modern computers does not change this conclusion.

"There is always a basic limitation upon any computational procedure that is to be used in design practice—the user must be able to trace a clear relation between each assumption and the result of making this assumption. In the case of soil engineering design there is an additional fact: it is almost impossible to ascertain the actual pattern of nonhomogeneity that exists in a particular soil deposit.

"Sophisticated models and procedures are useful only in applied research. The end objectives of any development of such models and procedures are the clarification of certain puzzling aspects of the behavior of soil masses to bring greater unity into empirical observations, and the determination of the reasonableness and accuracy of simplified methods to aid the development of such simplified methods for use in practical design situations."

The essential nature of the breakout problem differs from the ordinary footing problem (that is, prediction of the ultimate bearing capacity) in at least two important aspects.

First, the ordinary footing problem is generally analyzed statically by means of equations or charts developed by Terzaghi. Time-dependent effects are not considered, whereas for some preliminary breakout tests such effects were observed to be important. Second, the loading pattern applied to the soil mass by footings is relatively simple as compared to that which might exist before and after extraction of a full-scale submarine or deep-submergence vehicle. This is further complicated by the remolding of the soil in the vicinity of the object, whereas for footings the soil is assumed to be essentially undisturbed. The degree of remolding as a function of distance is unknown. Moreover, laboratory techniques for determining the stress-strain relationships for soils under compressive loadings are well established. These relationships are useful in soil engineering practice, since the tests from which they are derived correspond roughly to the loading patterns induced by footings. On the other hand, little comparable information has been developed for soils under tensile loadings. Thus, the symmetry or asymmetry of the stress-strain relationships for soils is not well established.

In view of these differences the use of a sophisticated model for analysis of the breakout process seems at least partially justified. The word partially is used since one might well argue that it is difficult if not impossible to model mathematically the very complicated two-phase material described generally as soil. If this premise were accepted, then predictions of breakout behavior would be required to rely exclusively on experiment followed by the use of relatively simple models.

The theoretical procedure used in this study is based on a systematic numerical procedure, developed by Harper and Ang (1963), for determining the displacements, strains and stresses within a plane continuum wherein certain regions have been strained beyond an elastic yield limit. The material of the continuum is considered to be isotropic, elastic–perfectly plastic, and the problems are solved for continuously increasing external loads.

The numerical procedure is essentially a relaxation technique applied to a discrete physical model composed of suitably arranged stress points and mass points. Once the externally applied loads have been raised to a

sufficiently high level, the more highly stressed stress points of the model begin to yield and flow plastically. The initiation of yielding is determined by the Mises-Hencky yield criterion. Thereafter, yielded regions are assumed to obey the plastic stress-strain relations postulated by the Prandtl-Ruess theory. The numerical method is presented in complete detail in Appendixes C through G. Only a brief resume is presented in the following paragraph.

The lumped parameter model, shown in Figure C-1, is used in the procedure developed by Harper and Ang. The model consists of mass points, at which the mass of the material is assumed to be concentrated, and stress points, which connect the neighboring mass points. Displacements in the continuum are defined only at the mass points, while stresses and strains are defined only at the stress points. The stresses at each stress point are related to the movements of the four surrounding mass points by using a finite-difference version of the stress-strain laws for the continuum. Boundary conditions are given in terms of either external loads acting on the mass points or specified displacements of these mass points.

Figures 19 through 21 are results of an example obtained by application of the numerical method. In this example, it is assumed that a 4 x 4 x 16-foot parallelepiped has penetrated a distance of 6 inches into a soft marine sediment having a yield strength in simple tension of 0.6 psi, a Poisson's ratio of 0.4, and an effective modulus of elasticity of 74 psi.

Figure 19 depicts the propagation of plastic straining with increasing force levels. Figure 20 shows the distribution of yield ratio percentiles for a given level of loading. The elastic displacements at first yielding are shown in Figure 21. Results given in Figures 19 through 31 are based on an arbitrary loading of the boundary mass points, which does not quite coincide with the loading pattern in the field tests. The application of uniform loads to the mass points (that is, load intensity is constant) results in unequal movement of these mass points, which corresponds to what happens with a flexible footing. But submarine keels and other appendages are very rigid and correspond to a rigid footing. Thus, the results given in Figures 19 through 21 must be considered with this reservation. Certain difficulties in adjusting the load increments within the plastic range have thus far prevented the processing of displacement-controlled loading pattern problems. In summary, no anomalies are present in the theoretical approach, even though only the gross features of the breakout process have thus far been studied.

In order to substantiate the results obtained by application of the numerical technique, a photoelastic study of the stress-strain patterns induced by tensile loadings on various boundary geometries was completed. The details are given in Appendix H. A urethane rubber having a modulus of elasticity of 500 psi and a Poisson's ratio of 0.48 was employed for these

tests. The tests support the results of the numerical technique in every detail, at least within the elastic range where the results are comparable. The condition of plasticity cannot be simulated by the photoelastic method. Thus, the numerical technique, which is applicable to both the elastic and plastic regimes, is much more versatile than the photoelastic method and can be applied to a wide range of problems not necessarily limited by laboratory equipment or the construction of special models. The present version of the numerical method, however, is limited to a two-dimensional treatment of the problem.

COMPARISON BETWEEN THEORETICAL AND EMPIRICAL PROCEDURES

An example is selected to compare the results of the theoretical procedure with those of the empirical formula. Data from the photoelastic model are also used to estimate the breakout force.

Let us assume that the keel of the nuclear research submarine NR-1 is buried 6 inches in a marine sediment similar to that in San Francisco Bay. This soil is saturated clay and can be assumed to have a Poisson's ratio of 0.40 and a yield shear strength of 0.6 psi. Let us further assume that the effective modulus of elasticity of the soil is 74 psi, which is equal to the average modulus of elasticity of the tested soil. This value is obtained through triaxial tests. The keel is considered as a parallelepiped 05 feet long and 4 feet wide.

The breakout force required for an immediate pullout is first calculated by the analytical method given in detail in Appendixes C through G. The soil properties and the object geometry are entered as inputs to the computer program according to the format. The force increment is then selected to give the desired accuracy. The final force which causes the soil to yield and the object to totally detach from the bottom is the breakout force. This force has been found from the computer output to be slightly larger than 01,000 pounds.

If the soil is considered a pure elastic material, then the breakout force may be estimated from the photoelastic model data. Based on model study theorem, we have

$$P = \frac{F_m L_r B_r (\tau_{max})}{L_m B_m (\tau_{max})_m}$$

where: m = model

F = breakout force

L = length of parallelopiped

B = width of parallelopiped

τ_{max} = maximum shear stress or strength

In this case

F_m	= 6.14 pounds	L	= 95 feet
L_m	= 0.75 inch	B	= 4 feet
B_m	= 0.25 inch	τ_{max}	= 0.6 psi
$(\tau_{max})_m$	= 11.5 psi		

Substituting these values in the equation we obtain

$$F = \frac{6.14(95)(4)(144)(0.6)}{0.75(0.25)(11.5)} = 93{,}500 \text{ pounds}$$

The Poisson's ratio for the model material is 0.46. The photoelastic model study is discussed in Appendix H.

The breakout force is also calculated from the empirical formula

$$F = 0.20\, q_u\, A_{max}\, e^{-R(t - t_o)}$$

where $q_u = 2.85[1 + (B/L)]\, q_u$

In this problem

A_{max}	= 95(4)(144) in.^{2} = 54,900 in.^{2}	B	= 4 feet (width of parallelopiped)
t_o	= 260 minutes	L	= 95 feet (length of parallelopiped)
t	= 0 min (instant breakout)	q_u	= 0.6 psi
R	= 0.0054		

where q_u is the unconfined compressive strength and is assumed to be equal to the yield strength in simple shear.

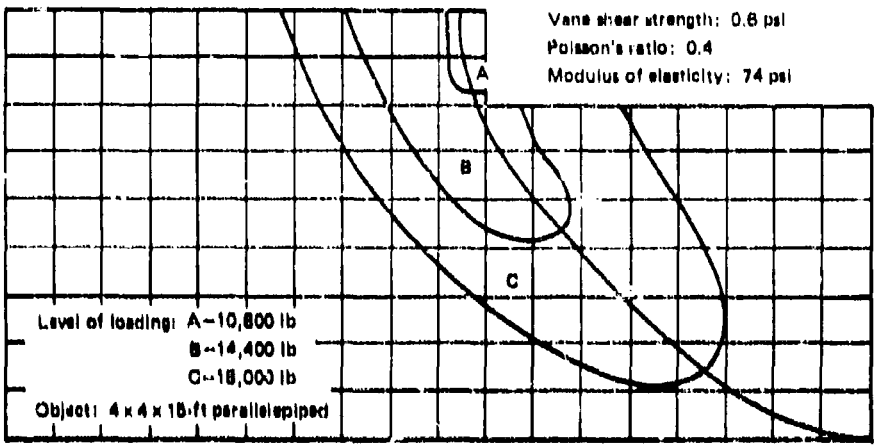

Figure 19. Propagation of plastic straining with increasing load levels.

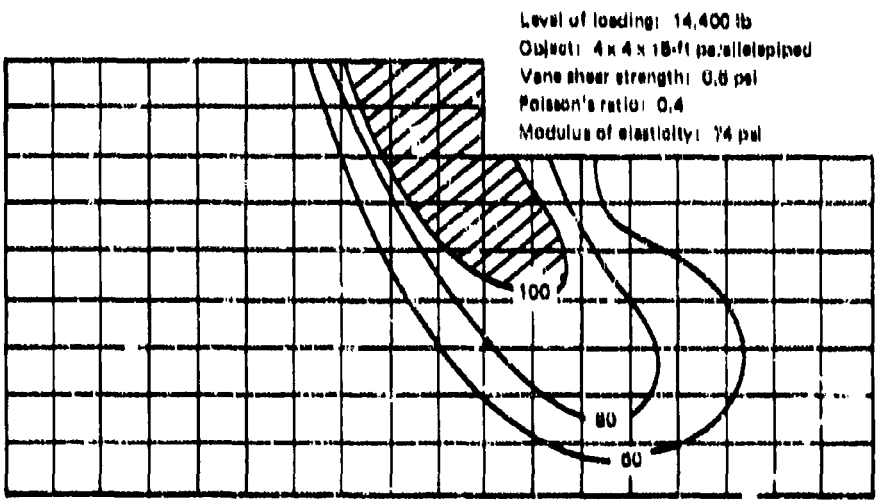

Figure 20. Distribution of yield ratio percentiles for given level of loading.

Substituting these values in the empirical formulae, we have

$$q_d = 2.85[1 + (4/95)](0.6) = 1.79 \text{ psi}$$

Thus $F = 0.20(1.79)(54{,}900)e^{-0.0054(0-260)} = 80{,}000$ pounds

Thus, comparable predictions of the breakout force for zero elapsed time according to the theoretical and empirical approaches are 91,000 and 80,000 pounds, respectively.

The theoretical procedure considers neither the effects of remolding or the increase in strength due to consolidation. In the San Francisco Bay tests (upon which the empirical constants were determined), the maximum bearing loads were very high, much higher than the capacity of the soil near the surface to support such loads. Thus, the soil in the immediate vicinity of the test object was disturbed and remolded to a considerable degree. Moreover, the object penetrated a certain distance until the bearing loads were reduced to a level within the capability of the soil to support the imposed loads. There is a natural increase in strength with depth due primarily to an increase in bulk density and a decrease in water content. However, the strength of the soil is also affected by the presence of the object in two opposing ways. One, referred to previously, is the reduction in strength due to remolding. The other is the gain in strength due to consolidation. Both effects occur on vastly different time scales. The loss in strength due to remolding takes place instantaneously, whereas the gain in strength due to consolidation is a long-term process depending initially to a large extent on the permeability of the soil.

It seems likely that for a given object two worst situations are possible. One, termed the shallow-penetration case, occurs when the soil has a high shear strength which is almost but not quite matched by the imposed bearing loads. This ensures a close bonding of the object skin surface to the sedimentary layer without inducing a strength reduction in the soil. The other, termed the deep-penetration case, occurs when penetration has been so deep that the volume of displaced soil becomes sufficiently large so as to completely dominate the breakout process. The latter situation is not to be confused with the volume of material lying between the failure surface and the object boundary, which is a function of the gross dimensions of the object. We are concerned here with a given geometry.

In the theoretical approach, the computational scheme permits loads of any magnitude to be applied to any or all mass points. Again, in the cited example, equal loads were applied to the mass points located on the boundary geometry. Thus, unequal relative movement between the mass points on the boundary are permitted, whereas in fact, such unequal movements are realized only for flexible membranes.

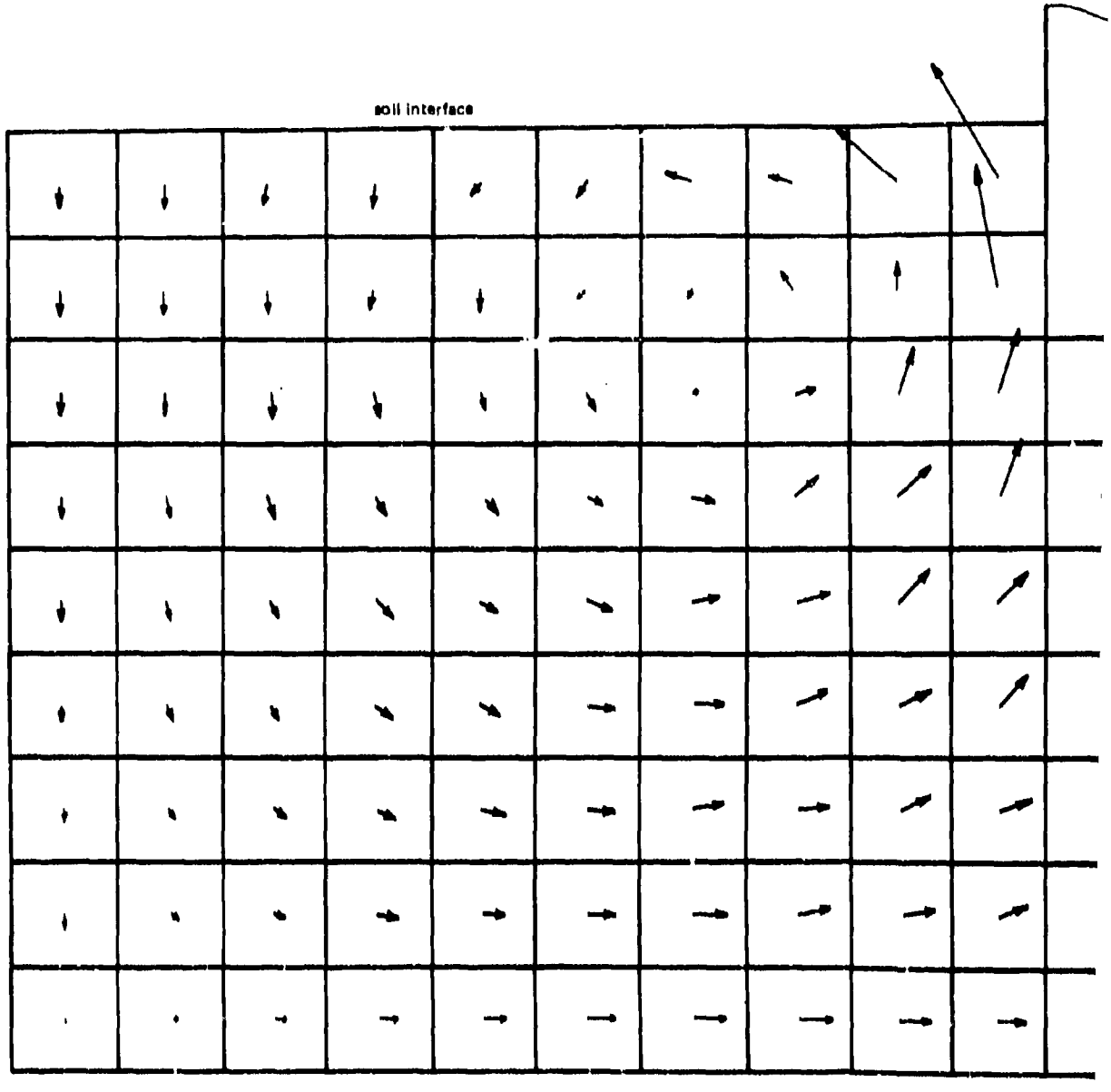

Figure 21. Displacement vector mapping of soil elements

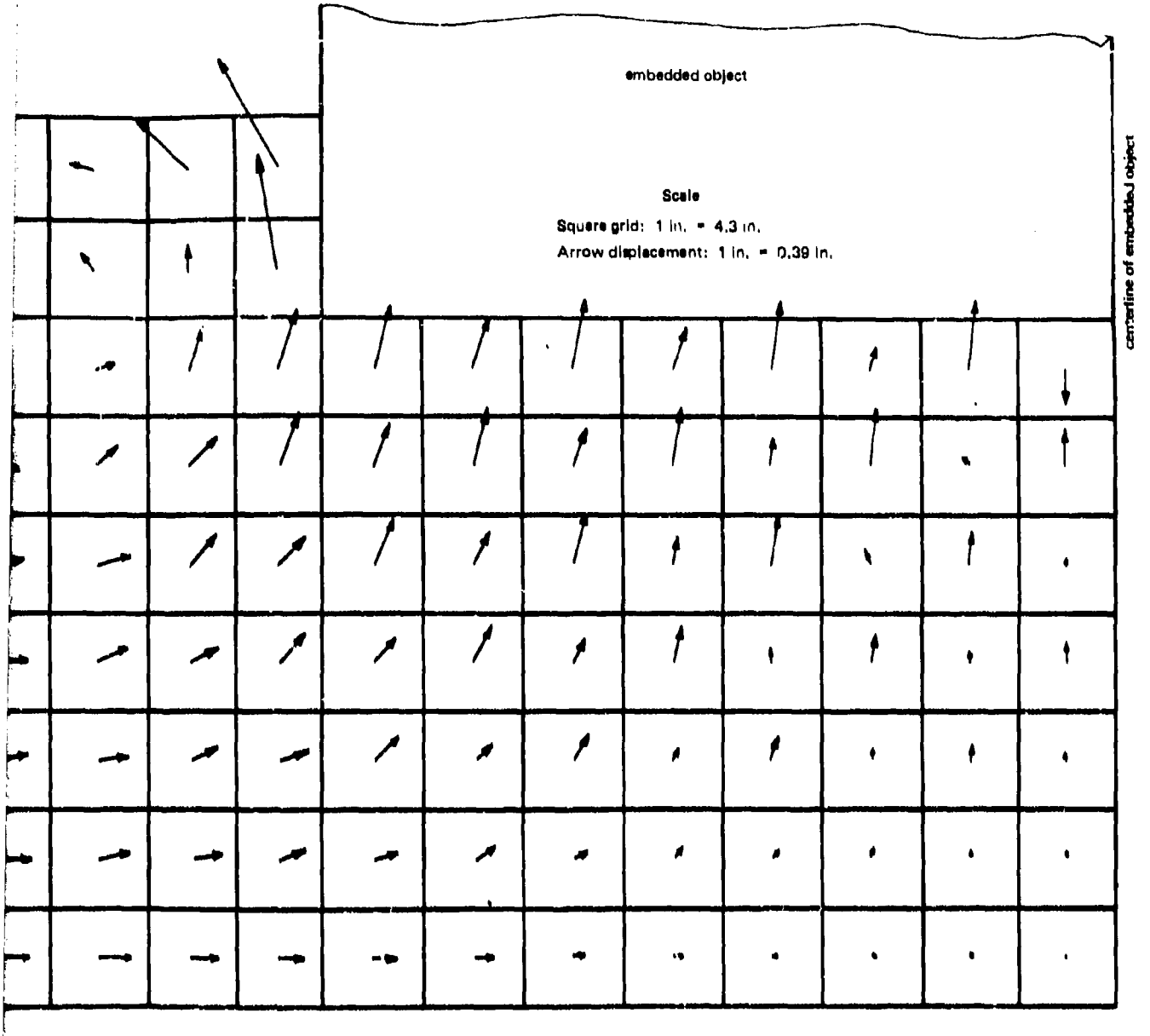

Displacement vector mapping of soil elements at first yield.

1

75

FINDINGS

1. A numerical method of predicting strains, stresses, and displacements in an elastic–perfectly plastic medium subject to loads applied to an arbitrary boundary geometry was found to be useful in developing a theoretical prediction of breakout forces.

2. A complicated computer program, which uses a lumped parameter model of the material and an iterative technique to obtain solutions, was found to be an integral part of the theoretical procedure. The program requires use of a high-speed large-memory-capacity computer.

3. The computational procedure traces the development of the stress and displacement fields in an elastic–perfectly plastic material under conditions of plane strain, with specified boundary conditions and force-controlled loading.

4. Results yielded by the computational procedure were found to be verified by separate photoelastic studies, at least within the elastic range.

5. Data from breakout tests with large specimens in San Francisco Bay were found to develop the following empirical formula:

$$F = 0.20\, A_{max}\, q_d\, e^{-0.00840(t - 260)}$$

The geometry of the breakout object seemed to have relatively little effect on the breakout force.

6. In a particular example, the breakout force requirement was estimated by the theoretical procedure to be 91,000 pounds and by the empirical procedure to be about 80,000 pounds.

CONCLUSIONS

1. The ocean bottom breakout force of an object of simple geometry can be estimated by means of an analytical method that uses numerical calculation by high-speed computers. The method takes into account the plastic behavior of soil beyond the elastic strain range.

2. The following empirical formula may be used to describe the breakout force for an ocean bottom soil:

$$F = O\, A_{max}\, q_d\, e^{-R(t - t_0)}$$

RECOMMENDATIONS

1. Whenever possible, engineers should use the analytical method outlined in this report and the appendixes to estimate the breakout force before any actual salvage operation.

2. When a computer is not available, the empirical formula should be used to determine the breakout force. The constants Q, R, and t_o can be derived from a limited number of in-situ field test data.

3. More field data should be collected to verify the analytical method for various object geometries and soil sediments.

4. More research should be conducted into methods for reducing the breakout force.

NOMENCLATURE

A	Horizontal projection of the contact area, $in.^2$
A_{max}	Horizontal projection of the maximum contact area, $in.^2$
B	Width of breakout object, feet
b	Numerical constant used to force $\underline{C} = C$ for very large t
C	Cohesion, or alternatively a measure of the vane shear strength, psi
$\underline{C}$	Effective average cohesion along the failure surface at the instant of breakout, psi
F	Breakout force, pounds
k	Constant which is a function of object size, object shape, time duration of applied force, rate force is applied, soil sensitivity, and the elapsed time which the object has been in place after the initial disturbance
L	Length of breakout object, feet
Q	Constant
q_d	Average supporting pressure provided by the soil to maintain the embedded object in static equilibrium, psi
q_u	Unconfined compressive strength, psi
R	Slope of the "failure line" when log $(F/\underline{C}A)$ is plotted versus time, t
s	Degree of soil sensitivity
t	Time allowed for breakout, minutes
t_1	Reference time related to the thixotropic behavior of a material in regaining a stated percentage of its strength after initial disturbance, minutes
t_o	Reference time, minutes
τ_{max}	Maximum shear stress or strength

BLANK PAGE

Appendix A

SITE SELECTION AND LABORATORY TESTS

by M. C. Hironaka

The field tests were carried out in San Francisco Bay about 300 yards southeast of Pier 3 at Hunters Point (Figure A-1). San Francisco Bay was selected because it is the only location on the West Coast in relatively shallow water where there exist large undisturbed deposits of fine grain sediments whose physical characteristics are reasonably similar to those of the deep ocean basins.

The specific site is one which is relatively free of the shells and debris which are generally found adjacent to piers, wharves, and sea walls, and which make such locations unsuitable for field tests. Figure A-2 shows the depth contours at the site and the soil-profile locations along which soil cores were retrieved. Figures A-3 through A-5 are schematic elevations of the soil layering based on a detailed examination of the soil cores. Table A-1 gives statistical information on the laboratory soil tests for certain selected cores.

Finally, Figure A-6 presents a typical sample of the results of triaxial tests of certain soil samples. Values of cohesion obtained from the triaxial tests appeared to agree with corresponding values obtained from vane shear tests. The bulging of the soil sample, which occurred in the latter stage of the triaxial tests, tends to make the remainder of the triaxial test results somewhat less than meaningful.

Table A 1. Test Results From Selected Core Samples

Core Sample 10

(Polar angle = 97.7°, radial distance = 961 ft)

Properties	Interval (in.)							
	12-16	24-27	36-39	48-51	72-75	84-87	96-99	108-111
Bulk wet density (pcf)	91	96	98	96	98	94	95	91
Vane shear strength (psf)	90	112	104	112	153	108	100	81
Remolded strength (psf)	11	17	23	16	24	23	24	16
Sensitivity	8,4	6,1	4,6	6,1	6,3	7,3	6,7	5,5
Original water content (%)	106,3	93,1	81,4	90,6	86,2	97,0	79,4	73,6
Specific gravity of solids	2,61	2,63	2,61	2,68	2,67	2,65	2,64	2,63
Dry density (pcf)	44	50	54	49	52	47	54	52
Void ratio	2,73	2,30	2,02	2,32	2,32	2,48	2,06	2,13
Porosity (%)	73,2	69,7	66,9	69,9	69,9	71,3	67,3	68,1
Saturated void ratio	2,83	2,44	2,13	2,49	2,27	2,67	1,99	1,94
Liquid limit (%)	73	64	62	73	66	62	64	64
Plastic limit (%)	40	33	28	35	33	29	30	30
Plasticity index	33	31	34	38	33	43	34	34
Liquidity index	207	190	196	161	169	134	134	128
Compression index	,67	,49	,47	,67	,60	,66	,48	,49

Core Sample 14

(Polar angle = 90,0°, radial distance = 741 ft)

Properties	Interval (in.)							
	12-16	24-27	36-39	60-63	72-75	84-87	96-99	108-111
Bulk wet density (pcf)	94	92	97	98	93	96	100	98
Vane shear strength (psf)	68	82	103	101	141	113	407	97
Remolded strength (psf)	11	17	18	19	24	20	46	8
Sensitivity	6,1	4,8	5,7	5,3	6,0	5,6	9,0	4,8
Original water content (%)	109,6	100,6	88,7	83,7	86,6	86,1	83,7	80,6
Specific gravity of solids	2,69	2,66	2,71	2,75	2,68	2,69	2,66	2,72
Dry density (pcf)	46	46	51	53	47	52	51	54
Void ratio	2,67	2,61	2,30	2,19	2,50	2,26	1,71	2,12
Porosity (%)	72,7	72,3	69,7	68,7	71,7	69,4	63,1	68,0
Saturated void ratio	2,84	2,67	2,40	2,28	2,66	2,31	1,69	2,19
Liquid limit (%)	80	72	67	66	77	64	68	68
Plastic limit (%)	43	34	31	31	38	30	36	36
Plasticity index	38	38	36	34	39	34	32	32
Liquidity index	200	176	172	164	149	227	60	138
Compression index	,63	,68	,59	,54	,60	,38	,52	,62

Continued

Table A 1. Continued

Core Sample 17

(Polar angle = 110.2°, radial distance = 495 ft)

Properties	Interval (ft.)							
	0-3	12-15	24-27	36-39	48-51	60-63	72-75	84-87
Bulk wet density (pcf)	94	91	94	90	89	91	95	94
Vane shear strength (psf)	83	81	90	92	113	94	120	93
Remolded strength (psf)	16	16	14	17	16	14	21	17
Sensitivity	5.5	5.0	6.4	5.5	7.1	6.7	5.7	5.5
Original water content (%)	97.3	104.0	91.1	112.9	114.6	99.5	81.5	88.0
Specific gravity of solids	2.84	2.87	2.88	2.86	2.89	2.87	2.88	2.86
Dry density (pcf)	66	46	49	42	42	46	59	60
Void ratio	1.94	2.74	2.47	2.94	3.04	2.66	2.17	2.34
Porosity (%)	66.0	73.3	70.3	74.6	75.2	72.7	68.5	70.0
Saturated void ratio	1.78	2.78	2.42	3.01	3.09	2.66	2.16	2.34
Liquid limit (%)	46	71	67	68	67	63	64	70
Plastic limit (%)	30	32	33	41	41	36	32	29
Plasticity index	16	39	34	47	46	47	32	41
Liquidity index	291	187	169	169	194	136	140	128
Compression index	.31	.66	.52	.71	.70	.66	.61	.62

Core Sample 18

(Polar angle = 91.1°, radial distance = 417 ft)

Properties	Interval (ft.)							
	12-15	24-27	36-39	48-51	60-63	72-75	84-87	96-99
Bulk wet density (pcf)	87	93	93	91	93	91	91	93
Vane shear strength (psf)	82	70	86	84	100	143	100	101
Remolded strength (psf)	9	12	14	13	22	20	18	17
Sensitivity	9.0	6.0	6.4	6.4	4.6	7.1	5.6	5.9
Original water content (%)	117.8	104.5	103.0	93.0	90.8	83.0	94.5	89.1
Specific gravity of solids	2.83	2.90	2.88	2.86	2.88	2.86	2.88	2.70
Dry density (pcf)	40	46	46	48	48	51	47	48
Void ratio	3.01	2.67	2.72	2.62	2.64	2.36	2.67	2.60
Porosity (%)	77.0	72.0	73.1	70.7	71.0	69.3	72.0	71.4
Saturated void ratio	3.01	2.71	2.86	2.60	2.64	2.31	2.61	2.40
Liquid limit (%)	80	70	69	72	70	69	64	70
Plastic limit (%)	40	35	31	31	31	34	40	30
Plasticity index	40	40	40	41	39	35	43	40
Liquidity index	189	173	166	164	166	140	126	141
Compression index	.77	.60	.66	.60	.64	.61	.66	.62

Continued

Table A-1. Continued

Core Sample 19
(Polar angle = 98.0°; radial distance = 692 ft)

Properties	Interval (in.)							
	12-15	24-27	36-39	48-51	72-75	84-87	96-99	108-111
Bulk wet density (pcf)	92	106	91	92	91	93	96	94
Vane shear strength (psf)	83	146	79	100	124	129	124	130
Remolded strength (psf)	13	16	18	28	29	31	46	10
Sensitivity	6.3	9.1	4.4	3.7	4.3	4.1	2.7	13.0
Original water content (%)	102.0	68.1	107.8	84.5	94.7	87.6	82.3	83.6
Specific gravity of solids	2.66	2.69	2.66	2.66	2.66	2.67	2.66	2.66
Dry density (pcf)	46	67	44	50	47	50	53	51
Void ratio	2.02	1.62	2.79	2.34	2.63	2.36	2.16	2.24
Porosity (%)	72.4	60.3	73.6	70.1	71.7	70.3	68.2	69.1
Saturated void ratio	2.70	1.80	2.87	2.25	2.82	2.34	2.19	2.21
Liquid limit (%)	74	42	69	69	82	77	72	76
Plastic limit (%)	36	22	40	33	38	35	36	36
Plasticity index	38	20	43	36	44	42	36	39
Liquidity index	176	180	157	143	128	124	127	123
Compression index	.57	.29	.66	.53	.65	.61	.66	.64

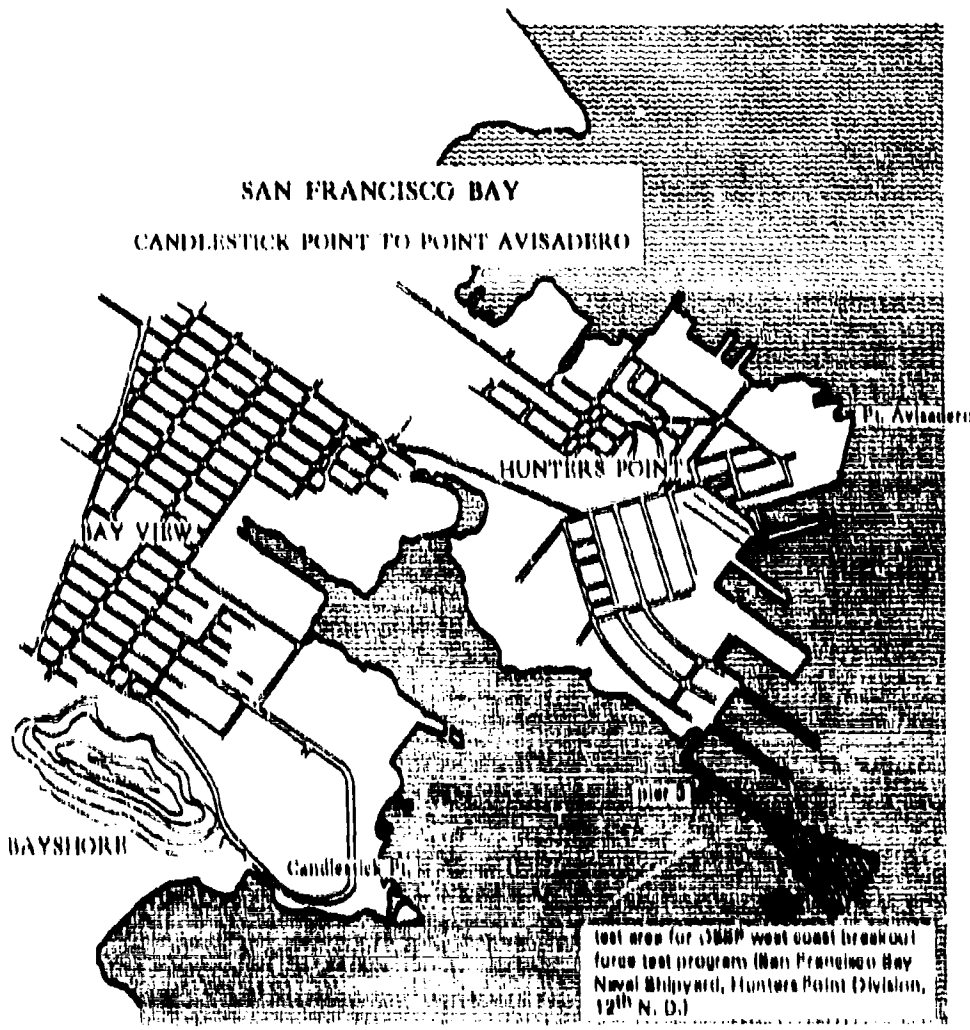

Figure A-1. Location of test site.

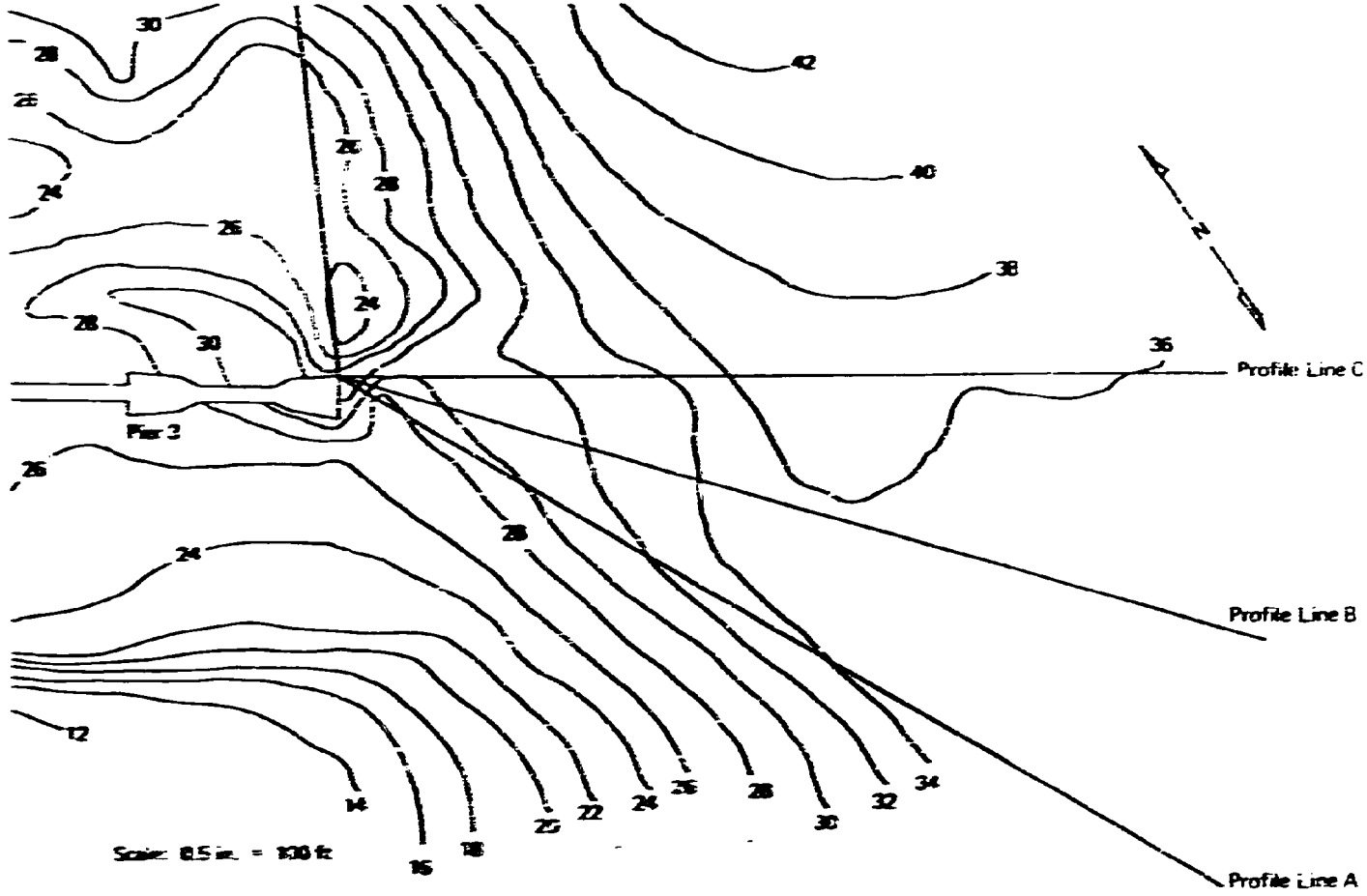

Figure A-2. Depth contours at test site.

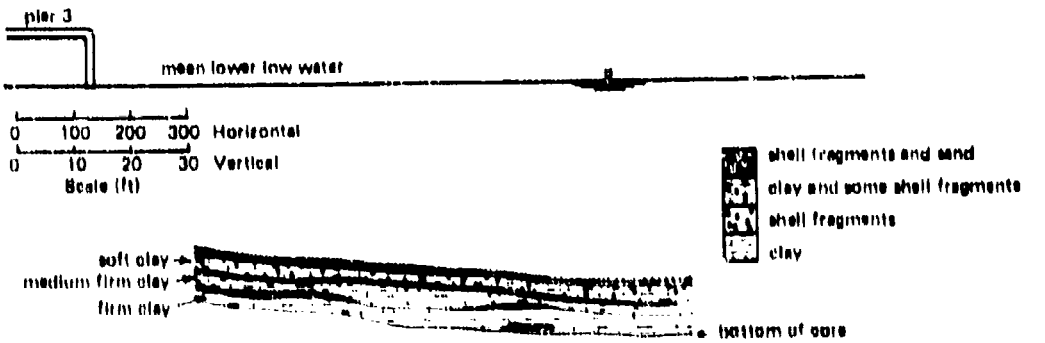

Figure A-3. Schematic of soil layering along profile A.

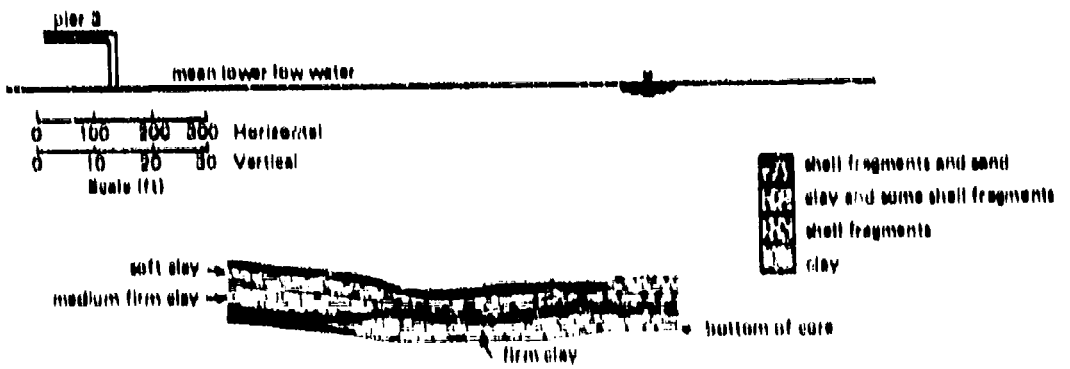

Figure A-4. Schematic of soil layering along profile B.

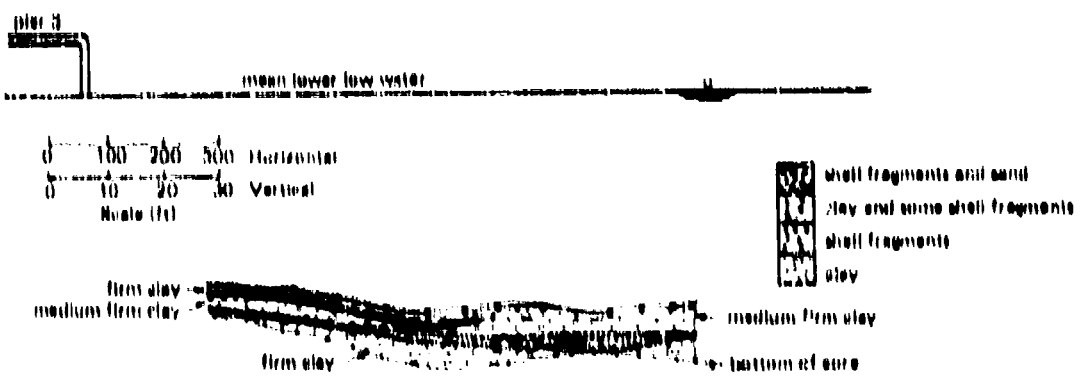

Figure A-5. Schematic of soil layering along profile C.

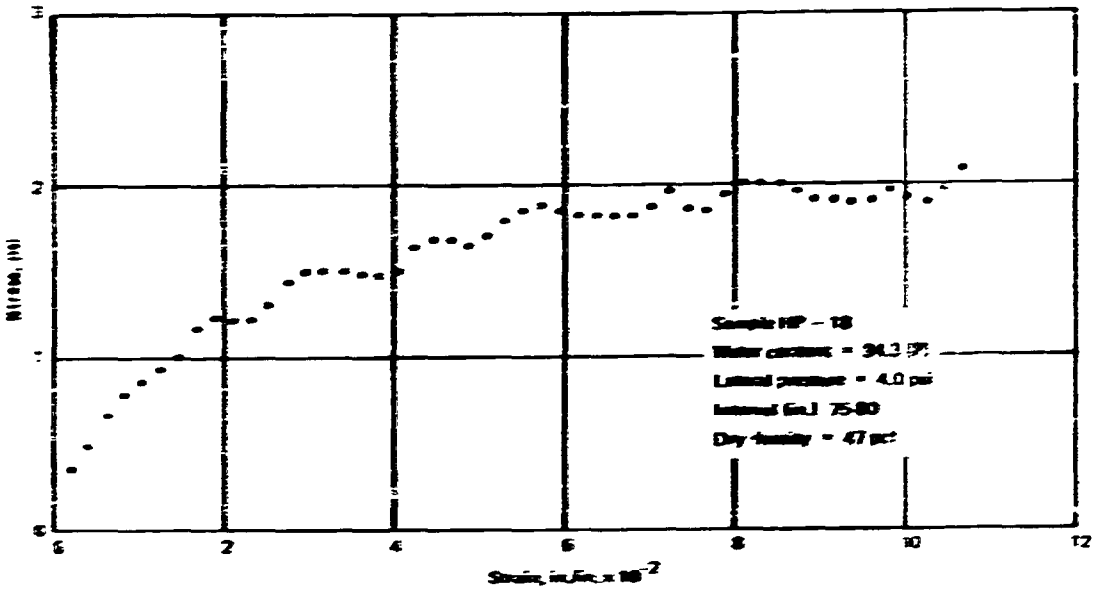

Figure A-6. Typical sample of results of triaxial tests (core sample 18).

Appendix B

LITERATURE SURVEY OF BODY SHAPES AND DIMENSIONS

by S. J. Muga

A thorough review of the literature on existing body shapes and dimensions of possible interest to the breakout force problem was conducted for the purpose of establishing specific guidelines for designing the experimental test program. One large class of body shapes, namely anchors, was excluded from this study. It was felt that the irregular nonformalized shapes presented by anchors constituted a complete study in itself and that there would be little to gain from the attempted extrapolation of data available from tests on anchor shapes to other shapes.

Although it was known that the shapes of certain classified objects would be of interest, they also were excluded in order to maintain a wide dissemination and distribution of the results of the test program. The study was focused on two categories of body shapes. The first category included full-size U. S. Navy submarines, the various types of which are indicated in Table B-1. All of these vessels have essentially a cylindrical hull. However, at least one of the target submarines (SST) has a prismatic rectangular keel attached to the underside of the hull. The second category included the growing family of deep submergence vehicles, summarized in Table B-2. It is to be noted that the DOLPHIN (AGSS-555) is listed in both categories. However, data on the DOLPHIN pertinent to the breakout force problem did not appear in the open published literature. Of the other vessels, the MOHAY, NR-1, and PX-15 seem to fall into the larger class of deep submergence vehicles having approximately the same contact area. For some vessels, such as the ALUMINAUT and ALVIN, data on surface contact area was not readily available.

The shapes of the bottom contact members of the deep submergence vehicles varied from ellipsoids and prisms (rectangular and cylindrical) having large length-to-diameter ratios to more compact bodies such as cones and spheres.

From the foregoing tabulations, the basic shapes, sizes, and weights were selected for the test program. Sizes and weights were selected on the basis of (1) bearing load similar to that which might be experienced in the worst possible situation, (2) surface contact area, and (3) available weight-handling capability.

Dimensions and additional descriptions of the test objects are shown in Table B-3.

Table B-1. Selected Data on U.S. Navy Submarines

Symbol	Class	Name	Number	Displacement (tons)			Length (ft)	Beam (ft)
				Minimum Surface	Maximum Surface	Submerged		
SSBN	Lafayette	--	31	6,650	7,250	8,250	425	33
SSBN	Ethan Allen	--	5	6,,300	,900	7,900	410-1/2	33
SSBN	G. Washington	--	5	5,400	5,900	6,700	381-2/3	33
SSN	--	Nautilus	1	3,215	3,532	4,091	320	28
SSN	--	Seawolf	1	3,470	2,721	4,287	3,0	28
SSN	Skate	Skate & Sargo	2	2,270	2,555	2,350	200	25
SSN	Skate	Swordfish & Scorpion	2	2,270	2,552	2,881	200	25
SSN	Skipjack	--	6	2,850	3,070	3,500	252	32
SSN	--	Triton	1	5,662	5,940	7,781	447-1/2	37
SSN	Thresher	--	22	3,526	3,750	4,310	278-1/2	31-2/3
SSN	Sturgeon	--	22	--	4,140	4,630	292-1/4	--
SSN	Narwhal	--	1	--	--	--	--	--
SSN	--	Halibut	1	3,002	3,845	4,895	350	30
SSN	--	Tullibee	1	2,177	2,317	2,607	272-3/4	24
SS	Tang	--	4	1,650	1,870	2,380	279	27
SS	Gudgeon	--	2	1,600	1,800	2,200	269-1/6	27-1/6
SS	Sailfish	--	2	2,048	2,426	3,170	300-1/2	30
SS	Porter	--	1	1,800	1,870	2,372	298-1/2	27-1/6
SS	Barbel	--	3	1,700	2,150	2,640	219	29
SS	Guppy III	--	9	1,850	1,975	2,540	319-5/6	27
SS	Guppy IIA	--	16	1,800	1,840	2,445	306	27
SS	Guppy II	--	14	1,800	1,870	2,420	307-1/2	27-1/3
SS	Guppy IA	--	10	1,847	1,870	2,440	308	27
SS	Fleet Snorkel	--	10	1,800	1,820	2,400	312	27-1/3
SS	Tench	--	1	1,490	1,840	2,400	312	27-1/3
SS	Balao	--	1	1,480	1,810	2,400	312	27
SS	Gato	--	3	1,810	1,870	2,420	309-1/3	27-1/3
AGSS	--	Grayback	1	2,310	2,671	3,000	322-1/2	[illegible]
AGSS	--	Growler	1	2,200	2,044	3,010	322-1/2	27-1/6
AGSS	Con. Balao	Barbero	1	1,826	1,816	2,426	311-1/2	27
AGSS	Con. Gato	Tunny	1	1,826	1,816	2,426	311-3/4	27
AGSS	Albacore		1	1,200	1,517	1,810	203-3/4	27-1/3
AGSS	Con. Gato		2	1,826	1,816	2,426	311-1/4	27
AGSS	Con. Gato		4	1,760	1,800	2,500	343	27
AGSS	Con. Balao	Dove	1	1,826	1,900	2,250	314-3/4	27
AGSS	Con. Balao	Manta	1	1,826	1,900	2,366	311-1/2	27
AGSS		Dolphin	1					
AGSC	Test	Barracuda	1	760	800	1,100	100	26
AGSS	1	Macdonald & Marlin	2	270	300	340	141-1/6	14
AGSS	Midget		1	31		35	49-1/4	7
APSS	Con. Balao		2	1,826	1,816	2,426	311-1/2	27
ADSS	Con. Balao	--	1	1,760	2,000	2,250	311-1/2	27

Table D-1. Deep Submergence Vehicles

Name	Builder and or Owner	Operating Depth (ft)	Weight (tons)		Dimensions (ft)		
			Dry	Displacement Submerged	Length	Width or Diameter	Height
Aluminaut	Electric Boat/Reynolds Aluminum	15,000	73.2	81.1	30		9.6
Alvin	Office of Naval Research, Woods Hole	6,000	13		10.6		
AquaSub 300	American Submarine	300	1.1		2.2		1.6
AquaSub 600	American Submarine	600	1.75		3.9		
Archimede	French Navy	unmanned	61	105.0	50	10	12
Asherah (Star II)	Electric Boat/Univ. of Penn. Museum	600	4.25	4.35	4		0.5
Auguste Piccard	Swiss National Exhibition	2,500	164.37	218.8			
Beaver MK III	North American Aviation	1,000	7.5		8.0	6.0	
Benthos V	Lear Siegler Inc.	600	2.1		11.3	6	
Submarine PC3A	Perry Submarine Builders Inc.	300	2.4	3.0	8		0.3
Submarine PC3B	Perry Submarine Builders Inc.	600	3.13	3.30	8.3		0.2
Deep Diver	Ocean Systems Inc	1,350	0.20		6.4	2.4	
Deep Jeep	U.S. Naval Ordnance Test Station	2,000	d			3.0 diam	1.75
Deep Star 2000	Westinghouse	2,000	d				
Deep Star 4000	Westinghouse	4,000	9.6				
Deep Star 12000	Westinghouse	12,000	9.0				
Deep Star 20000	Westinghouse	20,000	11.0				
Diving Saucer SP-300	Westinghouse	1,000	0.20		6.0	4.7	
Diving Saucer SP-1200	Westinghouse	4,000	6				
Dolphin AGDS (4th)	U.S. Navy		200	0.26	162	10	
DOWB	General Motors	6,000	7.13			8 diam	0.6
DSV 1 (Modified Px-15)	Ortomman Ocean Systems	2,000					
Moray	U.S. Naval Ordnance Test Station	6,000	10	10	30	6.1	
NR-1 (Nuclear)	U.S. Navy Special Projects Office		297				
Pisces	International Hydrodynamics, Canada	6,000	6.6				
PX-15	Ortomman Ocean Systems	2,000	1.80		40.6	6.9	8
SeaRover VI	General Mills	6,000	0.4		8.0	0.26	0.26
Star I	Electric Boat	200	1.4		11		
Star III	Electric Boat	2,000	9		43		6.6
Trieste II	DEEP to Sold for Cost						
(Deep Submergence)		20,000	60	220		7	
(Deep Submergence)		estimated	60	330		7.4	
Yamato	Mitsubishi Heavy Industries, Japan	1,000	4.0		20.4	10.2.4	6.0

Table B-2 Deep Submergence Vehicles

...n)	Bottom Contact Member					Additional Features	Status
	Dimensions (ft)			Approximate Geometric Shape	Approximate Horizontal Contact Area (ft^2)		
...tcrement merged	Length	Width or Diameter	Height				
11.1	30		2.5	prism (rectangle)			operational
	10.6					after-body can be jettisoned	operational
	2.2		1.5			releasable lead keel	operational
	3.9					releasable lead keel	operational
15.0	20	1.8	1.2	prism (rectangle)	40.4		operational
0.00	4		0.5			releasable skid-300 pounds	operational
0.5							operational
	0.3	0.0		prism (rectangle)	30.3		operational
	11.3	6		conical	64		operational
3.3	4		0.3			droppable lead keel-180 pounds	operational
3.00	0.3		0.2			droppable keel-200 pounds	operational
	0.4	2.4		prism (cylinder)	14.5		operational
		3.0 diam	1.75	vertical cylinder	9.4		operational
							under construction
				segment of sphere			operational
	0.6	4.7		ellipsoid			
20	162	10		ellipsoid	4 000		under construction
		8 diam	0.8	prism cylinder	20		under construction
							design
10	33	6.3		ellipsoid	200		operational
				prism (rectangle)	333		under construction
							operational
	40.5	5.2	1	prism (rectangle)	210		
	8.6	0.75	0.25	prism (rectangle)	6.4	2 skids	
	1.6					telescoping keel (2 cm. legs)	operational
	4.0		0.5				under construction
20		7		hemisphere	77		operational
20		7.2		hemisphere	81.5		operational
	20.4	10.2.4	6.8	prism (rectangle)	61	telescoping keel (1,070 cm.)	operational

Table B.3 Dimension of Test Objects

Test Objects	Weight in Air (lb)	Weight in Water (lb)	Dimensions (in.)
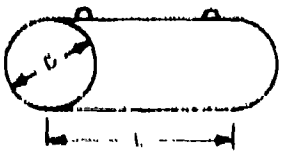	40,250	21,750	D = 64 L = 211.5
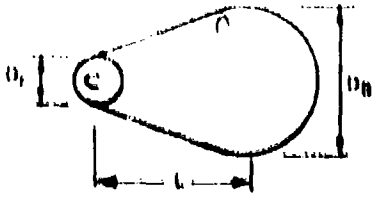	22,250	10,600	D_1 = 21 D_B = 76.5 L = 103
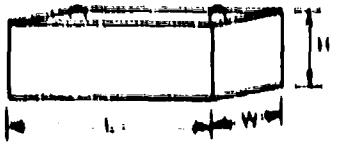	38,800	22,200	L = 186 W = 40 H = 40
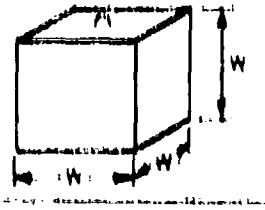	36,600	20,000	W = 74
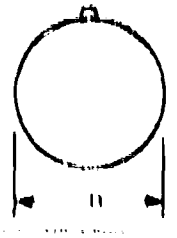	23,500	14,100	D = 76.0
	34,600	10,200	D = 40 L = 204

Appendix C

THEORETICAL ANALYSES

Table of Contents

Appendix C

THEORETICAL ANALYSIS

by B. J. Muga and W. D. Atkins

INTRODUCTION

The cost of full scale breakout tests, with varying test specimens and soil properties, makes it attractive to formulate a less expensive method of predicting breakout forces. This appendix reports on a theoretical study which is based on a numerical method of predicting bottom breakout forces. It is intended that confidence can be developed in the method by calibrating the analytical model to a relatively small number of full-scale field tests. Thereafter, the analytical method can be used to predict breakout under a very wide range of circumstances.

The following sections present in detail pertinent background information, describe the numerical method, develop the constitutive equations from the theory of perfectly plastic solids, and indicate how these equations can be combined to provide a systematic numerical solution of contained plastic flow problems. Finally, some example problems are given to demonstrate the use of the computer program.

BACKGROUND

Harper and Ang (1963) have developed a systematic numerical procedure for determining the displacements, strains, and stresses within a plane continuum wherein certain regions have been strained beyond an elastic yield limit. As adapted for use in this study, the procedure is restricted to static problems with plane strain conditions. The material of the continuum is considered to be isotropic, elastic - perfectly plastic and the problems are solved for continuously increasing external loads. Unloading from a plastically strained state is not considered.

Harper and Ang state that "the numerical procedure is essentially a relaxation technique applied to a discrete physical model composed of suitably arranged stress points and mass points." Once the external loading has been raised to a sufficiently high level, the more highly stressed regions of the model begin to yield and flow plastically. The initiation of yielding is determined by the Mises-Hencky yield criterion. Thereafter, yielded regions are assumed to obey the plastic stress-strain relations postulated by the Prandtl-Reuss theory.

Use of the discrete model permits a problem in continuum mechanics with an infinite number of degrees of freedom to be replaced by a corresponding problem in particle mechanics having a finite number of degrees of freedom. The basic advantage of such a technique is that it makes possible the solution of problems not easily solved by mathematical analysis, particularly problems involving partial loadings and complicated boundary conditions. This is of considerable importance to the breakout force problem since many different-shaped objects are to be retrieved under a variety of embedment conditions. The basic disadvantage of the use of a discrete model, as pointed out by Harper and Ang, is its very finiteness; that is, stresses and displacements are determined only at a finite number of points. Hence, frequently the finite model can furnish only a rough quantitative measure of the true but unknown solution in the continuum.

To gain some notion of the accuracy of the model, Harper and Ang solved a problem in plane elasticity using an analytical solution and compared the results to those from the numerical solution using the model. The results from the two solutions agreed very well.

Whitman (1964) has considered the use of the numerical method developed by Harper and Ang for analyzing two-dimensional and three-dimensional boundary value problems involving soil.* Whitman concluded that immediate progress with the problem of multidimensional contained plastic flow would result from application of the numerical method, and that the use of the theory for a perfectly plastic solid permits a first step in the development of procedures for analyzing contained plastic flow in soils.

Christian (1966) has used the numerical method developed by Harper and Ang to investigate the stress and displacement fields for an elastic porous material under conditions of plane strain with rectangular boundaries and force- or displacement-controlled loading.

Whitman and Hoeg (1965) have examined the performance and accuracy of the Harper and Ang numerical method and used it to analyze the development of the plastic zone beneath a strip footing resting on an elastic-perfectly plastic foundation material. The computed results for the flexible and rigid strip footings analyzed in their study showed the gradual development of the plastic zone, the corresponding displacement fields, and the accumulation of footing settlements as the full shearing resistance of the foundation material was mobilized. The load settlement curves approached asymptotically the bearing capacity, which was in agreement with the ultimate load predicted by plastic theory.

* In a boundary value problem, one seeks to determine the response (that is, stresses, strains, displacements) of a system (that is, a deformable mass of soil) to a specified set of boundary conditions (that is, applied loads or displacement).

While the medium properties in the study performed by Harper and Ang corresponded to steel rather than soil, and therefore the conclusions are based on the behavior of such an idealized "foundation" material, the results do provide valuable insights into the behavior attendant on the loading of soils. The lumped parameter model can tolerate any type of stress-strain relationship, and future studies can introduce stress-strain properties and yield phenomena better representing soil materials.

Although the basic calculations used in the Harper and Ang numerical method are very simple, the large number of calculations required to solve even a simple practice problem preclude the use of hand calculations. Therefore the entire procedure for handling plane strain problems of contained plastic flow in an elastic–perfectly plastic continuum has been coded in FORTRAN II for use on the IBM 7094 digital computer. The computer program used in this study is an extensive revision of a program written for Whitman (1964) at the Stanford Research Institute. By revising the program, compilation and execution time has been reduced, some logical errors have been corrected, and the output has been reorganized to facilitate its use.

This appendix presents the numerical method developed by Harper and Ang and documents the revised Whitman program. No attempt has been made to extend the theory.

LUMPED PARAMETER MODEL

Harper and Ang (1963) note that there are very few solutions for problems of contained plastic flow. That is, there are very few solutions which trace the development of the stress and strain patterns in a body of material from the time that yielding first develops at some point in the material until the deformations finally increase beyond all bounds.

One criterion that has been used in the selection of a mathematical model is that there be mathematical consistency between the finite difference equations governing the behavior of the model and the differential equations governing the behavior of the continuum. This means that the equations for stresses, strains, equilibrium, and compatibility, which are derived directly from the model, should be the same as a set of finite difference equations of the corresponding differential relations governing the continuum. Harper and Ang point out that if this requirement is met, the requirement of equal deformations in the model and corresponding continuum will be automatically satisfied. The model proposed by Harper and Ang, and used herein, satisfies this criterion.

Description of the Model

Figure C-1 shows the lumped parameter model used in the procedure developed by Harper and Ang. This model consists of mass points and stress points.

The mass of the material is assumed to be concentrated at the mass points and the strains within the material are given in terms of the displacements of the mass points. Each of the mass points is connected through the stress points to the neighboring mass points. Three components of stress and strain are defined at each stress point (two normal components and a shear component). Displacements in the continuum are defined only at the mass points while stresses and strains are defined only at the stress points. In the model representation, springs are shown at the stress points for conceptual purposes only. The stresses at each stress point are related to the movements of the four surrounding mass points using a finite difference version of the stress-strain laws for the continuum. No attempt is made to define a set of springs whose action would be equivalent to the action of the continuum.

Actual computations are carried out in terms of the forces F_x, F_y, F_{xy} at each stress point (Figure C-2). These forces are equal to the corresponding components of the stress tensor multiplied by the appropriate fraction of the grid spacing.

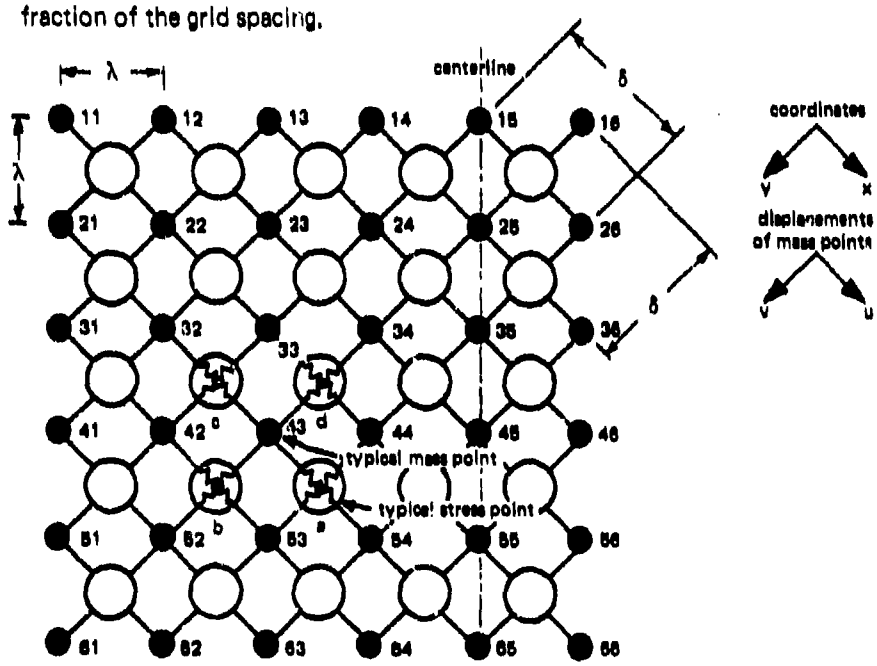

Figure C-1. Lumped parameter model for continuum.

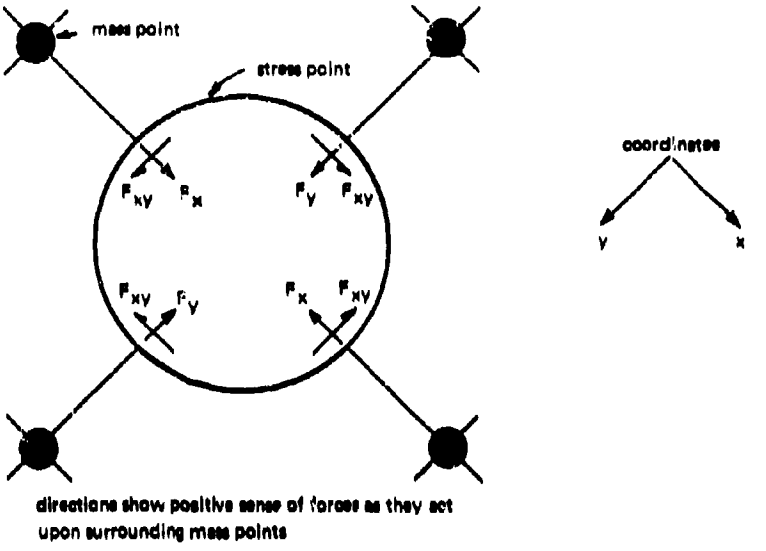

Figure C-2. Forces at stress point of lumped parameter model.

Harper and Ang and Whitman note that there are two important advantages of the model configuration. First, all elements of the strain and stress tensors are defined at the same point. This is especially important in extending the use of the model to problems of plasticity. Second, the horizontal and vertical boundaries of the model contain only mass points. Thus, boundary conditions given in terms of either external loads acting on the mass points or specified displacements of the mass points can be applied with equal ease.

Relation of the Model to the Finite Difference Equations of the Continuum

The notation and example presented by Harper and Ang are used to illustrate the relation of the numerical model to the finite difference equations of the continuum. The following notation is used:

1. Superscript letters refer to stress point locations.
2. Subscript letters x and y refer to the direction of the axes.
3. Subscript numbers refer to mass point locations.
4. Displacement components in the x and y directions are given by u and v, respectively.
5. Sign convention is that shown in Figure C-2.

For Figure C-1 the components of the strains at a typical stress point, a, are defined as follows:

$$\epsilon_x^a = \frac{u_{54} - u_{43}}{\delta}$$

$$\epsilon_y^a = \frac{v_{53} - v_{44}}{\delta} \qquad \text{(C-1)}$$

$$\gamma_{xy}^a = \frac{u_{53} - u_{44}}{\delta} + \frac{v_{54} - v_{43}}{\delta}$$

where ϵ = normal strain

γ = shear strain

δ = diagonal distance between mass points

These strains, which are derived directly from the model, are identical to the finite difference expressions for the differential strain-displacement relations from the classical theory for plane continua under small deformations:

$$\epsilon_x = \frac{\partial u}{\partial x} \quad \epsilon_y = \frac{\partial v}{\partial y} \quad \gamma_{xy} = \frac{\partial u}{\partial y} + \frac{\partial v}{\partial x}$$

Using the sign convention of Figure C-2, the equation of equilibrium in the x direction for a typical interior mass point, 43, is

$$(F_x^a - F_x^c) + (F_{xy}^b - F_{xy}^d) + \frac{X\delta^2}{2} = 0 \qquad \text{(C-2)}$$

where X = body force per unit volume

F = component force at stress point

The volume of a parallelepiped of unit thickness and area $\lambda^2 = \delta^2/2$ is considered concentrated at each mass point. If the thickness of the model is taken as unity in the z direction, forces at the stress point a can be obtained from the stresses:

$$F_x^a = \sigma_x^a \cdot \frac{\delta}{2} \cdot 1$$

$$F_y^a = \sigma_y^a \cdot \frac{\delta}{2} \cdot 1 \qquad \text{(C-3)}$$

$$F_{xy}^a = \tau_{xy}^a \cdot \frac{\delta}{2} \cdot 1$$

Using Equations C-2 and C-3, the following equation of equilibrium, in terms of stresses, is obtained:

$$\frac{\sigma_x^a - \sigma_x^c}{\delta} + \frac{\tau_{xy}^b - \tau_{xy}^d}{\delta} + X = 0 \qquad \text{(C-4a)}$$

A similar equation is obtained for the y direction:

$$\frac{\sigma_y^b - \sigma_y^d}{\delta} + \frac{\tau_{xy}^a - \tau_{xy}^c}{\delta} + Y = 0 \qquad \text{(C-4b)}$$

These equilibrium equations, C-4a and C-4b, are identical to the finite difference expressions for the differential equations of equilibrium governing the corresponding continuum:

$$\frac{\partial \sigma_x}{\partial x} + \frac{\partial \tau_{xy}}{\partial y} + X = 0$$

$$\frac{\partial \sigma_y}{\partial y} + \frac{\partial \tau_{xy}}{\partial x} + Y = 0$$

Harper and Ang state that "the strains in the model will necessarily satisfy the compatibility relation, since strain compatibility is essentially a requirement placed on the three components of strain in order to insure that they correspond to a physically possible displacement configuration. The model deals directly with displacements, and the strains are defined directly in terms of these displacements. Hence, it can be expected that the strains derived from the displacements of the model will exactly satisfy the compatibility condition."

It is also possible to express the equations of equilibrium in terms of displacements. For an elastic continuum, the stress-strain relations for plane strain, as given by Prager and Hodge (1951), are

$$\sigma_x = \frac{E}{(1+\nu)(1-2\nu)}\,[(1-\nu)\epsilon_x + \nu\epsilon_y]$$

$$\sigma_y = \frac{E}{(1+\nu)(1-2\nu)}\,[(1-\nu)\epsilon_y + \nu\epsilon_x] \qquad \text{(C-5)}$$

$$\tau_{xy} = \frac{E}{2(1+\nu)}\,\gamma_{xy}$$

where E = modulus of elasticity of the material

ν = Poisson's ratio of the material

Combining Equations C-1, C-3, and C-5, the three force components at stress point a in terms of displacements are

$$F_x^a = \frac{E}{(1+\nu)(1-2\nu)}\left[(1-\nu)\,\frac{u_{54}-u_{43}}{\delta} + \nu\,\frac{v_{53}-v_{44}}{\delta}\right]\frac{\delta}{2}$$

$$F_y^a = \frac{E}{(1+\nu)(1-2\nu)}\left[(1-\nu)\,\frac{v_{53}-v_{44}}{\delta} + \nu\,\frac{u_{54}-u_{43}}{\delta}\right]\frac{\delta}{2} \qquad \text{(C-6)}$$

$$F_{xy}^a = \frac{E}{2(1+\nu)}\left[\frac{u_{53}-u_{44}}{\delta} + \frac{v_{54}-v_{43}}{\delta}\right]\frac{\delta}{2}$$

The three expressions in Equation C-6 are Hooke's stress-strain relationships for plane strain in terms of displacements. Substitution of these and similar relations for the forces originating at the other stress points (b, c, and d) into Equation C-2 results in the following equation of equilibrium in the x direction, in terms of displacements as given by Harper and Ang:

$$\frac{E}{2(1+\nu)(1-2\nu)}\left[2(1-\nu)\,\frac{u_{54}-2u_{43}+u_{32}}{\delta^2} + (1-2\nu)\,\frac{u_{52}-2u_{43}+u_{34}}{\delta^2} + \frac{(v_{53}-v_{42})-(v_{44}-v_{33})}{\delta^2}\right] + X = 0 \qquad \text{(C-7)}$$

A similar equation exists for equilibrium in the y direction. Note that Equation C-7 is the same as a finite difference equation for the differential equation of equilibrium governing the continuum:

$$\frac{E}{2(1+\nu)(1-2\nu)}\left[2(1-\nu)\frac{\partial^2 u}{\partial x^2} + (1-2\nu)\frac{\partial^2 u}{\partial y^2} + \frac{\partial^2 v}{\partial x\,\partial y}\right] + X = 0$$

Boundary Conditions

In general, boundary conditions (for either continua or discrete models) can be of two types: either the forces acting along some boundary or the displacements on the boundary are prescribed. It has been previously noted that the model is suited to either type of prescribed condition. Some of the more common boundary conditions which may be imposed on the model are described in the following paragraphs.

Symmetric. If the continuum is known to possess symmetry about a vertical axis through a column of mass points, as shown in Figure C-1, then the boundary condition on the right edge of the model may be specified as follows:

$$\left.\begin{aligned} u_{i6} &= v_{i4} \\ v_{i6} &= u_{i4} \end{aligned}\right\} \quad i = 1,2,\ldots,6$$

Infinite. The model may be used to simulate an infinite half-space. In Figure C-1, consider the problem of imposing boundary conditions on the far-left column of mass points. For vertical loadings which are symmetric about the centerline, it has been assumed that the horizontal displacements of this far-left column are zero, and that the vertical displacements of this far-left column will be equal to the vertical displacements of the column of mass points immediately to the right of this boundary column. When these vertical and horizontal motions are resolved into displacements in the x and y directions, the boundary conditions become

$$\left.\begin{aligned} u_{i1} &= \frac{1}{2}(u_{i2} + v_{i2}) \\ v_{i1} &= \frac{1}{2}(u_{i2} + v_{i2}) \end{aligned}\right\} \quad i = 1,2,\ldots,6$$

Specified by Loading Arrangement. If an external load is to be applied to the top surface of the continuum, the model will have the appropriate concentrated loads applied to the top row of mass points. These concentrated loads may approximate a distributed load or represent actual concentrated loads.

Fixed. If it is desired to hold the base of the continuum fixed against displacement, the displacement components of the bottom row of mass points are simply set equal to zero.

These examples indicate the manner in which boundary conditions are prescribed for the model. A variety of practical, significant conditions can be conceived, but an extensive treatment of possible boundary conditions is beyond the scope of this study.

CONSTITUTIVE EQUATIONS FROM THE THEORY OF PERFECTLY PLASTIC SOLIDS

Prager and Hodge (1951) have provided a careful definition for the perfectly plastic solid.

Any constitutive relationship of the theory of plasticity may be divided into the following three parts:

1. Stress-strain relations for the elastic region
2. Yield criterion to define the initiation of yielding
3. Stress-strain relations for the plastic region

These three major divisions of the theory will be discussed after the associated assumptions and limitations are listed, and after a set of notation that will be useful in the discussion of the theory is introduced.

Harper and Ang (1963) state: "There are three main assumptions underlying the theory of perfectly plastic material used in this investigation. These can be stated as follows:

"1. It is assumed that the Mises-Hencky yield condition accurately determines the beginning of yield. General considerations of isotropy and symmetry can furnish only the general form of the yield condition. Beyond this, any yield condition is a hypothesis which only tests can justify.

"2. It is assumed that there is no permanent volume change. This assumption, justified on the basis of experimental evidence for metals, leads to the result that the plastic strain is equal to the plastic deviator strain.

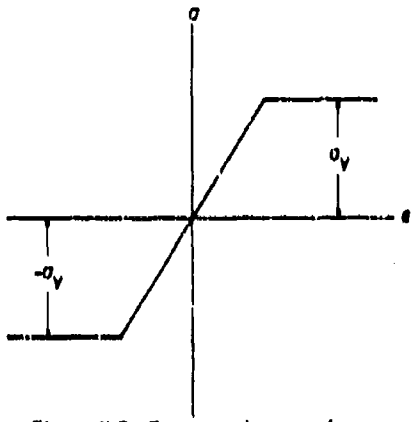

Figure C-3. Stress-strain curve for elastic-perfectly plastic material in simple tension or compression.

"3. During the plastic flow, it is assumed that the deviator strain rate tensor is proportional to the instantaneous deviator stress. This is the familiar Prandtl-Reuss postulate.

"In addition to those three main assumptions, it is possible to list several other restrictions on the theory:

"4. The material must be isotropic. This condition is used in developing the general form of the yield condition.

"5. There is no work hardening, and the material follows the stress-strain diagram of [Figure C-3] when subjected to simple tension or compression.

"6. No unloading occurs. Once a stress point has yielded, it remains yielded under successive increments of external load.

"7. Time effects of loading, such as creep, are ignored.

"8. Displacements are small so that the small deformation theory of elasticity applies."

The following definitions and notation are introduced for the purpose of describing the pertinent constitutive equations used in this study:

$$\text{Total stress tensor} = S^T = \begin{bmatrix} \sigma_x & \tau_{xy} & \tau_{xz} \\ \tau_{xy} & \sigma_y & \tau_{yz} \\ \tau_{xz} & \tau_{yz} & \sigma_z \end{bmatrix}$$

$$\text{Spherical stress tensor} = S^S = \begin{bmatrix} s & 0 & 0 \\ 0 & s & 0 \\ 0 & 0 & s \end{bmatrix}$$

$$\text{Deviator stress tensor} = S^D = \begin{bmatrix} s_x & \tau_{xy} & \tau_{xz} \\ \tau_{xy} & s_y & \tau_{yz} \\ \tau_{xz} & \tau_{yz} & s_z \end{bmatrix}$$

where s = mean normal stress = $1/3\,(\sigma_x + \sigma_y + \sigma_z)$

s_x = normal x component of S^D = $\sigma_x - s$

s_y = normal y component of S^D = $\sigma_y - s$

s_z = normal z component of S^D = $\sigma_z - s$

With this notation

$$S^T = S^S + S^D$$

$$s_x + s_y + s_z = \sigma_x + \sigma_y + \sigma_z - 3s = 0$$

Principal normal stresses are designated by σ_1, σ_2, and σ_3. Principal normal components of the stress deviator are

$$s_1 = \sigma_1 - s$$
$$s_2 = \sigma_2 - s$$
$$s_3 = \sigma_3 - s$$

A completely similar notation exists for strains:

$$\text{Total strain tensor} = E^T = \begin{bmatrix} e_x & \frac{1}{2}\gamma_{xy} & \frac{1}{2}\gamma_{xz} \\ \frac{1}{2}\gamma_{xy} & e_y & \frac{1}{2}\gamma_{yz} \\ \frac{1}{2}\gamma_{xz} & \frac{1}{2}\gamma_{yz} & e_z \end{bmatrix}$$

$$\text{Spherical strain tensor} = E^S = \begin{bmatrix} e & 0 & 0 \\ 0 & e & 0 \\ 0 & 0 & e \end{bmatrix}$$

$$\text{Deviator strain tensor} = E^D = \begin{bmatrix} e_x & \frac{1}{2}\gamma_{xy} & \frac{1}{2}\gamma_{xz} \\ \frac{1}{2}\gamma_{xy} & e_y & \frac{1}{2}\gamma_{yz} \\ \frac{1}{2}\gamma_{xz} & \frac{1}{2}\gamma_{yz} & e_z \end{bmatrix}$$

where e = mean normal strain $= 1/3\,(\epsilon_x + \epsilon_y + \epsilon_z)$

e_x = normal x component of $E^D = \epsilon_x - e$

e_y = normal y component of $E^D = \epsilon_y - e$

e_z = normal z component of $E^D = \epsilon_z - e$

With this notation

$$E^T = E^S + E^D$$

$$e_x + e_y + e_z = \epsilon_x + \epsilon_y + \epsilon_z - 3e = 0$$

Principal normal strains are designated as ϵ_1, ϵ_2, and ϵ_3. Principal normal components of the strain deviator are

$$e_1 = \epsilon_1 - e$$
$$e_2 = \epsilon_2 - e$$
$$e_3 = \epsilon_3 - e$$

Elastic Stress-Strain Relations

In the elastic range the relationship between the elements of the stress and strain tensors is assumed to be that of Hooke's law. It is convenient to express this linear relationship in terms of the elements of the deviator stress and deviator strain tensors:

$$s_x = 2Ge_x \qquad s_y = 2Ge_y \qquad s_z = 2Ge_z$$
$$\tau_{xy} = G\gamma_{xy} \qquad \tau_{xz} = G\gamma_{xy} \qquad \tau_{yz} = G\gamma_{yz} \qquad \text{(C-8)}$$

$$\sigma_x + \sigma_y + \sigma_z = 3K(\epsilon_x + \epsilon_y + \epsilon_z) \qquad \text{(C-9)}$$

where $G = \frac{E}{2(1 + \nu)}$

$K = \frac{E}{3(1 - 2\nu)}$

The relationships in Equation C-8 can be expressed more concisely as

$$S^D = 2GE^D \qquad \text{(C-10)}$$

Note that the expressions in Equation C-8 or Equation C-10 are not six independent relations since addition of $s_x + s_y + s_z = 0$ gives an identity. Therefore, Equation C-9 is needed to give a complete statement of Hooke's law.

Yield Criterion

The yield point is determined by the Mises-Hencky yield criterion:

$$J_2 = k^2 \qquad \text{(C-11)}$$

where J_2 = second invariant of the stress deviator tensor

k = yield stress in simple shear

J_2 is defined by

$$J_2 = \frac{1}{2}(s_1^2 + s_2^2 + s_3^2) = \frac{1}{2}(s_x^2 + s_y^2 + s_z^2) + \tau_{yz}^2 + \tau_{xz}^2 + \tau_{xy}^2$$

$$= \frac{1}{6}(\sigma_x - \sigma_y)^2 + (\sigma_y - \sigma_z)^2 + (\sigma_z - \sigma_x)^2$$

$$+ \tau_{yz}^2 + \tau_{xz}^2 + \tau_{xy}^2$$

For plane strain problems, the yield condition reduces to

$$J_2 = \left(\frac{\sigma_x - \sigma_y}{2}\right)^2 + \tau_{xy}^2 = k^2 \qquad \text{(C-12)}$$

Combining Equations C-12 and C-3, we obtain for any yielded stress point

$$J_2 \frac{\delta^2}{4} = \left(\frac{F_x - F_y}{2}\right)^2 + F_{xy}^2 = \frac{k^2 \delta^2}{4}$$

Still another useful form for the yield criterion is obtained by substituting the expressions in Equation C-5 into Equation C-12:

$$(\epsilon_x - \epsilon_y)^2 + \gamma_{xy}^2 = \left[\frac{2(1+\nu)k}{E}\right]^2 = \left(\frac{k}{G}\right)^2$$

Using Equations C-1 for the strains at a typical stress point, a, the yield criterion becomes:

$$(u_{54} - u_{43} - v_{53} + v_{44})^2 + (u_{53} - u_{44} + v_{54} - v_{43})^2 = \left(\frac{k\delta}{G}\right)^2 \qquad \text{(C-13)}$$

Plastic Stress-Strain Relations

In order to relate stress and strain in a material which is undergoing plastic flow, it is convenient to express the strain tensor in terms of elastic and plastic components. Single primes will be used to denote an elastic component, and double primes will denote a plastic component. Dots will denote rate of change with respect to increment of external load.

The essential nature of the relations between stress and strain during plastic flow is given by Equations C-14 and C-15. The assumption of no permanent change of volume is stated mathematically as

$$\theta'' = \frac{1}{3}(\epsilon_x'' + \epsilon_y'' + \epsilon_z'') = 0 \qquad \text{(C-14)}$$

This implies that the plastic strain deviation is identical to the plastic strain, or

$$e_x'' = \epsilon_x'' \qquad e_y'' = \epsilon_y'' \qquad e_z'' = \epsilon_z''$$

The assumption that during plastic flow the deviator strain rate tensor is proportional to the instantaneous deviator stress tensor is stated mathematically as

$$2G\dot{e}_x'' = \phi s_x \quad 2G\dot{e}_y'' = \phi s_y \quad 2G\dot{e}_z'' = \phi s_z$$

$$G\dot{\gamma}_{xy}'' = \phi \tau_{xy} \quad G\dot{\gamma}_{xz}'' = \phi \tau_{xz} \quad G\dot{\gamma}_{yz}'' = \phi \tau_{yz} \qquad \text{(C-15)}$$

where ϕ = a proportionality factor

The expressions in Equation C-15 are in the same form as the elastic stress-strain relations given in Equation C-8.

The basic relationships which are assumed during plastic flow have been presented. At this point it is necessary to apply these relations, along with the yield criterion (Equation C-11) and the elastic relations (Equations C-8 and C-9), in order to develop the final relationships between the stress rates (incremental stresses), strain rates (incremental strains), and instantaneous stresses.

The plastic strain rates have been expressed in terms of stresses by Equation C-15. Similarly, the elastic strain rates are expressed in terms of stress rates by differentiating the expressions in Equation C-8 with respect to external load:

$$2G\dot{e}_x' = \dot{s}_x \quad 2G\dot{e}_y' = \dot{s}_y \quad 2G\dot{e}_z' = \dot{s}_z$$

$$G\dot{\gamma}_{xy}' = \dot{\tau}_{xy} \quad G\dot{\gamma}_{xz}' = \dot{\tau}_{xz} \quad G\dot{\gamma}_{yz}' = \dot{\tau}_{yz}$$

Combining the elastic and plastic strain rates gives the total strain rate:

$$\begin{aligned}
2G\dot{e}_x &= 2G\dot{e}_x' + 2G\dot{e}_x'' = \dot{s}_x + \phi s_x \\
2G\dot{e}_y &= 2G\dot{e}_y' + 2G\dot{e}_y'' = \dot{s}_y + \phi s_y \\
2G\dot{e}_z &= 2G\dot{e}_z' + 2G\dot{e}_z'' = \dot{s}_z + \phi s_z \\
G\dot{\gamma}_{xy} &= G\dot{\gamma}_{xy}' + G\dot{\gamma}_{xy}'' = \dot{\tau}_{xy} + \phi \tau_{xy} \\
G\dot{\gamma}_{xz} &= G\dot{\gamma}_{xz}' + G\dot{\gamma}_{xz}'' = \dot{\tau}_{xz} + \phi \tau_{xz} \\
G\dot{\gamma}_{yz} &= G\dot{\gamma}_{yz}' + G\dot{\gamma}_{yz}'' = \dot{\tau}_{yz} + \phi \tau_{yz}
\end{aligned} \qquad \text{(C-16)}$$

Note that these relations apply only during plastic flow, that is, when

$$J_2 = k^2 \quad \text{and} \quad \dot{J}_2 = 0$$

In order to eliminate the proportionality factor ϕ from the expressions in Equation C-16, it is convenient to introduce the notation

$$\dot{W} = s_x \dot{e}_x + s_y \dot{e}_y + s_z \dot{e}_z + \tau_{xy} \dot{\gamma}_{xy} + \tau_{xz} \dot{\gamma}_{xz} + \tau_{yz} \dot{\gamma}_{yz}$$

where $\dot{W}$ may be interpreted as the rate at which stresses do work during a change of shape, and to note that

$$\dot{J}_2 = s_x \dot{s}_x + s_y \dot{s}_y + s_z \dot{s}_z + 2\tau_{xy} \dot{\tau}_{xy} + 2\tau_{xz} \dot{\tau}_{xz} + 2\tau_{yz} \dot{\tau}_{yz}$$

By multiplying the first three expressions of Equation C-16 by s_x, s_y, s_z, and the last three by $2\tau_{xy}$, $2\tau_{xz}$, $2\tau_{yz}$, respectively, and adding, we get

$$\begin{aligned} 2G\dot{W} &= s_x \dot{s}_x + \phi s_x^2 + s_y \dot{s}_y + \phi s_y^2 + s_z \dot{s}_z + \phi s_z^2 \\ &\quad + 2\tau_{xy} \dot{\tau}_{xy} + 2\phi \tau_{xy}^2 + 2\tau_{xz} \dot{\tau}_{xz} + 2\phi \tau_{xz}^2 \\ &\quad + 2\tau_{yz} \dot{\tau}_{yz} + 2\phi \tau_{yz}^2 \\ &= \dot{J}_2 + \phi(s_x^2 + s_y^2 + s_z^2 + 2\tau_{xy}^2 + 2\tau_{xz}^2 + 2\tau_{yz}^2) \\ &= \dot{J}_2 + 2\phi J_2 \end{aligned}$$

But during plastic flow, $J_2 = k^2$ and $\dot{J}_2 = 0$. Hence, $2G\dot{W} = 2\phi k^2$ and $\phi = G\dot{W}/k^2$.

Substituting this value of ϕ into the expressions in Equation C-16, it is possible to solve for the deviator stress rates, which gives

$$\begin{aligned} \dot{s}_x &= 2G\left(\dot{e}_x - \frac{\dot{W}}{2k^2} s_x\right) \qquad \dot{\tau}_{xy} = G\left(\dot{\gamma}_{xy} - \frac{\dot{W}}{k^2} \tau_{xy}\right) \\ \dot{s}_y &= 2G\left(\dot{e}_y - \frac{\dot{W}}{2k^2} s_y\right) \qquad \dot{\tau}_{xz} = G\left(\dot{\gamma}_{xz} - \frac{\dot{W}}{k^2} \tau_{xz}\right) \\ \dot{s}_z &= 2G\left(\dot{e}_z - \frac{\dot{W}}{2k^2} s_z\right) \qquad \dot{\tau}_{yz} = G\left(\dot{\gamma}_{yz} - \frac{\dot{W}}{k^2} \tau_{yz}\right) \end{aligned} \tag{C-17}$$

To obtain the total stress rates it is necessary to add the deviator stress rates from the expressions in Equation C-17 to the spherical stress rate, which can be obtained by differentiating Equation C-9 with respect to external load:

$$\dot{s} = 3K\dot{e} \tag{C-18}$$

Adding Equations C-17 and C-18 results in the total stress rates:

$$\begin{aligned}
\dot{\sigma}_x &= \dot{s}_x + \dot{s} = 2G\left(\dot{e}_x - \frac{\dot{W}}{2k^2} s_x\right) + 3K\dot{e} \\
\dot{\sigma}_y &= \dot{s}_y + \dot{s} = 2G\left(\dot{e}_y - \frac{\dot{W}}{2k^2} s_y\right) + 3K\dot{e} \\
\dot{\sigma}_z &= \dot{s}_z + \dot{s} = 2G\left(\dot{e}_z - \frac{\dot{W}}{2k^2} s_z\right) + 3K\dot{e} \\
\dot{\tau}_{xy} &= G\left(\dot{\gamma}_{xy} - \frac{\dot{W}}{k^2} \tau_{xy}\right) \\
\dot{\tau}_{xz} &= G\left(\dot{\gamma}_{xz} - \frac{\dot{W}}{k^2} \tau_{xz}\right) \\
\dot{\tau}_{yz} &= G\left(\dot{\gamma}_{yz} - \frac{\dot{W}}{k^2} \tau_{yz}\right)
\end{aligned} \tag{C-19}$$

The expressions in Equation C-19 give the desired relationships between the stress rates, strain rates, and instantaneous stresses.

To apply the expressions in Equation C-19 to the numerical model, it is necessary to reduce them to an incremental form. Note that for plane strain problems the number of relations is reduced from six to three. Therefore

$$\begin{aligned}
\Delta\sigma_x &= \Delta s_x + \Delta s \\
\Delta\sigma_y &= \Delta s_y + \Delta s \\
\Delta\tau_{xy} &= G\left(\Delta\tau_{xy} - \frac{\Delta W}{k^2} \tau_{xy}\right)
\end{aligned} \tag{C-20}$$

For plane strain conditions, the expressions in Equation C-17 are reduced to

$$\Delta s_x = 2G\left(\Delta e_x - \frac{\Delta W}{2k^2} s_x\right)$$

$$\Delta s_y = 2G\left(\Delta e_y - \frac{\Delta W}{2k^2} s_y\right)$$

$$\Delta \tau_{xy} = G\left(\Delta \gamma_{xy} - \frac{\Delta W}{k^2} \tau_{xy}\right)$$

and Equation C-18 becomes

$$\Delta s = 3K\Delta e = K(\Delta \epsilon_x + \Delta \epsilon_y)$$

The increment $\dot{W}$ becomes

$$\Delta W = s_x \Delta e_x + s_y \Delta e_y + s_z \Delta e_z + \tau_{xy} \Delta \gamma_{xy} \qquad \text{(C-21)}$$

But $$s_z = \sigma_z - \frac{1}{3}(\sigma_x + \sigma_y + \sigma_z)$$

Where, for plane strain

$$\sigma_z = \nu(\sigma_x + \sigma_y)$$

and during plastic flow

$$\nu = \frac{1}{2}$$

Hence $$s_z = \frac{1}{2}(\sigma_x + \sigma_y) - \frac{1}{3}\left(\sigma_x + \sigma_y + \frac{\sigma_x + \sigma_y}{2}\right) = 0$$

Thus $$s_x = \sigma_x - \frac{1}{3}\left(\sigma_x + \sigma_y + \frac{\sigma_x + \sigma_y}{2}\right) = \frac{\sigma_x - \sigma_y}{2}$$

$$s_y = \sigma_y - \frac{1}{3}\left(\sigma_y + \sigma_x + \frac{\sigma_x + \sigma_y}{2}\right) = \frac{\sigma_y - \sigma_x}{2} = -s_x \qquad \text{(C-22)}$$

$$e_x = \epsilon_x - \frac{1}{3}(\epsilon_x + \epsilon_y) = \frac{2\epsilon_x - \epsilon_y}{3}$$

$$\Delta e_x = \frac{2\Delta\epsilon_x - \Delta\epsilon_y}{3}$$

$$e_y = \epsilon_y - \frac{1}{3}(\epsilon_x + \epsilon_y) = \frac{2\epsilon_y - \epsilon_x}{3} \qquad \text{(C-22 con'td)}$$

$$\Delta e_y = \frac{2\Delta\epsilon_y - \Delta\epsilon_x}{3}$$

Substituting the values of Equation C-22 into Equation C-21 yields

$$\Delta W = \frac{1}{2}(\sigma_x - \sigma_y)(\Delta\epsilon_x - \Delta\epsilon_y) + \tau_{xy}\Delta\gamma_{xy} \qquad \text{(C-23)}$$

Substituting the expressions for ΔW, Δe_x, and s_x from Equations C-22 and C-23 in Equation C-20, $\Delta\sigma_x$ becomes

$$\Delta\sigma_x = 2G\left[\left(\frac{2\Delta\epsilon_x - \Delta\epsilon_y}{3}\right) - \frac{\frac{1}{2}(\sigma_x - \sigma_y)(\Delta\epsilon_x - \Delta\epsilon_y) + \tau_{xy}\Delta\gamma_{xy}}{2k^2}\left(\frac{\sigma_x - \sigma_y}{2}\right) + K(\Delta\epsilon_x + \Delta\epsilon_y)\right]$$

Collecting terms gives

$$\Delta\sigma_x = \Delta\epsilon_x\left[\frac{4G + 3K}{3} - \frac{G}{k^2}\left(\frac{\sigma_x - \sigma_y}{2}\right)^2\right] + \Delta\epsilon_y\left[\frac{-2G + 3K}{3} + \frac{G}{k^2}\left(\frac{\sigma_x - \sigma_y}{2}\right)^2\right] + \Delta\gamma_{xy}\left[\frac{-G\tau_{xy}}{k^2}\left(\frac{\sigma_x - \sigma_y}{2}\right)\right] \qquad \text{(C-24)}$$

Similar expressions are obtained for $\Delta\sigma_y$ and $\Delta\tau_{xy}$:

$$\Delta\sigma_y = \Delta e_x\left[\frac{-2G + 3K}{3} + \frac{G}{k^2}\left(\frac{\sigma_x - \sigma_y}{2}\right)^2\right]$$

$$+ \Delta e_y\left[\frac{-4G + 3K}{3} + \frac{G}{k^2}\left(\frac{\sigma_x - \sigma_y}{2}\right)^2\right]$$

$$+ \Delta\tau_{xy}\left[\frac{G}{k^2}\tau_{xy}\left(\frac{\sigma_x - \sigma_y}{2}\right)\right] \qquad \text{(C-25)}$$

$$\Delta\tau_{xy} = \Delta e_x\left[\frac{-G}{k^2}\tau_{xy}\left(\frac{\sigma_x - \sigma_y}{2}\right)\right]$$

$$+ \Delta e_y\left[\frac{G}{k^2}\tau_{xy}\left(\frac{\sigma_x - \sigma_y}{2}\right)\right]$$

$$+ \Delta\gamma_{xy}\left[G\left(1 - \frac{\tau^2_{xy}}{k^2}\right)\right] \qquad \text{(C-26)}$$

Combining Equations C-1 and C-3 with Equations C-24, C-25, and C-26, and rearranging, the three force components at the stress point a in terms of displacements are

$$\Delta F_x = A(\Delta u_{54} - \Delta u_{43}) + B(\Delta v_{53} - \Delta v_{44})$$

$$- C(\Delta u_{53} - \Delta u_{44} + \Delta v_{54} - \Delta v_{43}) \qquad \text{(C-27)}$$

$$\Delta F_y = B(\Delta u_{54} - \Delta u_{43}) + A(\Delta v_{53} - \Delta v_{44})$$

$$+ C(\Delta u_{53} - \Delta u_{44} + \Delta v_{54} - \Delta v_{43}) \qquad \text{(C-28)}$$

$$\Delta F_{xy} = -C(\Delta u_{54} - \Delta u_{43}) + C(\Delta v_{53} - \Delta v_{44})$$

$$+ D(\Delta u_{53} - \Delta u_{44} + \Delta v_{54} - \Delta v_{43}) \qquad \text{(C-29)}$$

where the Δ denotes change during an external load increment and

$$A = \frac{1}{2}\left[\frac{4G + 3K}{3} - \frac{G}{k^2\delta^2}(F_x - F_y)^2\right]$$

$$B = \frac{1}{2}\left[\frac{-2G + 3K}{3} + \frac{G}{k^2\delta^2}(F_x - F_y)^2\right]$$

$$C = \frac{G}{k^2\delta^2}F_{xy}(F_x - F_y)$$

$$D = \frac{1}{2}\left[G - \frac{4G}{k^2\delta^2}(F_{xy})^2\right]$$

Equations C-27, C-28, and C-29 are the relationships with which the incremental force components in a plastic region are computed. These incremental force components are added to the existing force components (F_x, F_y, and F_{xy}) at a yielded stress point to obtain the total forces.

In order to compute the quantities Δu and Δv which appear in Equations C-27, C-28, and C-29, two sets of displacements corresponding to two consecutive load levels are required. One set of displacements is the set which is being generated for the current load; the other set is that computed for the previous load. The quantities Δu and Δv are computed as the difference in displacements determined for these two loads.

Equations C-27, C-28, and C-29 are linear: that is, if A, B, C, and D are constants, then the changes in force are linear with regard to changes in displacement. Actually, the equations are not linear since in general F_x, F_y, F_{xy} will change during plastic flow. Thus, it is necessary to proceed in a step-wise linear fashion.

General Form of the Plasticity Equations

In general, the application of the plasticity equations to the Harper and Ang model is closely associated with the three stages of material behavior presented in the previous sections. The plasticity relations which describe these three stages of material behavior in terms of stress point forces and mass point displacements are used to describe the behavior of the numerical model.

These relations, which have been developed in the previous sections, can be generalized by adopting the following subscript notation:

LR = lower right
UL = upper left
LL = lower left
UR = upper right

Force-Displacement Relations: Elastic Case. The expressions (Equations C-6) which relate elastic stress point forces to mass point displacements can be generalized as

$$F_x = \frac{E}{2(1+\nu)(1-2\nu)}\left[(1-\nu)(u_{LR}-u_{UL}) + \nu(v_{LL}-v_{UR})\right]$$

$$F_y = \frac{E}{2(1+\nu)(1-2\nu)}\left[(1-\nu)(v_{LL}-v_{UR}) + \nu(u_{LR}-u_{UL})\right] \qquad \text{(C-30)}$$

$$F_{xy} = \frac{E}{4(1+\nu)}\,(u_{LL}-u_{UR}+v_{LR}-v_{UL})$$

Yield Criterion. The yield criterion (Equation C-13) in terms of mass point displacements can be generalized as

$$(u_{LR}-u_{UL}-v_{LL}+v_{UR})^2 + (u_{LL}-u_{UR}+v_{LR}-v_{UL})^2 = \left(\frac{kE}{G}\right)^2 \qquad \text{(C-31)}$$

Force-Displacement Relations: Plastic Case. The expressions (Equations C-27, C-28, and C-29) which relate incremental plastic stress point forces to mass point displacements can be generalized as

$$\begin{aligned}
\Delta F_x &= A(\Delta u_{LR}-\Delta u_{UL}) + B(\Delta v_{LL}-\Delta v_{UR}) \\
&\quad - C(\Delta u_{LL}-\Delta u_{UR}-\Delta v_{LR}-\Delta v_{UL}) \\
\Delta F_y &= B(\Delta u_{LR}-\Delta u_{UL}) + A(\Delta v_{LL}-\Delta v_{UR}) \\
&\quad + C(\Delta u_{LL}-\Delta u_{UR}-\Delta v_{LR}-\Delta v_{UL}) \qquad \text{(C-32)} \\
\Delta F_{xy} &= -C(\Delta u_{LR}-\Delta u_{UL}) + C(\Delta v_{LL}-\Delta v_{UR}) \\
&\quad + D(\Delta u_{LL}-\Delta u_{UR}-\Delta v_{LR}-\Delta v_{UL})
\end{aligned}$$

where $A = \frac{1}{2}\left[\frac{4G + 3K}{3} - \frac{G}{k^2\delta^2}(F_x - F_y)^2\right]$

$B = \frac{1}{2}\left[\frac{-2G + 3K}{3} + \frac{G}{k^2\delta^2}(F_x - F_y)^2\right]$

$C = \frac{G}{k^2\delta^2} F_{xy}(F_x - F_y)$

$D = \frac{1}{2}\left[G - \frac{4G}{k^2\delta^2}(F_{xy})^2\right]$

Equations C-30, C-31, and C-32 are the form of the plasticity relations actually used in the numerical method.

NUMERICAL METHOD

When a problem in continuum mechanics is replaced by a corresponding problem in particle mechanics involving a discrete model, the displacements to satisfy equilibrium must be determined. One method is to write and solve the set of simultaneous linear algebraic equations (equations similar to Equation C-7) for the unknown displacement components u and v at each mass point. Harper and Ang (1963) note that such an approach has significant disadvantages. The preparation of the equations, whether it is done by hand or by an intricate program for the computer, involves a considerable amount of labor. In addition, even with machines as large as the IBM 7094, the number of equations which can be solved by the standard library subroutines is limited. Perhaps most important, the changes in the coefficients for the displacements resulting from the yielding of one or more stress points are not easy to determine.

A more flexible and practical approach to the problem as suggested by Harper and Ang (1963) and Whitman (1964) is to employ a relaxation technique. Such an approach eliminates completely the preparation of simultaneous equations, and can handle several thousand displacement components. An additional advantage of the relaxation method is the physical meaning that can be attached to each step of the procedure. This is very helpful in determining plastic forces and displacements.

Relaxation Procedure

The relaxation procedure used for determining the equilibrium displacements is summarized by the flow diagram in Figure C-4. Following the discussion given by Harper and Ang, all mass points of the model are initially in equilibrium with zero displacements and no external load. The first increment of external load is then applied to any or all mass points, thus destroying the equilibrium of the loaded mass points. The following operations are then performed for each mass point of the model.

The forces acting on a mass point are determined as follows: External forces acting on the mass point are given as a part of the loading pattern applied to the model. Internal forces, originating at the stress points, are determined uniquely by Equation C-30 in the elastic range from the displacements surrounding the stress points. After a stress point has yielded, the force components at that stress point are determined both by the surrounding displacements and the past history of that particular stress point. Incremental plastic forces (Equation C-32) are then added to the last set of equilibrium forces at the stress point to obtain the current total plastic forces acting at the yielded stress point.

After the forces acting on a given mass point are determined, a summation of all the forces acting in the x direction is made. In general, this will result in a residual force which is an indication of the amount by which the mass point is out of equilibrium in the x direction. The mass point is then displaced through a small distance in the x direction equal to the product of the residual force and a flexibility coefficient.

Similar operations are performed for the y direction. These operations place the current mass point in equilibrium, though in general the equilibrium of surrounding mass points will be upset by a small amount. The procedure is repeated for each mass point until every mass point has been moved once in the x direction and once in the y direction, thus completing one cycle of relaxation.

After every relaxation cycle, each mass point is inspected to determine if it is in equilibrium. If not, the relaxation process is repeated until all mass points are in equilibrium within the accuracy prescribed by a convergence criterion. After all mass points are in equilibrium, all the stress points are inspected for yielding by Mises-Hencky yield criterion (Equation C-31) and the yielded regions are recorded. All the displacements and forces for the equilibrium configuration just obtained are also recorded.

If desired, the external load is given a new increment, and the complete procedure is repeated for each load increment in order to trace the development of plastic yielding from one stress point to another.

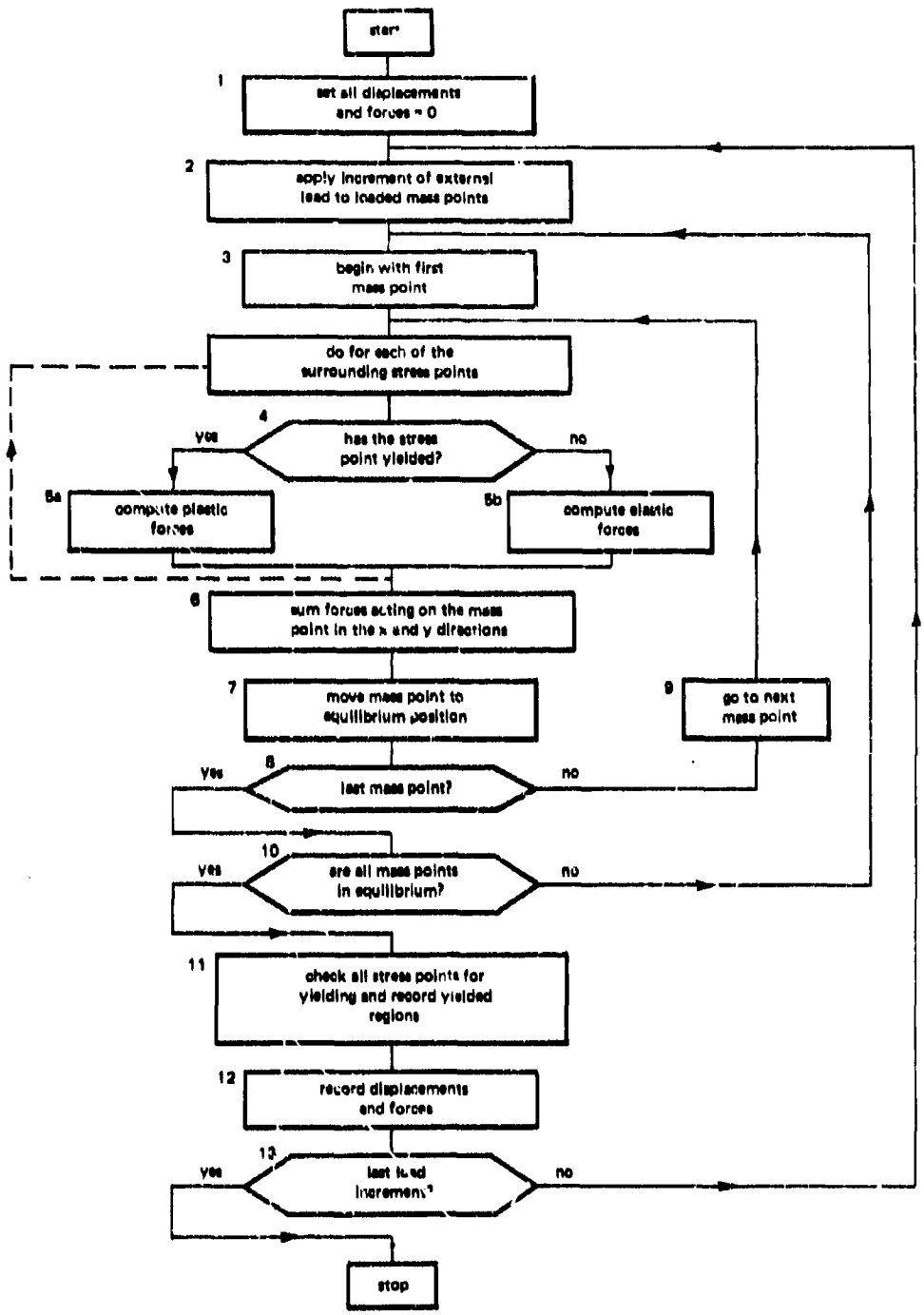

Figure C-4. Flow diagram for relaxation procedure.

This relaxation procedure has been coded for use on the digital computer. Although the basic calculations are simple, a complex program is needed to handle all of the logical decisions that the computer must make as it distinguishes between yielded and unyielded stress points and computes the magnitude of the load increment needed to just cause yielding at one additional stress point.

Program PERFPLAS II

The computer program used in this study is a revision of the program (PERFPLAS I) developed for Whitman (1964) at the Stanford Research Institute. The revised program has been named PERFPLAS II (PERFectly PLAStic) and is written in FORTRAN II for the IBM 7094 digital computer.

At present, program PERFPLAS II will permit the use of up to a 36 x 36 grid of mass points (35 x 35 stress points). The allowable grid size can be increased by increasing the storage allocated by the program's dimension statements.

The boundary conditions can be of four types: free, fixed, reflected, or infinite. A free boundary is one in which the mass points can move in any direction and a fixed boundary is one in which the mass points cannot move. A reflected boundary is a line of symmetry between two halves of a symmetrical problem for which it is necessary to solve only one half. An infinite boundary is an approximation of the condition far from the loaded area, in that mass points can move only parallel to the boundary in such a manner that normal lines remain normal to the boundary.

In PERFPLAS II, the left boundary is limited to a fixed or an infinite boundary. The right boundary is limited to a fixed, a symmetrical, or an infinite boundary. The top boundary is limited to a free boundary.

The basic step in the program is the application of a trial load increment and the successive relaxation of mass points until the system comes to equilibrium. The program keeps track of stress points which have yielded and uses the plastic equations accordingly (Equation C-32).

Two load options have been programmed into PERFPLAS II. These load options are the same when the material deformations are elastic, and differ only after the material has yielded at some point. Initially, a small load (known to be less than the load required to cause first yielding) is applied. When the specified standard load increment is used, the initial load is incremented until the first stress point yields. Thereafter, the two load options differ:

1. When the first load option is used, the load will continue to be incremented by the specified standard load increment until the load attains the specified maximum value.

2. When the second load option is used, the load will be incremented by the specified standard load increment, but each time a new stress point yields the load will be reduced to a level which will just cause this stress point to yield. This process continues until the load attains or slightly exceeds the specified maximum load.

The relations required to downgrade the load when the second load option is is used are presented in Appendix D.

Whenever an adjustment is to be made in the results of a trial load increment, the program determines the amount by which the load increment must be changed and then adjusts all computed displacements and forces accordingly. By using the second load option, the propagation of yielding within the material may be studied in detail (one stress point at a time). However, the execution time of the program will be increased. It was found convenient to use the first load option for the first run of all new problems.

In the range where plastic deformations occur, the load increments should be sufficiently small so that the development of the plastic zone is gradual. This keeps the errors due to linear extrapolation to a minimum.

As mentioned previously, approximate linearized equations (Equation C-32) are used to compute the forces at already yielded stress points. For this reason, the yield condition may be exceeded at these stress points at the end of an increment of plastic straining, and a correction must be introduced to bring the forces back to the yield surface. The relations required to make this correction are presented in Appendix D. In PERFPLAS II, subroutine CORRECT makes this correction. Subroutine CORRECT is applied after equilibrium has been established under the given load increment. This subroutine alters the forces at each previously yielded stress point without altering any displacements. As a result, the surrounding mass points are slightly out of equilibrium.

A convergence criterion is needed to specify what accuracy is desired in the iteration process following each applied load increment. The criterion adopted is that the ratio of the next incremental adjustment in displacement to the total displacement at the mass point should be less than or equal to a prescribed value. The next incremental adjustment in displacement is determined by multiplying the unbalanced force acting on a mass point by an elastic flexibility coefficient. Displacements are adjusted in both the x and y directions to bring the mass points into equilibrium, and the convergence criterion is applied to all mass points.

The elastic flexibility coefficient for a mass point is developed subsequently. This coefficient is used for both elastic and plastic deformations. As a result, the number of iterations required to establish equilibrium increases sharply after a large number of stress points have yielded.

In program PERFPLAS II, the mass points are identified by a double subscript (I,J). I indicates the vertical position of the mass point (the row) and increases vertically downward. J indicates the horizontal position of the mass point (the column) and increases from left to right. Stress points are identified by a double subscript (I,J) corresponding to the mass point above and to the left of the stress point. This subscript notation is illustrated in Figure C-5.

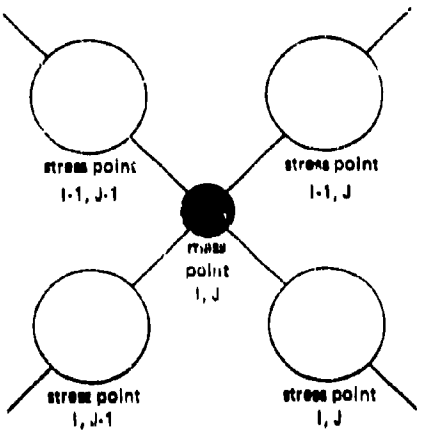

Figure C-5. Mass point and stress point subscript notation used in program PERFPLAS II.

Using Program PERFPLAS I, Whitman and Hoeg (1965) have studied the performance and accuracy of the Harper and Ang mathematical model. From this study, it is suggested that a convergence criterion of 10^{-5} or 10^{-6} should be used. Christian (1965) has shown that the number of iterations required for equilibrium increases sharply if Poisson's ratio exceeds 0.45. This is because the expression $(1 - 2\nu)$ appears in the denominator of the elastic force displacement equations (Equation C-30). As Poisson's ratio approaches 0.5, the expression $(1 - 2\nu)$ approaches zero.

The FORTRAN deck of program PERFPLAS II can be compiled in less than 3 minutes on the IBM 7094. Compiling time can be eliminated by using a binary deck on production runs. Execution time increases (for a given value of Poisson's ratio) as the number of mass points increases and as the number of yielded stress points increases. A detailed study of execution time has not been made.

The user of program PERFPLAS II must provide certain data describing the problem. The data can be in any consistent set of units, and the output will be in the same units. A data input guide is given in Appendix E.

A glossary of notation used in PERFPLAS II is given in Appendix F and a listing of the FORTRAN deck is given in Appendix G. Also listed in Appendix G is the input data for the sample problem which will be discussed subsequently. Program output will be discussed in connection with the sample problem.

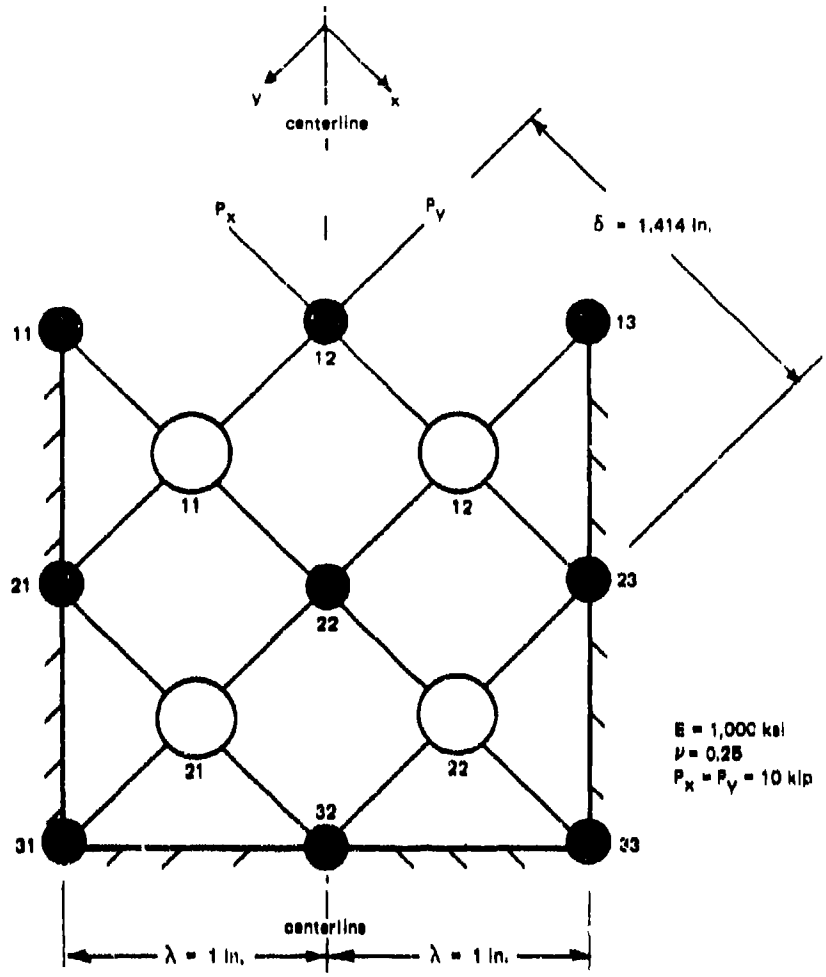

Figure C-6. Schematic of sample problem.

SAMPLE PROBLEM

A sample problem has been selected to familiarize the reader with the numerical method and program PERFPLAS II.

The problem selected is the same as that presented by Harper and Ang (1963). This elementary problem (Figure C 6) was selected because it can be readily solved by hand. Therefore, the numerical procedure can be illustrated in detail.

In Figure C-6, only mass points 12 and 22 are free to move, and due to symmetry about a vertical line through these mass points, the u and v displacements at a mass point are equal:

$$u_{12} = v_{12} \quad u_{22} = v_{22}$$

Hence there are only two unknown displacements, u_{12} and u_{22}. By means of the material constants, dimensions, and loading shown in Figure C-6, it is possible to write two simultaneous linear algebraic equations (similar to Equation C-7) for the elastic behavior of the system in terms of the two unknowns, u_{12} and u_{22}. Solution of these two equations yields

$$\begin{aligned} u_{12} &= v_{22} = 1.429 \times 10^{-2} \text{ inches} \\ u_{22} &= v_{22} = 3.571 \times 10^{-3} \text{ inches} \end{aligned} \tag{C-33}$$

These values will now be used to measure the progress of the relaxation procedure. Converting these displacements to elastic force components at stress point 12 by using Equation C-30 gives

$$\begin{aligned} (F_x)_{12} &= -7.857 \text{ kips} \\ (F_y)_{12} &= -0.714 \text{ kip} \\ (F_{xy})_{12} &= -2.143 \text{ kips} \end{aligned} \tag{C-34}$$

Before the systematic relaxation procedure is begun, it is first necessary to convert external loads to concentrated loads for application at the loaded mass points and to determine the flexibility coefficients for each mass point. For example, if an external vertical pressure of 14.14 ksi is acting on the top surface of the model shown in Figure C-6, the concentrated vertical force acting on mass point 12, which arises from this pressure acting over a distance of $\lambda/2$ = 1/2 inch on either side of mass point 12, is

$$P_v = (14.14 \text{ ksi})\left(\frac{1}{2} + \frac{1}{2} \text{ inch}\right)(1 \text{ inch}) = 14.14 \text{ kips}$$

where the thickness of the model is 1 inch. This vertical force is then resolved into components in the x and y directions for application to mass point 12:

$$P_x = \frac{P_v}{\sqrt{2}} = 10 \text{ kips} \quad P_y = \frac{P_v}{\sqrt{2}} = 10 \text{ kips}$$

The flexibility coefficient for a mass point is obtained by determining the deflection caused at the mass point by a unit component force. All adjacent mass points are assumed fixed, and the flexibility coefficient determined will be for the direction of the applied unit force. For example, a unit force of 1 kip applied in the x direction at mass point **22** is resisted by internal force components at stress points **11**, **12**, **21**, and **22**. By using the sign convention shown in Figure C-2 and by summing the forces in the x direction at mass point **22**, we get

$$(\Sigma F_x)_{22} = (F_x)_{22} - (F_x)_{11} + (F_{xy})_{21} - (F_{xy})_{12} + 1 = 0$$

Expressing $(F_x)_{22}$, $(F_x)_{11}$, $(F_{xy})_{21}$, and $(F_{xy})_{12}$ in terms of displacements by means of Equation C-30, and noting that all displacement components except u_{22} are zero, we get

$$1 = \left[\frac{E(1-\nu)}{(1+\nu)(1-2\nu)} + \frac{2E}{4(1+\nu)}\right] u_{22} \qquad \text{(C-35)}$$

or $$u_{22} = \frac{2(1+\nu)(1-2\nu)}{(3-4\nu)E} = (f_x)_{22} = (f_y)_{22}$$

Equation C-35 gives the flexibility coefficient for a typical interior mass point in the x direction and has units of inches/kip. Due to symmetry, this is also the flexibility coefficient for a typical interior mass point in the y direction.

From Figure C-1 it can be seen that the flexibility coefficient for mass point **12**, which is a typical top boundary mass point, is twice that of the flexibility coefficient for mass point **22**, or

$$(f_x)_{12} = 2(f_y)_{22} = \frac{4(1+\nu)(1-2\nu)}{(3-4\nu)E}$$

If E and ν take on the values 1,000 ksi and 0.25, respectively, as shown in Figure C-6, these flexibility coefficients become

$$(f_x)_{12} = (f_y)_{12} = 1.25 \times 10^{-3} \text{ in./kip}$$

$$(f_x)_{22} = (f_y)_{22} = 6.25 \times 10^{-4} \text{ in./kip}$$

With the values for the concentrated external loads and the flexibility coefficients known, it is possible to begin the relaxation procedure. The following step numbers refer to the flow diagram of Figure C-4.

Step	Operation
1	Set $u_{12} = v_{12} = u_{22} = v_{22} = 0$. Also set force components = 0.
2	Apply increment of external load to mass point **12**: $(P_x)_{12} = 10$ kips $(P_y)_{12} = 10$ kips
3	Begin with mass point **12**.
4	No stress point has yielded, since all stress components are initially zero. Go to 5b.
5b	On the first cycle, all force components are zero since the mass points have not moved.
6	On the first cycle, only external forces are nonzero. Hence $(F_x)_{12} = (P_x)_{12} = +10$ kips $(F_y)_{12} = (P_y)_{12} = +10$ kips
7	Now u_{12} = old $u_{12} + (f_x)_{12} \Sigma (F_x)_{12}$ $u_{12} = 0 + (0.00125)(10) = 0.0125$ inch Similarly $v_{12} = 0 + (0.00125)(10) = 0.0125$ inch Note that those displacements of mass point **12** destroy the equilibrium of mass point **22**.
8	The current mass point, **12**, is not the last mass point. Go to 9.
9	Take mass point **22**. Go to 4.
4	Again no stress point has yielded, since yielding can occur only after equilibrium is reached. Go to 5b.

Step	Operation
5b	Force components at stress points 11 and 12 are computed from Equation C-30, taking into account that all displacements are zero except $u_{12} = v_{12}$ and $u_{22} = v_{22}$. Note that only those components acting on mass point 22 are computed.

$$(F_v)_{12} = \frac{E}{2(1+\nu)(1-2\nu)}\left[(1- \quad)(v_{22} - v_{13}) + \nu(u_{23} - u_{12})\right]$$

$$= \frac{1{,}000}{2(1+0.25)(1-0.5)}\left[(1-0.25)(0) - 0.25(0.0125)\right]$$

$$= -2.5 \text{ kips}$$

$$(F_{uv})_{12} = \frac{E}{4(1+\nu)}(u_{23} - u_{13} + v_{23} - v_{12})$$

$$= \frac{1{,}000}{4(1+0.25)}(0 - 0 + 0 - 0.0125)$$

$$= -2.5 \text{ kips}$$

$$(F_u)_{11} = \frac{E}{2(1+\nu)(1-2\nu)}\left[(1-\nu)(u_{22} - u_{11}) + \nu(v_{21} - v_{12})\right]$$

$$= \frac{1{,}000}{2(1+0.25)(1-0.5)}\left[(1-0.25)(0) - 0.25(0.0125)\right]$$

$$= -2.5 \text{ kips}$$

$$(F_{uv})_{11} = \frac{E}{4(1+\nu)}(u_{21} - u_{12} + v_{22} - v_{11})$$

$$= \frac{1{,}000}{4(1+0.25)}(0 - 0.0125 + 0 - 0)$$

$$= -2.5 \text{ kips}$$

Note that for the first cycle, mass point 22 has not been moved. Hence, $u_{22} = v_{22} = 0$ and all force components at stress points 21 and 22 = 0. From symmetry, it can also be concluded that

Step	Operation

$$(F_y)_{12} = (F_x)_{11} \qquad (F_{xy})_{12} = (F_{xy})_{11}$$

The equality of the shearing forces and the normal forces at a stress point on this first cycle is a coincidence.

6 Following the sign convention of Figure C-2

$$\Sigma(F_x)_{22} = -(F_{xy})_{12} - (F_x)_{11} + (F_{xy})_{21} + (F_x)_{22}$$

$$= -(-2.5) - (-2.5) = +5.0 \text{ kips}$$

$$\Sigma(F_y)_{22} = -(F_y)_{12} - (F_{xy})_{11} + (F_y)_{21} + (F_{xy})_{22}$$

$$= -(-2.5) - (-2.5) = +5.0 \text{ kips}$$

7 New u_{22} = old u_{22} + $(f_x)_{22}\Sigma(F_x)_{22}$

$$u_{22} = 0 + (0.000625)(5) = 3.125 \times 10^{-3} \text{ inches}$$

Similarly

$$v_{22} = 0 + (0.000625)(5) = 3.125 \times 10^{-3} \text{ inches}$$

Note that these displacements of mass point 22 destroy the equilibrium of mass point 12.

8 This is the last mass point and the end of the first cycle of relaxation. Go to 10.

10 All mass points are not in equilibrium since the displacements u_{22} and v_{22} under step 7 above destroyed the equilibrium of mass point 12. Therefore, there must be a second cycle of relaxation, beginning at step 3. Note, however, that in only one cycle of relaxation and displacement, components have attained nearly 90% of their final values.

The operations listed above demonstrate the procedure for elastic behavior. Suppose that a sufficient number of relaxation cycles have been performed to bring both mass points to within an acceptable error in the equilibrium equations. The following discussion indicates how the yield criterion is applied (Step 11 of Figure C-4) and how the force components at a yielded stress point (Step 9a of Figure C-4) are computed.

To illustrate the application of the yield criterion, assume that the yield stress in simple tension for the material is 35 ksi. Then the yield stress in simple shear is

$$k = \frac{\sigma_{yield}}{2} = \frac{35}{2} = 17.5 \text{ ksi}$$

Using the equilibrium displacements from Equation C-22 and applying the yield criterion (Equation C-31) to stress point 12, we get

$$(u_{23} - u_{12} - v_{22} + v_{13})^2 + (u_{22} - u_{13} + v_{23} - v_{12})^2 \leq \left(\frac{k\delta}{G}\right)^2$$

$$(0 - 0.01429 - 0.003571 + 0)^2$$

$$+ (0.003571 - 0 + 0 - 0.01429)^2 \leq \left[\frac{(17.5)(1.414)}{\frac{1,000}{2(1 + 0.25)}}\right]^2$$

$$0.000434 < 0.00383$$

and for stress point 22 we get

$$(u_{33} - u_{22} - v_{32} + v_{23})^2 + (u_{32} - u_{23} + v_{33} - v_{22})^2 \leq \left(\frac{k\delta}{G}\right)^2$$

$$(0 - 0.003571 - 0 + 0)^2$$

$$+ (0 - 0 + 0 - 0.0003571)^2 \leq \left[\frac{(17.5)(1.414)}{\frac{1,000}{2(1 + 0.25)}}\right]^2$$

$$0.0000255 < 0.00383$$

Therefore, both stress points have not yielded at an external pressure of 14.14 ksi. First yielding will take place at stress point 11 and 12 at an external pressure of

$$\left(\sqrt{\frac{0.00383}{0.000434}}\right) 14.14 \text{ ksi} = 42 \text{ ksi}$$

Note that this value of external stress is considerably greater than the yield stress in simple tension or compression of 35 ksi assumed for the material. This is a characteristic of failure or yielding in two dimensional stress systems.

Until the external load level has reached 42 ksi, all forces and displacements increase linearly. When this elastic limit has been reached, the corresponding forces and displacements are 42/14.14 times those of Equations C-33 and C-34:

$$u_{12} = v_{12} = 4.244 \times 10^{-2} \text{ inches}$$

$$u_{22} = v_{22} = 1.061 \times 10^{-2} \text{ inches}$$

$$(F_x)_{12} = -23.34 \text{ kips} \qquad \text{(C-36)}$$

$$(F_y)_{12} = -2.12 \text{ kips}$$

$$(F_{xy})_{12} = -6.37 \text{ kips}$$

These values are recorded and are used to determine the total forces and displacements for the first load increment above the 42-ksi load level.

Suppose now that the external load level is increased to 49.08 ksi. As a first approximation to the final displacements at this new load level, the displacements of Equation C-36 are increased in the same ratio as the loads:

$$u_{12} = v_{12} = \left(\frac{49.08}{42.0}\right)(0.04244) = 0.04959 \text{ inch}$$

$$u_{22} = v_{22} = \left(\frac{49.08}{42.0}\right)(0.01061) = 0.01240 \text{ inch} \qquad \text{(C-37)}$$

Note that two sets of displacements are available: the last set of equilibrium displacements, Equation C-36, and the current set of displacements, Equation C-37 (which in general is not compatible with the condition of equilibrium). These two sets of displacements are necessary in order to compute the incremental plastic force components as discussed previously.

These incremental plastic force components can be computed from Equation C-32 for stress point 12 as follows:

$$(F_x)_{12} = A(\Delta u_{23} - \Delta u_{12}) + B(\Delta v_{22} - \Delta v_{13})$$

$$-C(\Delta u_{22} - \Delta u_{13} - \Delta v_{23} - \Delta v_{12})$$

$$(F_y)_{12} = B(\Delta u_{23} - \Delta u_{12}) + A(\Delta v_{22} - \Delta v_{13})$$

$$+ C(\Delta u_{22} - \Delta u_{13} - \Delta v_{23} - \Delta v_{12})$$

$$(F_{xy})_{12} = -C(\Delta u_{23} - \Delta u_{12}) + C(\Delta v_{22} - \Delta v_{13})$$

$$+ D(\Delta u_{22} - \Delta u_{13} - \Delta v_{23} - \Delta v_{12})$$

where $$A = \frac{1}{2}\left\{\frac{4G + 3K}{3} - \frac{G}{k^2\delta^2}\left[(F_x)_{12} - (F_y)_{12}\right]^2\right\}$$

$$B = \frac{1}{2}\left\{\frac{-2G + 3K}{3} + \frac{G}{k^2\delta^2}\left[(F_x)_{12} - (F_y)_{12}\right]^2\right\}$$

$$C = \frac{G}{k^2\delta^2}(F_{xy})_{12}\left[(F_x)_{12} - (F_y)_{12}\right]$$

$$D = \frac{1}{2}\left[G - \frac{4G}{k^2\delta^2}(F_{xy})_{12}^2\right]$$

$$G = \frac{E}{2(1 + \nu)}$$

$$K = \frac{E}{3(1 - 2\nu)}$$

Note that these equations require instantaneous values of the force components if the incremental force components are to be computed. For small increments in the external loading, the instantaneous forces are very nearly equal to the forces at the last equilibrium configuration, Equation C-36.

Thus, the incremental relationships by which the incremental force components in the plastic region can be computed may be determined. The next step requires an approximation of the forces at the stress points by adding the incremental forces to the last set of forces. Finally, the forces acting at a yielded stress point are computed, and the relaxation technique proceeds as before.

Appendix D

DERIVATION OF SELECTED EQUATIONS

by W. D. Atkins

In this appendix, the equations necessary to apply the downgrade option in PERFPLAS II are derived and then the equations used in subroutine CORRECT are presented.

Downgrade Option

The yield criterion equation is the equation of a circle with its center at the origin and a radius of δk:

$$\frac{(F_x - F_y)^2}{4} + F_{xy}^2 = \frac{\delta^2 k^2}{4}$$

or $$(F_x - F_y)^2 + 4F_{xy}^2 = \delta^2 k^2$$

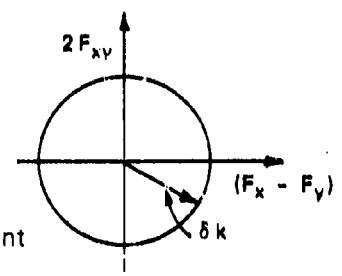

where F_x = force in x direction at a stress point

F_y = force in y direction at a stress point

F_{xy} = shear force on the x-y plane at a stress point

δ = diagonal distance between mass points

k = yield stress in simple shear of material

Only the linear elastic case will be considered. That is, it is assumed that the forces at any stress point will vary linearly with variations in applied loads. Further it will be assumed that the forces at a stress point which has yielded at the current loading are computed using the elastic equations. Referring to Figure D-1, the subscripts 1, 2, and 3 denote conditions before, at, and after yield.

Mathematically

$$\left[\left(F_{x_1} - F_{y_1}\right)^2 + 4F_{xy_1}^2\right]^{1/2} < \delta k$$

$$\left[\left(F_{x_2} - F_{y_2}\right)^2 + 4F_{xy_2}^2\right]^{1/2} = \delta k, \text{ yield criterion}$$

$$\left[\left(F_{x_3} - F_{y_3}\right)^2 + 4F_{xy_3}^2\right]^{1/2} > \delta k$$

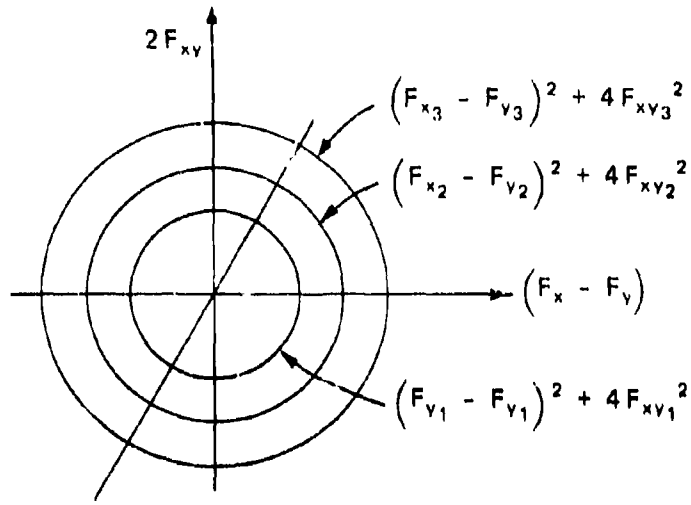

Figure D-1. Soil yield criterion.

What is required to be found is the load increment, $\Delta\ell$, necessary to change the state of stress from condition 3 to condition 2. Setting the load equal to L, then $L_3 - L_1 = \Delta L$, or change in load and $L_2 - L_2 = \Delta\ell$, or load increment. If there is a change in $\left[(F_x - F_y)^2 + 4F_{xy}^2\right]^{1/2}$, then a unit change in load is

$$\frac{\left[\left(F_{x_3} - F_{y_3}\right)^2 + 4F_{xy_3}^2\right]^{1/2} - \left[\left(F_{x_1} - F_{y_1}\right)^2 + 4F_{xy_1}^2\right]^{1/2}}{\Delta L}$$

and that the value of

$$\left[\left(F_{x_2} - F_{y_2}\right) + 4F_{xy_2}^2\right]^{1/2} = \delta k$$

Then

$$\frac{\left[\left(F_{x_3} - F_{y_3}\right)^2 + 4F_{xy_3}^2\right]^{1/2} + \Delta\ell\left\{\left[\left(F_{x_3} - F_{y_3}\right)^2 + 4F_{xy_3}^2\right]^{1/2} - \left[\left(F_{x_1} - F_{y_1}\right)^2 + 4F_{xy_1}^2\right]^{1/2}\right\}}{\Delta L} = \delta k$$

Finally

$$\Delta\ell = \frac{\left\{\delta k - \left[\left(F_{x_3} - F_{y_3}\right)^2 + 4F_{xy_3}^2\right]^{1/2}\right\}\Delta L}{\left[\left(F_{x_3} - F_{y_3}\right)^2 + 4F_{xy_3}^2\right]^{1/2} - \left[\left(F_{x_1} - F_{y_1}\right)^2 + 4F_{xy_1}^2\right]^{1/2}}$$

Subroutine CORRECT

At the end of an increment of plastic straining, the stresses at an already yielded point may exceed the yield condition, since approximate linearized equations are used. For any assumed increment of plastic strain along a chosen direction, the force-displacement relations given in Appendix C will indicate changes in stress lying along the tangent to the Mohr circle.

Thus, after several successive plastic strain increments, the stress condition might well be in excess of the yield condition. To prevent this, a correction must be made at the end of each increment to bring the stresses back to the yield surface along the radius through the stress state existing at the end of the increment. The correction to be applied is derived in the following pages.

Referring to Figure D-2, the following quantities are known:

$$F_{x_2} = \frac{\sigma_{x_2}\delta}{2} \; ; \quad F_{y_2} = \frac{\sigma_{y_2}\delta}{2} \; ; \quad F_{xy_2} = \frac{\tau_{xy_2}\delta}{2}$$

$$H = \frac{\sigma_{x_1} + \sigma_{y_1}}{2} = \frac{\sigma_{x_2} + \sigma_{y_2}}{2}$$

It is required to find

$$F_{x_1} = \frac{\sigma_{x_1}\delta}{2} \; ; \quad F_{y_1} = \frac{\sigma_{y_1}\delta}{2} \; ; \quad F_{xy_1} = \frac{\tau_{xy_1}\delta}{2}$$

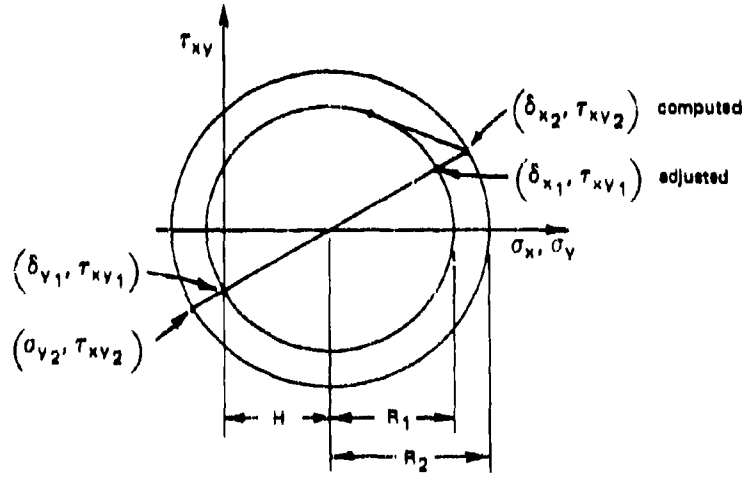

Figure D-2. Mohr circle.

It is necessary to define

$$\tau_{max_2} = R^2 = \sqrt{\left(\frac{\sigma_{x_2} - \delta_{y_2}}{2}\right)^2 + \tau_{xy_2}^2}$$

$$= \sqrt{\left(\frac{\frac{2F_{x_2}}{\delta} - \frac{2F_{y_2}}{\delta}}{2}\right)^2 + \left(\frac{2F_{xy_2}}{\delta}\right)^2}$$

$$= \frac{2}{\delta}\sqrt{\left(\frac{F_{x_2} - F_{y_2}}{2}\right)^2 + F_{xy_2}^2}$$

$$= \sqrt{J_2}$$

Thus $$R_2 = \sqrt{J_2}$$

and since after adjustment

$$J_2 = k$$

then $$R_1 = k$$

The derivation then proceeds as follows: From the low of similar triangles

$$\frac{\sigma_{x_1} - H}{R_1} = \frac{\sigma_{x_2} - H}{R_2}$$

$$\sigma_{x_1} = \frac{R_1}{R_2}\left(\sigma_{x_2} - H\right) + H$$

$$\sigma_{x_1} = \frac{R_1}{R_2}\left(\sigma_{x_2} - \frac{\sigma_{x_2}}{2} - \frac{\sigma_{y_2}}{2}\right) + \frac{\sigma_{x_2} + \sigma_{y_2}}{2}$$

$$= \frac{R_1}{R_2}\left(\frac{\sigma_{x_2} - \sigma_{y_2}}{2}\right) + \frac{\sigma_{x_2} + \sigma_{y_2}}{2}$$

$$\frac{2F_{x_1}}{\delta} = \frac{R_1}{R_2}\left(\frac{\frac{2F_{x_2}}{\delta} - \frac{2F_{y_2}}{\delta}}{2}\right) + \frac{2F_{x_2} + 2F_{y_2}}{2\delta}$$

$$2F_{x_1} = \frac{R_1}{R_2}\left(F_{x_2} - F_{y_2}\right) + \left(F_{x_2} + F_{y_2}\right)$$

$$F_{x_1} = \frac{R_1}{R_2}\left(\frac{F_{x_2} - F_{y_2}}{2}\right) + \frac{F_{x_2} + F_{y_2}}{2}$$

$$F_{x_1} = \frac{k}{\sqrt{J_2}}\left(\frac{F_{x_2} - F_{y_2}}{2}\right) + \frac{F_{x_2} + F_{y_2}}{2}$$

or

$$F_x{}^1 = \frac{k}{\sqrt{J_2}}\left(\frac{F_x - F_y}{2}\right) + \frac{F_x + F_y}{2}$$

$$= \frac{k}{\sqrt{J_2}}\left(\frac{F_x}{2}\right) - \frac{kF_y}{\sqrt{J_2}} + \frac{F_x}{2} + \frac{F_y}{2}$$

$$F_x{}^1 = \frac{F_x}{2}\left(1 + \frac{k}{\sqrt{J_2}}\right) + \frac{F_y}{2}\left(1 - \frac{k}{\sqrt{J_2}}\right)$$

similarly

$$\frac{\sigma_{y_1} - H}{R_1} = \frac{\sigma_{y_2} - H}{R_2}$$

$$\sigma_{y_1} = \frac{R_1}{R_2}\left(\sigma_{y_2} - H\right) + H$$

$$\sigma_{y_1} = \frac{R_1}{R_2}\left(\sigma_{y_2} - \frac{\sigma_{x_2}}{2} - \frac{\sigma_{y_2}}{2}\right) + \frac{\sigma_{x_2} + \sigma_{y_2}}{2}$$

$$= \frac{R_1}{R_2}\left(\frac{\sigma_{y_2} - \sigma_{y_2}}{2}\right) + \frac{\sigma_{x_2} + \sigma_{y_2}}{2}$$

$$\frac{2F_{y_1}}{\delta} = \frac{R_1}{R_2}\left(\frac{\frac{2F_{y_2}}{\delta} - \frac{2F_{x_2}}{\delta}}{2}\right) + \frac{\frac{2F_{x_2}}{\delta} + \frac{2F_{y_2}}{\delta}}{2}$$

$$F_{y_2} = \frac{R_1}{R_2}\left(\frac{F_{y_2} - F_{x_2}}{2}\right) + \frac{F_{x_2} + F_{y_2}}{2}$$

or $$F_y{}^1 = \frac{k}{\sqrt{J_2}}\left(\frac{F_y - F_x}{2}\right) + \frac{F_x + F_y}{2}$$

$$F_y{}^1 = \frac{F_x}{2}\left(1 - \frac{k}{\sqrt{J_2}}\right) + \frac{F_y}{2}\left(1 + \frac{k}{\sqrt{J_2}}\right)$$

and again

$$\frac{\tau_{xy_1}}{R_1} = \frac{\tau_{xy_2}}{R_2}$$

$$\tau_{xy_1} = \frac{R_1}{R_2}\left(\tau_{xy_2}\right)$$

$$\frac{2F_{xy_1}}{\delta} = \frac{R_1}{R_2}\left(\frac{2F_{xy_2}}{\delta}\right)$$

$$F_{xy_1} = \frac{R_1}{R_2} F_{xy_2}$$

or $$F_{xy}{}^1 = \frac{k}{\sqrt{J_2}} F_{xy}$$

Appendix E

DATA INPUT GUIDE FOR PROGRAM PERFPLAS II

by

N. Shoemaker

GENERAL PROGRAM NOTES

1. THE DATA CARDS MUST BE STACKED IN PROPER ORDER FOR THE PROGRAM TO RUN.
2. ANY NUMBER OF PROBLEMS CAN BE SOLVED WITH ONE RUN BY STACKING THE DATA.
3. CONSISTENT UNITS MUST BE USED WITHIN A PROBLEM. BUT UNITS MAY VARY BETWEEN PROBLEMS.
4. ALL 5-SPACE WORDS ARE FIXED POINT NUMBERS AND SHOULD BE RIGHT JUSTIFIED.
5. ALL 10-SPACE WORDS ARE FLOATING POINT NUMBERS AND SHOULD CONTAIN A DECIMAL POINT.
6. ANY DESIRED INFORMATION MAY BE READ IN ON THE HEADER CARD.
7. THE DIMENSION STATEMENT RESERVES STORAGE FOR 36 X 36 MASS POINTS AND 35 X 35 STRESS POINTS.
8. THE MATHEMATICAL MODEL HAS MASS POINTS ALONG ALL FOUR BOUNDARIES.
9. LOADS MAY BE APPLIED TO ANY OR ALL MASS POINTS.

INPUT CARD FORMS

1. HEADER CARD... (80H)

   A. COLUMN 1. ONE(1)

   B. COLUMNS 2-80. ANY ALPHANUMERIC INFORMATION WHICH MAY BE USED TO

IDENTIFY THE PROBLEM.

2. FIRST PARAMETER CARD... (8I5)

   A. COLUMNS 4-5. NUMBER OF ROWS OF MASS POINTS, N.

   B. COLUMNS 9-10. NUMBER OF COLUMNS OF MASS POINTS, M.

   C. BOUNDARY CONDITIONS... (SEE NOTE 1 BELOW.)

      (1) COLUMN 15. BOUNDARY CONDITION OPTION FOR THE LEFT BOUNDARY, NLEFT. (SEE NOTE 2 BELOW.)

(2) COLUMN 20. BOUNDARY CONDITION OPTION FOR THE RIGHT BOUNDARY, NRIGHT. (SEE NOTE 3 BELOW.)

(3) COLUMN 25. BOUNDARY CONDITION OPTION FOR THE TOP BOUNDARY, NTOP. (SEE NOTE 4 BELOW.)

(4) COLUMN 30. BOUNDARY CONDITION OPTION FOR THE BOTTOM BOUNDARY, NBOT. (SEE NOTE 5 BELOW.)

D. COLUMN 35. LOAD OPTION, NALPHA. (SEE NOTE 6 BELOW.)

E. COLUMNS 36-40. NUMBER OF LOAD CARDS, NLDPT.

3. SECOND PARAMETER CARD... (6E10.5)

A. COLUMNS 1-10. MODULUS OF ELASTICITY OF THE MATERIAL, E.

B. COLUMNS 11-20. POISSONS RATIO FOR THE MATERIAL, GNU.

C. COLUMNS 21-30. YIELD STRESS IN SIMPLE SHEAR FOR THE MATERIAL, FK.

D. COLUMNS 31-40. SHORTEST DISTANCE BETWEEN MASS POINTS, FLAMDA.

E. COLUMNS 41-50. CONVERGENCE CRITERION, EPSI. (SEE NOTE 7 BELOW.)

F. COLUMNS 51-60. INITIAL VALUE OF THE MAXIMUM-COMPONENT LOAD APPLIED, TL. (SEE NOTES 8 AND 10 BELOW.)

G. COLUMNS 61-70. VALUE OF THE STANDARD MAXIMUM-COMPONENT LOAD INCREMENT, DELP. (SEE NOTE 10 BELOW.)

H. COLUMNS 71-80. MAXIMUM VALUE WHICH THE MAXIMUM-COMPONENT LOAD MAY ATTAIN, TTOTAL. (SEE NOTE 10 BELOW.)

4. LOAD CARDS...(2I5,2E10.5,I5) - (SEE NOTES 8,9 AND 10 BELOW.)

A. COLUMNS 4-5. ROW INDEX, I OF THE LOADED MASS POINT.

B. COLUMNS 5-10. COLUMN INDEX, J OF THE LOADED MASS POINT.

C. COLUMNS 11-20. X COMPONENT, PX OF THE INITIAL LOAD APPLIED TO MASS POINT (I,J).

D. COLUMNS 21-30. Y COMPONENT, PY OF THE INITIAL LOAD APPLIED TO MASS POINT (I,J).

E. COLUMN 35. BEND CODE,K, TO DESCRIBE SHAPE OF LOADED BOUNDRY (SEE NOTE 11 BELOW.)

NOTES

1. BOUNDARY CONDITIONS...

A. BOUNDARY CONDITION OPTION = 1 SPECIFIES A FREE BOUNDARY.

B. BOUNDARY CONDITION OPTION = 2 SPECIFIES A FIXED BOUNDARY.

C. BOUNDARY CONDITION OPTION = 3 SPECIFIES A BOUNDARY OF SYMMETRY.

D. BOUNDARY CONDITION OPTION = 4 SPECIFIES AN APPROXIMATION OF AN INFINITE BOUNDARY.

2. THE LEFT BOUNDARY IS CURRENTLY LIMITED TO A FIXED OR AN APPROXIMATION OF AN INFINITE BOUNDARY. NLEFT = 2 OR 4 RESPECTIVELY.

3. THE RIGHT BOUNDARY IS CURRENTLY LIMITED TO A FIXED BOUNDARY, A BOUNDARY OF SYMMETRY OR AN APPROXIMATION OF AN INFINITE BOUNDARY. NRIGHT = 2, 3 OR 4 RESPECTIVELY.

4. THE TOP BOUNDARY IS CURRENTLY LIMITED TO A FREE BOUNDARY. NTOP = 1.

5. THE BOTTOM BOUNDARY IS CURRENTLY LIMITED TO A FIXED BOUNDARY OR AN APPROXIMATION OF AN INFINITE BOUNDARY. NBOT = 2 OR 4 RESPECTIVELY.

6. TO USE THE STANDARD LOAD INCREMENT WITH NO ADJUSTMENTS, NALPHA = 1.
TO USE THE STANDARD LOAD INCREMENT WITH THE DOWNGRADE ROUTINE SO THAT THE STRESS POINTS WILL YIELD ONE AT A TIME, NALPHA = 2.

7. A CONVERGENCE CRITERION, EPSI OF 10^{-5} OR 10^{-6} IS SUGGESTED.

8. THE VALUE OF TL SHOULD BE THE SAME AS THE MAXIMUM VALUE OF PX AND PY INPUT FOR A PROBLEM.

9. THE NUMBER OF LOAD CARDS IS EQUAL TO THE NUMBER OF LOADED MASS POINTS, NLOPT.

10. ALL LOADS ARE COMPONENT LOADS IN THE X AND Y DIRECTIONS AND ARE APPLIED TO MASS POINTS. THE POSITIVE X-AXIS POINTS TO THE SOUTHEAST AND THE POSITIVE Y-AXIS POINTS TO THE SOUTHWEST. DOWNWARD LOADS ARE POSITIVE. HALF LOADS MAY BE APPLIED TO END MASS POINTS WHERE REQUIRED.

11. THE BEND CODE, K, INDICATES THE SHAPE OF THE LOADED BOUNDRY (WHICH IS ALWAYS IN THE UPPER RIGHT PORTION OF THE GRID.) K=1 ON A LOAD CARD WITH INDICES,(I,J), MEANS THAT MASS POINT I,J IS ON AN 'L' SHAPED PORTION OF THE LOADED BOUNDRY. K=2, THE BOUNDRY IN HORIZONTAL. K=3, THE BOUNDRY IS AN INVERTED 'L' SHAPE. K=4, THE BOUNDRY IS VERTICAL. K=5, THE MASS POINT IS ON THE FAR RIGHT VERTICAL BOUNDRY.

Appendix F

NOTATION FOR PROGRAM PERFPLAS II

by

N. Shoemaker

NOTATION

A	COEFFICIENT IN PLASTIC FORCE-DISPLACEMENT EQUATIONS
A1	COEFFICIENT IN QUADRATIC EQUATION SOLVED IN DOWNGRADE OPTION
B	COEFFICIENT IN PLASTIC FORCE-DISPLACEMENT EQUATIONS
B1	COEFFICIENT IN QUADRATIC EQUATION SOLVED IN DOWNGRADE OPTION
BDY	BOUNDARY CONDITION
BEGIN	FIRST WORD IN COMMON - USED AS AN ARGUMENT IN LIBRARY SUBROUTINE XLOCF
BMK	BULK MODULUS - PROBLEM CONSTANT
C	COEFFICIENT IN PLASTIC FORCE-DISPLACEMENT EQUATIONS
C1	COEFFICIENT IN QUADRATIC EQUATION SOLVED IN DOWNGRADE OPTION
D	COEFFICIENT IN PLASTIC FORCE-DISPLACEMENT EQUATIONS
DELOLD	MOST RECENT MAXIMUM-COMPONENT LOAD INCREMENT
DELP	STANDARD MAXIMUM-COMPONENT LOAD INCREMENT - INPUT PARAMETER
DELTA	DIAGONAL DISTANCE BETWEEN MASS POINTS

DELTL	CURRENT MAXIMUM-COMPONENT LOAD INCREMENT
E	YOUNGS MODULUS OF ELASTICITY - INPUT PARAMETER
ENDT	LAST WORD IN COMMON - USED AS AN ARGUMENT IN LIBRARY SUBROUTINE XLOCF
EOV2V	PROBLEM CONSTANT USED IN ELASTIC EQUATIONS FOR FX AND FY
EOV4V	PROBLEM CONSTANT USED IN ELASTIC EQUATION FOR FXY
EPSI	CONVERGENCE CRITERION FOR MASS POINT DISPLACEMENTS WHICH IS COMPARED WITH DU/U AND DV/V AT EACH MASS POINT - INPUT PARAMETER
FJ2	SECOND INVARIANT OF STRESS DEVIATION TENSOR
FK	YIELD STRESS IN SIMPLE SHEAR - INPUT PARAMETER
FLAMDA	SHORTEST DISTANCE BETWEEN MASS POINTS - INPUT PARAMETER
FLEX	ELASTIC FLEXIBILITY COEFFICIENT FOR X DIRECTION USED IN BOTH ELASTIC AND PLASTIC DISPLACEMENT CALCULATIONS - IT IS THE DEFLECTION OF A MASS POINT IN THE DIRECTION OF AN APPLIED UNIT LOAD WITH THE DISPLACEMENT AT ALL ADJACENT MASS POINTS HELD FIXED. THE MORE APPROPRIATE THE VALUE OF FLEX, THE FASTER THE CONVERGENCE.
FLEY	ELASTIC FLEXIBILITY COEFFICIENT FOR Y DIRECTION USED IN BOTH ELASTIC AND PLASTIC DISPLACEMENT CALCULATIONS - SEE FLEX
FMAX	INDEX TO STRESS CONDITION AT A STRESS POINT - A STRESS POINT IS PLASTIC, HAS JUST YIELDED, OR IS ELASTIC IF FMAX IS GREATER THAN, EQUAL TO, OR LESS THAN SKORD RESPECTIVELY.

FX	CURRENT VALUE OF X-COMPONENT FORCE AT ELASTIC STRESS POINTS - FORCE IN X DIRECTION FOR MOST RECENT LOADING AT PLASTIC STRESS POINTS
FXOLD	X-COMPONENT FORCE AT STRESS POINT ISTORE, JSTORE FOR MOST RECENT LOADING
FXONE	X-COMPONENT FORCE AT STRESS POINT WHICH IS TO LOWER RIGHT OF MASS POINT I, J
FXTWO	X-COMPONENT FORCE AT STRESS POINT WHICH IS TO UPPER LEFT OF MASS POINT I, J
FXY	CURRENT VALUE OF SHEAR FORCE AT ELASTIC STRESS POINTS - SHEAR FORCE FOR MOST RECENT LOADING AT PLASTIC STRESS POINTS
FXYOLD	SHEAR FORCE AT STRESS POINT ISTORE, JSTORE FOR MOST RECENT LOADING
FY	CURRENT VALUE OF Y-COMPONENT FORCE AT ELASTIC STRESS POINTS - FORCE IN Y DIRECTION FOR MOST RECENT LOADING AT PLASTIC STRESS POINTS
FYOLD	Y-COMPONENT FORCE AT STRESS POINT ISTORE, JSTORE FOR MOST RECENT LOADING
FYONE	Y-COMPONENT FORCE AT STRESS POINT WHICH IS TO LOWER LEFT OF MASS POINT I, J
FYTWO	Y-COMPONENT FORCE AT STRESS POINT WHICH IS TO UPPER RIGHT OF MASS POINT I, J

G	SHEAR MODULUS - PROBLEM CONSTANT USED IN PLASTIC EQUATIONS FOR FXY
GMIK	PROBLEM CONSTANT USED IN PLASTIC EQUATIONS FOR FX AND FY
GNU	POISSONS RATIO - INPUT PARAMETER
GOKK	PROBLEM CONSTANT USED IN PLASTIC EQUATIONS FOR FX, FY AND FXY
GPLK	PROBLEM CONSTANT USED IN PLASTIC EQUATIONS FOR FX AND FY
HD	HORIZONTAL DISPLACEMENT OF MASS POINT
HS	HORIZONTAL STRESS AT STRESS POINT
I	ROW INDEX
II	INDEX OF DO LOOP WHICH SETS ALL COMMON STORAGE LOCATIONS TO ZERO
ISTORE	ROW INDEX OF THE HIGHEST STRESSED STRESS POINT WHICH HAS JUST YIELDED
J	COLUMN INDEX
JSTORE	COLUMN INDEX OF THE HIGHEST STRESSED STRESS POINT WHICH HAS JUST YIELDED
K	TEMPORARY STORAGE FOR MUGA
K	ROW INDEX OF STRESS POINT WHOSE FORCES ARE TO BE DETERMINED
L	COLUMN INDEX OF STRESS POINT WHOSE FORCES ARE TO BE DETERMINED

M	NUMBER OF COLUMNS OF MASS POINTS - INPUT PARAMETER
MM1	NUMBER OF COLUMNS OF STRESS POINTS, M-1
MUSA	INDICATOR OF SHAPE OF LOADED MASS POINT BOUNDRY
MJM	NUMBER OF MASS POINTS IN ROW I
N	NUMBER OF ROWS OF MASS POINTS - INPUT PARAMETER
NALPHA	LOAD OPTION - INPUT PARAMETER
NBOT	BOUNDARY CONDITION OPTION FOR BOTTOM BOUNDARY - INPUT PARAMETER
NIN	STANDARD INPUT TAPE
NL	INDEX OF DO LOOP WHICH READS LOAD CARDS
NLDPT	NUMBER OF LOAD CARDS IN INPUT DATA AND EQUAL TO NUMBER OF LOADED MASS POINTS - INPUT PARAMETER
NLEFT	BOUNDARY CONDITION OPTION FOR LEFT BOUNDARY - INPUT PARAMETER
NN1	NUMBER OF ROWS OF STRESS POINTS, N-1
NNYT	STRESS POINT YIELD CODE - NNYT = 0, 1, OR 2 IF STRESS POINT HAS NOT YIELDED, YIELDED AT A PREVIOUS LOADING, OR HAS JUST YIELDED RESPECTIVELY.

%OUT	STANDARD OUTPUT TAPE
%RIGHT	BOUNDARY CONDITION OPTION FOR RIGHT BOUNDARY - INPUT PARAMETER
%SIGN	DISPLACEMENT CONVERGENCE FLAG - IF NEGATIVE, MASS POINT DISPLACEMENT MATRIX HAS NOT CONVERGED
%SW1	INTERNAL SWITCH - NSW1 = 1 OR 0 IF DOWNGRADE OPTION HAS OR HAS NOT BEEN EXECUTED RESPECTIVELY
%SW2	INTERNAL SWITCH
%SW3	INTERNAL SWITCH - IF NSW3 = 0 CURRENT EQUILIBRIUM VALUES OF MASS POINT DEFLECTIONS ARE STORED. IF OTHERWISE, DOWNGRADE OPTION IS BEING EXERCISED AND CURRENT EQUILIBRIUM VALUES OF MASS POINT DEFLECTIONS ARE NOT STORED.
%SW4	INTERNAL SWITCH - NSW4 = 1 OR 2, EDIT AND WRITE OUT INPUT DATA OR WRITE OUT RESULTS RESPECTIVELY
%TEMP	NUMBER OF STRESS POINTS WHICH HAVE JUST YIELDED
%TOP	BOUNDARY CONDITION OPTION FOR TOP BOUNDARY - INPUT PARAMETER
%UC	NUMBER OF STORAGE LOCATIONS USED FOR COMMON VARIABLES
%UEPY	DOUBLE CONSTANT USED IN ELASTIC EQUATIONS FOR Fx AND Fy
PX	DISPLACEMENT INDEPENDENT FORCE APPLIED IN X DIRECTION AT A GIVEN MASS POINT - INITIAL VALUE IS INPUT BUT SUBSEQUENT VALUES ARE DETERMINED INTERNALLY

PY	DISPLACEMENT INDEPENDENT FORCE APPLIED IN Y DIRECTION AT A GIVEN MASS POINT - INITIAL VALUE IS INPUT BUT SUBSEQUENT VALUES ARE DETERMINED INTERNALLY
SF	TEMPORARY VALUE OF THE SHEAR FORCE AT PLASTIC STRESS POINT K, L
SKORD	PROBLEM CONSTANT USED TO DETERMINE IF A STRESS POINT HAS YIELDED
SQRT2	SQUARE ROOT OF TWO
SS	SHEAR STRESS AT STRESS POINT
SUMFX	SUM OF ALL FORCES ACTING ON A MASS POINT IN X DIRECTION
SUMFY	SUM OF ALL FORCES ACTING ON A MASS POINT IN Y DIRECTION
SX	TEMPORARY VALUE OF X-COMPONENT FORCE AT PLASTIC STRESS POINT K, L
SXYONE	SHEAR FORCE AT STRESS POINT WHICH IS TO LOWER LEFT OF MASS POINT I, J
SXYTWO	SHEAR FORCE AT STRESS POINT WHICH IS TO UPPER RIGHT OF MASS POINT I, J
SY	TEMPORARY VALUE OF Y-COMPONENT FORCE AT PLASTIC STRESS POINT K, L
SYXONE	SHEAR FORCE AT STRESS POINT WHICH IS TO LOWER RIGHT OF MASS POINT I, J
SYXTWO	SHEAR FORCE AT STRESS POINT WHICH IS TO UPPER LEFT OF MASS POINT I, J

TEMP1 TEMP2 TEMP3 TEMP4	TEMPORARY STORAGE - USED TO GROUP VARIABLES COMMON TO SEVERAL EQUATIONS
TL	INITIAL VALUE OF MAXIMUM-COMPONENT LOAD APPLIED - INPUT PARAMETER
TTOTAL	MAXIMUM VALUE WHICH THE MAXIMUM-COMPONENT LOAD WILL ATTAIN WHEN STANDARD LOAD INCREMENT OPTION IS USED (NALPHA = 1) BUT IT WILL BE EXCEEDED SLIGHTLY WHEN DOWNGRADE OPTION IS USED (NALPHA = 2) - INPUT PARAMETER
U	CURRENT DISPLACEMENT OF MASS POINT IN X DIRECTION
UOLD	DISPLACEMENT OF MASS POINT IN X DIRECTION FOR MOST RECENT LOADING
V	CURRENT DISPLACEMENT OF MASS POINT IN Y DIRECTION
VD	VERTICAL DISPLACEMENT OF MASS POINT
VOLD	DISPLACEMENT OF MASS POINT IN Y DIRECTION FOR MOST RECENT LOADING
VS	VERTICAL STRESS AT STRESS POINT
XLCCF	LIBRARY SUBROUTINE USED TO DETERMINE NUMBER OF STORAGE LOCATIONS USED FOR COMMON VARIABLES, NWK
YR	YIELD RATIO - SQUARE ROOT OF SECOND INVARIANT OF STRESS DEVIATION TENSOR, FJ2, DIVIDED BY YIELD STRESS IN SIMPLE SHEAR
YT	YIELD STRESS IN SIMPLE SHEAR, FK, DIVIDED BY SQUARE ROOT OF SECOND INVARIANT OF STRESS DEVIATION TENSOR, FJ2

Appendix G

LISTING OF PROGRAM PERFPLAS II

by

N. Shoemaker

```
$EXECUTE        FORTRAN
*       KEC
C-------PROGRAM PEPFPLAS II  -  WRITTEN IN FORTRAN II FOR THE IBM 7094.
C       THIS IS THE PRINCIPLE PROGRAM.  IT READS THE INPUT DATA, CALLS SUBROUTINES
C       OUT, MAIN AND SEARCH, AND CALCULATES CONSTANTS USED IN THE SUBROUTINES.
        DIMENSION MUGA(36,36),MUM(36)
        DIMENSION BEGIN(1),PX(36,36),PY(36,36),U(36,36),V(36,36),
       1UOLD(36,36),VOLD(36,36),FX(35,35),FY(35,35),FXY(35,35),NNYT(35,35)
        COMMON BEGIN,FXONE,FXTWO,SXYONE,SXYTWO,FYONE,FYTWO,SYXONE,SYXTWO,
       1ONEFV,EOV2V,EOV4V,G,SOKK,SPLK,SMIK,SKORD,FK,DELTA,DELTL,TL,GNU,
       2EPSI,E,FLAMDA,TTOTAL,DELP,FLEX,FLEY,DELOLD,U,V,PX,PY,FX,FY,FXY,
       3SQRT2,UOLD,VOLD,N,M,NLEFT,NRIGHT,NTOP,NBOT,NP1,NM1,NNYT,NALPHA,
       4NIN,NOUT,MUGA,MUM,ENDT
 1000 FORMAT (20H
      1                                                  1
 1001 FORMAT (8I5)
 1002 FORMAT(8E10.5)
 1004 FORMAT  (2I5, 2E10.5,I5)
C-------SET ALL COMMON STORAGE LOCATIONS TO ZERO.
  100 NNK=XLOCF(BEGIN)-XLOCF(ENDT)+1
      DO 101 I=1,NNK
  101 BEGIN(I)=0.
C-------DEFINE INPUT AND OUTPUT TAPES.
      NIN=5
      NOUT=6
C-------READ AND PRINT HEADER CARD.
      READ INPUT TAPE NIN,1000
      WRITE OUTPUT TAPE NOUT,1000
C-------READ NO. ROWS, NO. COLUMNS, BOUNDARY CONDITIONS, LOAD OPTION, AND NO. OF
C       LOAD CARDS.
      READ INPUT TAPE NIN, 1001, N, M, NLEFT, NRIGHT, NTOP, NBOT,
     1     NALPHA, NLOPT
```

```
C------READ MATERIAL PROPERTIES, SHORTEST DISTANCE BETWEEN MASS POINTS, CLOSURE
C      CRITERION, AND LOAD DATA.
       READ INPUT TAPE NIN, 1002, E, GNU, FK, FLAMDA, EPSI, TL,
      1     DELP, TITAL
C------READ THE COORDINATES OF EACH LOADED MASS POINT AND THE COMPONENTS OF THE
C      LOAD AT THE MASS POINT, AND THE BEND CODE.
       DO 102 KL = 1, NLOPT
       READ INPUT TAPE NIN, 1004, I, J, (PX(I,J)), PY(I,J),K
       NUSA(I,J)=K
     1 NUM(I)=J
   102 CONTINUE
       DO 2 I=1,N
       IF(NUM(I)-3,3,2
     3 NUM(I)=M
     2 CONTINUE
       CALL OUT (1)
C------DEFINE PROBLEM CONSTANTS.
       NM1=N-1
       MM1=M-1
       SQRT2=1.414213562
       DELTA=FLAMDA*SQRT2
       DELTL = TL
       DELOLD = TI
       FLEX=2.*(1.+GNU)*(1.-2.*GNU)/(E*( 3.-4.* GNU))
       FLEY=FLEX
       ONEPV=1.-GNU
       EOV2V=E*.5/((1. + GNU)*(1. - 2. * GNU))
       EOV4V=E*.25/(1. + GNU)
       SMK=E/(3.*(1.-2.*GNU))
       G=E/(2.*(1.+GNU))
```

```
      GOKK=G/(FK*FK)
      GPLK=(3.*GMK  +  4. * G)/3.
      GMIK=(3.* GMK -2.*G )/3.
      SKORD = (FK*DELTA/G)*(FK*DELTA/G)
  310 CALL MAIN
      CALL SEARCH
C-----CHECK TO SEE IF THE PROBLEM HAS BEEN COMPLETED.
      IF ( ABSF(TL) - ABSF(TTOTAL) ) 311, 100, 100
  311 DELTL = DELP
      CALL ADD (2)
      DELOLD = DELP
      GO TO 310
      END
      SUBROUTINE MAIN
C-----ITERATIVE SUBROUTINE WHICH ADJUSTS THE MASS POINTS DEFLECTIONS UNTIL THEY
C     ARE IN EQUILIBRIUM UNDER THE GIVEN LOADING AND BOUNDARY CONDITIONS.
      DIMENSION MGA(36,36),MGP(36)
      DIMENSION BEGIN(1),PX(36,36),PY(36,36),U(36,36),V(36,36),
     1UOLD(36,36),VOLD(36,36),FX(35,35),FY(35,35),FXY(35,35),MAYT(35,35)
      COMMON BEGIN,FXONE,FXTWO,SXYONE,SXYTWO,FYONE,FYTWO,SYXONE,SYXTWO,
     1ONEPY,ECVZY,ECY4Y,G,GOKK,GPLK,GMIK,SKORD,FK,DELTA,DELTL,TL,GNU,
     2EPSI,E,FLAMDA,TTOTAL,DELP,FLEX,FLEY,DELOLD,U,V,PX,PY,FX,FY,FXY,
     3SORT2,UOLD,VOLD,N,M,NLEFT,NRIGHT,NTOP,NBOT,NM1,MM1,MAYT,NALPHA,
     4NI,NOUT,MGA,MGP,ENDT
C-----SET NON-CONVERGED FLAG SO THAT THERE WILL BE AT LEAST TWO ITERATIONS.
      NSIGN=-1
      GO TO 104
  103 NSIGN=+1
  104 CALL TOP
      DO 500 I=2,NM1
```

```
      CALL LEFT (I)
      [illegible]=[illegible](I)-1
      DO 510 J=2,[illegible]
      KICK=[illegible](I,J)+1
      GO TO (370,371,372),KICK
  371 CALL FORCE(3,I,J)
      CALL FORCE(2,I,J)
      CALL FORCE(1,I,J)
      SUMFX=FXONE-FXTWO+SXYONE+PX(I,J)
      SUMFY=FYONE+SYXONE-SYXTWO+PY(I,J)
      GO TO 373
  372 CALL FORCE(2,I,J)
      CALL FORCE(1,I,J)
      SUMFX=FXONE+SXYONE+PX(I,J)
      SUMFY=FYONE+SYXONE+PY(I,J)
      GO TO 373
  370 CALL FORCE (4, I, J)
      CALL FORCE (1, I, J)
      CALL FORCE (3, I, J)
      CALL FORCE (2, I, J)
C-----SUM FORCES IN THE X AND Y DIRECTIONS.
      SUMFX=FXONE-FXTWO+SXYONE-SXYTWO+PX(I,J)
      SUMFY=FYONE-FYTWO+SYXONE-SYXTWO+PY(I,J)
C---- -CHECK FOR CONVERGENCE.
  373 IF (ABSF(SUMFX*FLEX/U(I,J)) - EPS) 520, 520, 540
  520 IF (ABSF(SUMFY*FLEY/V(I,J)) - EPS) 411, 411, 540
  540 NSIGN=-1
C-----ADJUST MASS POINT DEFLECTIONS FOR EQUILIBRIUM OF FORCES ON THE MASS POINT.
  411 U(I,J)=U(I,J)+FLEX*SUMFX
      V(I,J)= V(I,J)+FLEY*SUMFY
```

```
  510 CONTINUE
      IF (NNN+1-M)492,499,492
  492 J=NNN+1
      KICK=MUGA(I,J)-2
      GO TO(493,494,499),KICK
  493 CALL FORCE(2,I,J)
      SUMFX=SXYONE*PX(I,J)
      SUMFY=FYONE*PY(I,J)
      GO TO 11
  494 CALL FORCE(3,I,J)
      CALL FORCE(2,I,J)
      SUMFX=SXYONE-FXTWO*PX(I,J)
      SUMFY=FYONE-SYXTWO*PY(I,J)
   11 U(I,J )=U(I,J)+FLEX*SUMFX
      V(I,J )=V(I,J)+FLEY*SUMFY
      GO TO 500
  496 CALL RIGHT (I)
  500 CONTINUE
      CALL BOTTOM
C-----CHECK CONVERGENCE FLAG.
      IF(NSIGN)103,103,509
  509 RETURN
      END
      SUBROUTINE SEARCH
C-----CHECK STRESS CONDITION OF EACH STRESS POINT AND SET ITS YIELD FLAG, NNYT
C     ACCORDINGLY.  UPDATE FX, FY, AND FXY AT EACH STRESS POINT AND INVOKE THE
C     DOWNGRADE OPTION IF DESIRED.
      DIMENSION MUGA(36,36),NUM(36)
      DIMENSION BEGIN(1),PX(36,36),PY(36,36),U(36,36),V(36,36),
     1OLD(36,36),VOLD(36,36),FX(35,35),FY(35,35),FXY(35,35),NNYT(35,35)
      COMMON BEGIN,FXONE,FXTWO,SXYONE,SXYTWO,FYONE,FYTWO,SYXONE,SYXTWO,
```

```
     1DREPY,EQY2V,EQY4Y,G,GOKK,GPLK,GMIK,SKORC,FK,DELTA,DELTL,TL,GNU,
     2EPSI,E,FLAMDA,TTOTAL,DELP,FLFX,FLEY,DELOLD,U,V,PX,PY,FX,FY,FXY,
     3SQRT2,UOLD,VOLD,*,*-NLEFT,NRIGHT,NTOP,NBOT,NM1,NP1,NNYT,NALPHA,
     4NIT,NOUT,NMI,NJM
      NTEMP=0
      NS=1 = 0
C-----CHECK TO SEE IF ANY NEW STRESS POINT HAS YIELDED.  IF YES, SET ITS YIELD
C     FLAG TO TWO.  SET TO ONE THE YIELD FLAG OF ANY STRESS POINT WHICH YIELDED
C     AT THE PREVIOUS LOADING.  YIELD FLAG OF ANY UNYIELDED STRESS POINT REMAINS
C     ZERO.
      DO 98 I=1,NM1
      NJM=NJ(I)-1
      DO 98 J=1,NJM
      IF(NNYT(I,J)-1)94,98,92
   92 NNYT(I,J)=1
      GO TO 98
   94 TEMP1 = U(I+1,J+1) - U(I,J) - V(I+1,J) + V(I,J+1)
      TEMP2 = U(I+1,J) - U(I,J+1) + V(I+1,J+1) - V(I,J)
      TEMP3 = TEMP1*TEMP1 + TEMP2*TEMP2
      IF (TEMP3 - SKORD) 98, 97, 97
   97 NNYT(I,J)=2
      NTEMP=NTEMP+1
   98 CONTINUE
      IF(NTEMP)5,99,5
    5 GO TO (99,804),NALPHA
C-----UPDATE FX, FY, AND FXY AT ALL STRESS POINTS.  THIS IS THE ONLY PLACE IN
C     THE PROGRAM WHERE ALL VALUES IN THE FORCE ARRAYS ARE UP TO DATE.
   99 DO 106 I=1,NM1
      NJM=NJ(I)-1
      DO 106 J=1,NJM
      CALL FORCE (5, I, J)
```

```
  105 CONTINUE
      IF(NSW1) 800, 800, 790
  790 NSW1 = 0
      MAT(ISTORE, JSTORE) = 2
  800 CALL CORECT
      CALL OUT (2)
      RETURN
C-----DOWNGRADE OPTION...
C     AT LEAST ONE STRESS POINT HAS YIELDED AT THE CURRENT LOADING.  ADJUST THE
C     LOADING SO THAT THE HIGHEST STRESSED ELASTIC STRESS POINT JUST YIELDS.
  804 FMAX=0
      NSW1 = 1
C-----FIND THE COORDINATES OF THE HIGHEST STRESSED STRESS POINT WHICH HAS JUST
C     YIELDED.
      DO 115 I=1,NP1
      NPV=NUM(I)-1
      DO 115 J=1,NPV
      IF(MAT(I,J)-2)115,117,115
  117 MAT(I,J)=2
      TEMP1=U(I+1,J+1)-U(I,J)-U(I+1,J)+V(I,J+1)
      TEMP2=U(I+1,J)-U(I,J+1)+V(I+1,J+1)-V(I,J)
      TEMP3 = TEMP1*TEMP1 + TEMP2*TEMP2
      IF (TEMP3 - FMAX) 115, 115, 119
  119 FMAX = TEMP3
      ISTORE=I
      JSTORE=J
  115 CONTINUE
C-----FOR THE PREVIOUS LOADING, GENERATE THE FORCES AT THE HIGHEST STRESSED
C     STRESS POINT WHICH HAS JUST YIELDED.
      I = ISTORE
      J = JSTORE
```

```
      FXOLD = EQV2V * (ONEPV*(UOLD(I+1,J+1) - UOLD(I,J)) + GNU*
     1        (VOLD(I+1,J) - VOLD(I,J+1)))
      FYOLD = EQV2V * (GNU*(UOLD(I+1,J+1) - UOLD(I,J)) + ONEPV*
     1        (VOLD(I+1,J) - VOLD(I,J+1)))
      FXYOLD = EQV4V * (UOLD(I+1,J) - UOLD(I,J+1) + VOLD(I+1,J+1) -
     1         VOLD(I,J))
C-----COMPUTE THE CHANGE IN LOADING REQUIRED TO JUST CAUSE YIELDING AT THE
C     HIGHEST STRESSED STRESS POINT WHICH YIELDED AT THE CURRENT LOADING.
      DIF1 = SQRTF ((FXOLD-FYOLD)*(FXOLD-FYOLD) + 4.0*FXYOLD*FXYOLD)
      DIF3 = SQRTF ((FX(ISTORE,JSTORE)-FY(ISTORE,JSTORE))*
     1       (FX(ISTORE,JSTORE)-FY(ISTORE,JSTORE)) + 4.0*
     2       FXY(ISTORE,JSTORE)*FXY(ISTORE,JSTORE))
      DELTL = (DELTA*FK-DIF3)*DELTL / (DIF3-DIF1)
      CALL ADD (1)
      DELOLD = DELP + DELTL
      CALL WAIT
      GO TO 99
      END
      SUBROUTINE FORCE (NSW2, I, J)
C-----GENERATE THE FORCES AT THE STRESS POINT INDICATED BY THE SWITCH NSW2.  IF
C     NSW2 = 5, UPDATE FORCES FX, FY, AND FXY.  IF NSW2 = 1, 2, 3, OR 4, UPDATE
C     FORCES FX, FY, AND FXY ONLY FOR AN UNYIELDED STRESS POINT.
      DIMENSION NOGA(36,36),NUM(36)
      DIMENSION BEGIN(1),PX(36,36),PY(36,36),U(36,36),V(36,36),
     1UOLD(36,36),VOLD(36,36),FX(35,35),FY(35,35),FXY(35,35),NNYT(35,35)
      COMMON BEGIN,FIONE,FITWO,SIYONE,SIYTWO,FYONE,FYTWO,SYYONE,SYYTWO,
     1ONEPV,EQV2V,EQV4V,G,SOKK,CPLK,SPIK,SKGRD,FK,DELTA,DELTL,TL,GNU,
     2EPS1,E,FLAMDA,FTOTAL,DELP,FLEX,FLEY,DELOLD,U,V,PX,PY,FX,FY,FXY,
     3SORT2,UOLD,VOLD,X,P,NLEFT,NRIGHT,NTOP,NBOT,NPI,NNI,NNYT,NALPHA,
     4NIN,NOUT,NOGA,NUM,SHOT
      GO TO (1, 2, 3, 4, 1), NSW2
```

```
C-----NSW2 = 1 OR 5. GENERATE FORCES AT THE STRESS POINT TO THE LOWER RIGHT OF
C     MASS POINT (I,J).
    1 K = I
      L = J
      GO TO 5
C-----NSW2 = 2. GENERATE FORCES AT THE STRESS POINT TO THE UPPER RIGHT OF MASS
C     POINT (I,J).
    2 K = I
      L = J - 1
      GO TO 5
C-----NSW2 = 3. GENERATE FORCES AT THE STRESS POINT TO THE UPPER LEFT OF MASS
C     POINT (I,J).
    3 K = I - 1
      L = J - 1
      GO TO 5
C-----NSW2 = 4. GENERATE FORCES AT THE STRESS POINT TO THE LOWER LEFT OF MASS
C     POINT (I,J).
    4 K = I - 1
      L = J
    5 TEMP1 = U(K+1,L+1) - U(K,L)
      TEMP2 = V(K+1,L) - V(K,L+1)
      TEMP3 = U(K+1,L) - U(K,L+1) + V(K+1,L+1) - V(K,L)
C-----CHECK STRESS POINT YIELD FLAG TO SEE IF THE STRESS POINT HAS YIELDED.
      IF (NYT(K,L)) 30, 19, 30
C-----EQUATIONS FOR ELASTIC STRESS POINT FORCES.
   10 FXY(K,L) = TEMP3 * EOV4V
      GO TO (11, 21, 11, 21, 51), NSW2
   11 FX(K,L) = (ONEPV*TEMP1 + GNU*TEMP2) * EOV2V
      IF (NSW2 - 1) 12, 12, 13
   12 FXONE = FX(K,L)
      SYXONE = FXY(K,L)
```

```
      RETURN
   13 FXTWO = FX(K,L)
      SYXTWO = FXY(K,L)
      RETURN
   21 FY(K,L) = (ONEPV*TEMP2 + GOU*TEMP1) * EOV2V
      IF (NSW2 - 2) 22, 22, 23
   22 FYONE = FY(K,L)
      SXYONE = FXY(K,L)
      RETURN
   23 FYTWO = FY(K,L)
      SXYTWO = FXY(K,L)
      RETURN
C-----EQUATIONS FOR PLASTIC STRESS POINT FORCES.
   30 TEMP1 = (U(K+1,L+1) - UOLD(K+1,L+1)) - (U(K,L) - UOLD(K,L))
      TEMP2 = (V(K+1,L) - VOLD(K+1,L)) - (V(K,L+1) - VOLD(K,L+1))
      TEMP3 = (U(K+1,L) - UOLD(K+1,L)) - (U(K,L+1) - UOLD(K,L+1)) +
     1        (V(K+1,L+1) - VOLD(K+1,L+1)) - (V(K,L) - VOLD(K,L))
      TEMP4 = (FX(K,L) - FY(K,L)) / DELTA
      A = 0.5 * (EPLK - GOKK*TEMP4*TEMP4)
      B = 0.5 * (EPIK + GOKK*TEMP4*TEMP4)
      C = GOKK/DELTA*FXY(K,L)*TEMP4
      D = 0.5 * (G - 4.0*GOKK/DELTA/DELTA*FXY(K,L)*FXY(K,L))
      SF = -(C*TEMP1 + C*TEMP2 + D*TEMP3 + FXY(K,L)
      GO TO (31, 41, 31, 41, 61), NSW2
   31 SX = A*TEMP1 + B*TEMP2 - C*TEMP3 + FX(K,L)
      IF (NSW2 - 1) 32, 32, 33
   32 FXONE = SX
      SYXONE = SF
      RETURN
   33 FXTWO = SX
      SYXTWO = SF
```

```
      RETURN
   41 SY = B*TEMP1 + A*TEMP2 + C*TEMP3 + FY(K,L)
      IF (NSW2 - 2) 42, 42, 43
   42 FYONE = SY
      SXYONE = SF
      RETURN
   43 FYTWO = SY
      SXYTWO = SF
      RETURN
   51 FX(K,L) = (ONEPV*TEMP1 + GNU*TEMP2) * EOV2V
      FY(K,L) = (ONEPV*TEMP2 + GNU*TEMP1) * EOV2V
      RETURN
   61 FX(K,L) = A*TEMP1 + B*TEMP2 - C*TEMP3 + FX(K,L)
      FY(K,L) = B*TEMP1 + A*TEMP2 + C*TEMP3 + FY(K,L)
      FXY(K,L) = SF
      RETURN
      END
      SUBROUTINE LEFT (I)
C-----DEFINE MASS POINT DEFLECTIONS FOR THE LEFT BOUNDARY ( = 1, NM1).
C     CURRENTLY LIMITED TO A FIXED OR AN APPROXIMATION OF AN INFINITE BOUNDARY.
      DIMENSION MUGA(36,36),MUM(36)
      DIMENSION BEGIN(1),PX(36,36),PY(36,36),U(36,36),V(36,36),
     1UOLD(36,36),VOLD(36,36),FX(35,35),FY(35,35),FXY(35,35),NNYT(35,35)
      COMMON BEGIN,FXONE,FXTWO,SXYONE,SXYTWO,FYONE,FYTWO,SYXONE,SYXTWO,
     1ONEPV,EOV2V,EOV4V,G,GOKK,GPLK,GMIK,SKORD,FK,DELTA,DELTL,TL,GNU,
     2EPSIL,FLAMDA,TTOTAL,DELP,FLEX,FLEY,DELOLD,U,V,PX,PY,FX,FY,FXY,
     3SQRT2,UOLD,VOLD,N,M,NLEFT,NRIGHT,NTOP,NBOT,NM1,MM1,NNYT,NALPHA,
     4NIN,NOUT,MUGA,MUM,ENDT
      GO TO (5, 5, 5, 4), NLEFT
C-----DEFINE MASS POINT DEFLECTIONS FOR AN APPROXIMATION OF AN INFINITE BOUNDARY
```

```
    4 U(I,1) = (U(I,2) + V(I,2)) * 0.5
      V(I,1)=U(I,1)
    5 RETURN
      END
      SUBROUTINE RIGHT (I)
C-----DEFINE MASS POINT DEFLECTIONS FOR THE RIGHT BOUNDARY (I = 1, NM1).
C     CURRENTLY LIMITED TO A FIXED BOUNDARY, A BOUNDARY OF SYMMETRY OR AN
C     APPROXIMATION OF AN INFINITE BOUNDARY.
      DIMENSION MUGA(36,36),MUM(36)
      DIMENSION BEGIN(1),PX(36,36),PY(36,36),U(36,36),V(36,36),
     1UOLD(36,36),VOLD(36,36),FX(35,35),FY(35,35),FXY(35,35),NNYT(35,35)
      COMMON BEGIN,FXONE,FXTWO,SXYONE,SXYTWO,FYONE,FYTWO,SYXONE,SYXTWO,
     1ONEPV,EOV2V,EOV4V,G,GOKK,GPLK,GMIK,SKORD,FK,DELTA,DELTL,TL,GNU,
     2EPSI,E,FLAMDA,TTOTAL,DELP,FLEX,FLEY,DELOLD,U,V,PX,PY,FX,FY,FXY,
     3SQRT2,UOLD,VOLD,N,M,NLEFT,NRIGHT,NTOP,NBOT,NM1,MM1,NNYT,NALPHA,
     4NIN,NCUT,MUGA,MUM,ENDT
      GO TO (50, 50, 40, 10), NRIGHT
C-----DEFINE MASS POINT DEFLECTIONS FOR AN APPROXIMATION OF AN INFINITE BOUNDARY
   10 U(I,M) = (U(I,MM1) + V(I,MM1)) * 0.5
      V(I,M) = U(I,M)
      RETURN
C-----DEFINE MASS POINT DEFLECTIONS FOR AN APPROXIMATION OF A BOUNDARY OF
C     SYMMETRY.
   40 J = M
      FXTWO = 0
      SYXTWO = 0
      IF(I - 1) 47, 47, 46
   46 CALL FORCE (3, I, J)
   47 CALL FORCE (2, I, J)
      FYTWO=FXTWO
```

```
      SXYTWO=SYXTWO
      FXONE=FYONE
      SYXONE=SXYONE
C-----SUM FORCES IN X AND Y DIRECTIONS.
      SUMFX=FXONE-FXTWO+SXYONE-SXYTWO+PX(I,J)
      SUMFY=FYONE-FYTWO+SYXONE-SYXTWO+PY(I,J)
C-----ADJUST MASS POINT DEFLECTIONS FOR EQUILIBRIUM OF FORCES ON THE MASS
C     POINT.
      U(I,M)=U(I,M)+FLEX*SUMFX
      V(I,M)=V(I,M)+FLEY*SUMFY
   50 RETURN
      END
      SUBROUTINE TOP
C-----DEFINE MASS POINT DEFLECTIONS FOR THE TOP BOUNDARY.  CURRENTLY LIMITED
C     TO THE FREE CONDITION.
      DIMENSION MUGA(36,36),MUM(36)
      DIMENSION BEGIN(1),PX(36,36),PY(36,36),U(36,36),V(36,36),
     1UOLD(36,36),VOLD(36,36),FX(35,35),FY(35,35),FXY(35,35),NNYT(35,35)
      COMMON BEGIN,FXONE,FXTWO,SXYONE,SXYTWO,FYONE,FYTWO,SYXONE,SYXTWO,
     1ONEPV,EOV2V,EOV4V,G,GCKK,GPLK,GMIK,SKORD,FK,DELTA,DELTL,TL,GNU,
     2EPSI,E,FLAMDA,TTOTAL,DELP,FLEX,FLEY,DELOLD,U,V,PX,PY,FX,FY,FXY,
     3SQRT2,UOLD,VOLD,N,M,NLEFT,NRIGHT,NTOP,NBOT,NM1,MM1,NNYT,NALPHA,
     4NIN,NOUT,MUGA,MUM,ENDT
      I = 1
      CALL LEFT (I)
      MMM=MUM(I)-1
      DO 101 J=2,MMM
      CALL FORCE (1, I, J)
      CALL FORCE (2, I, J)
C-----SUM FORCES IN THE X AND Y DIRECTIONS.
```

```
      SUMFX=FXONE+SXYONE+PX(I,J)
      SUMFY=FYONE+SYXONE+PY(I,J)
C-----ADJUST MASS POINT DEFLECTIONS FOR EQUILIBRIUM OF FORCES ON THE MASS POINT.
      U(I,J)=2.*FLEX*SUMFX+U(I,J)
  101 V(I,J)=2.*FLEY*SUMFY+V(I,J)
      J=MMM+1
      IF(J-M)599,500,500
  599 CALL FORCE(2,I,J)
      SUMFX=SXYONE+PX(I,J)
      SUMFY=FYONE+PY(I,J)
   11 U(I,J )=U(I,J)+FLEX*SUMFX
      V(I,J )=V(I,J)+FLEY*SUMFY
      GO TO 499
  500 CALL RIGHT (I)
  499 RETURN
      END
      SUBROUTINE BOTTOM
C-----DEFINE MASS POINT DEFLECTIONS FOR THE BOTTOM BOUNDARY.  CURRENTLY
C     LIMITED TO A FIXED BOUNDARY OR AN APPROXIMATION OF AN INFINITE BOUNDARY.
      DIMENSION MUGA(36,36),MUM(36)
      DIMENSION BEGIN(1),PX(36,36),PY(36,36),U(36,36),V(36,36),
     1UOLD(36,36),VOLD(36,36),FX(35,35),FY(35,35),FXY(35,35),NNYT(35,35)
      COMMON BEGIN,FXONE,FXTWO,SXYONE,SXYTWO,FYONE,FYTWO,SYXONE,SYXTWO,
     1ONEPV,EOV2V,EOV4V,G,GOKK,GPLK,GMIK,SKORD,FK,DELTA,DELTL,TL,GNU,
     2EPSI,E,FLAMDA,TTOTAL,DELP,FLEX,FLEY,DELOLD,U,V,PX,PY,FX,FY,FXY,
     3SQRT2,UOLD,VOLD,N,M,NLEFT,NRIGHT,NTOP,NBOT,NM1,MM1,NNYT,NALPHA,
     4NIN,NOUT,MUGA,MUM,ENDT
      GO TO (10, 10, 10, 4), NBOT
C-----DEFINE MASS POINT DEFLECTIONS FOR AN APPROXIMATION OF AN INFINITE BOUNDARY
    4 DO 5 J = 1, M
```

```
      U(N,J) = (U(NM1,J) - V(NM1,J)) * 0.5
      V(N,J) = -U(N,J)
    5 CONTINUE
   10 RETURN
      END
      SUBROUTINE CORECT
C-----BRING THE FORCES AT YIELDED STRESS POINTS BACK TO THE YIELD SURFACE.
      DIMENSION MUGA(36,36),MUM(36)
      DIMENSION BEGIN(1),PX(36,36),PY(36,36),U(36,36),V(36,36),
     1UOLD(36,36),VOLD(36,36),FX(35,35),FY(35,35),FXY(35,35),NNYT(35,35)
      COMMON BEGIN,FXONE,FXTWO,SXYONE,SXYTWO,FYONE,FYTWO,SYXONE,SYXTWO,
     1ONEPV,EOV2V,EOV4V,G,GOKK,GPLK,GMIK,SKORD,FK,DELTA,DELTL,TL,GNU,
     2EPSI,E,FLAMDA,TTOTAL,DELP,FLEX,FLEY,DELOLD,U,V,PX,PY,FX,FY,FXY,
     3SQRT2,UOLD,VOLD,N,M,NLEFT,NRIGHT,NTOP,NBOT,NM1,MM1,NNYT,NALPHA,
     4NIN,NOUT,MUGA,MUM,ENDT
      DO 10 I=1,NM1
      MMM=MUM(I)-1
      DO 10 J=1,MMM
      IF(NNYT(I,J))1,10,1
    1 FJ2 = ((FX(I,J) - FY(I,J))*(FX(I,J) - FY(I,J)) + 4.0*FXY(I,J)*
     1      FXY(I,J)) / (DELTA*DELTA)
      YT = FK / SQRTF(FJ2)
      TEMP1 = FX(I,J)*0.5*(1.+YT) + FY(I,J)*0.5*(1.-YT)
      TEMP2 = FX(I,J)*0.5*(1.-YT) + FY(I,J)*0.5*(1.+YT)
      FXY(I,J) = FXY(I,J) * YT
      FX(I,J) = TEMP1
      FY(I,J) = TEMP2
   10 CONTINUE
      RETURN
      END
```

```
      SUBROUTINE ADD (NSW3)
C-----INCREMENT MASS POINT LOADS, APPROXIMATE NEW MASS POINT DEFLECTIONS AND
C     STORE OLD EQUILIBRIUM MASS POINT DEFLECTION VALUES.
      DIMENSION MUGA(36,36),MUM(36)
      DIMENSION BEGIN(1),PX(36,36),PY(36,36),U(36,36),V(36,36),
     1UOLD(36,36),VOLD(36,36),FX(35,35),FY(35,35),FXY(35,35),NNYT(35,35)
      COMMON BEGIN,FXONE,FXTWO,SXYONE,SXYTWO,FYONE,FYTWO,SYXONE,SYXTWO,
     1ONEPV,EOV2V,EOV4V,G,GOKK,GPLK,GMIK,SKORD,FK,DELTA,DELTL,TL,GNU,
     2EPSI,E,FLAMDA,TTOTAL,DELP,FLEX,FLEY,DELOLD,U,V,PX,PY,FX,FY,FXY,
     3SQRT2,UOLD,VOLD,N,M,NLEFT,NRIGHT,NTOP,NBOT,NM1,MM1,NNYT,NALPHA,
     4NIN,NOUT,MUGA,MUM,ENDT
      DO 10 I = 1, N
      MM=MUM(I)
      DO 10 J = 1, MM
C-----ADJUST ALL MASS POINT DEFLECTIONS IN A LINEAR FASHION AS A FIRST
C     APPROXIMATION TO THEIR EQUILIBRIUM VALUES UNDER THE NEW LOADING.
      TEMP1 = U(I,J) + (U(I,J) - UOLD(I,J)) * DELTL/DELOLD
      TEMP2 = V(I,J) + (V(I,J) - VOLD(I,J)) * DELTL/DELOLD
C-----IF THE DOWNGRADE OPTION IS NOT BEING EXERCISED, STORE CURRENT EQUILIBRIUM
C     VALUES OF MASS POINT DEFLECTIONS.
      IF (NSW3) 5, 1, 5
    1 UOLD(I,J) = U(I,J)
      VOLD(I,J) = V(I,J)
    5 U(I,J) = TEMP1
      V(I,J) = TEMP2
C-----INCREMENT ALL MASS POINT FORCES BY THE CURRENT LOAD INCREMENT.
      PX(I,J) = PX(I,J) * (DELTL + TL)/TL
      PY(I,J) = PY(I,J) * (DELTL + TL)/TL
   10 CONTINUE
      TL = TL + DELTL
      RETURN
      END
```

```
      SUBROUTINE OUT (NSW4)
C-----WRITE OUT INPUT DATA AND RESULTS.
      DIMENSION MUGA(36,36),MUM(36)
      DIMENSION BEGIN(1),PX(36,36),PY(36,36),U(36,36),V(36,36),
     1UOLD(36,36),VOLD(36,36),FX(35,35),FY(35,35),FXY(35,35),NNYT(35,35)
      DIMENSION BDY(4)
      COMMON BEGIN,FXONE,FXTWO,SXYONE,SXYTWO,FYONE,FYTWO,SYXONE,SYXTWO,
     1ONEPV,EOV2V,EOV4V,G,GOKK,GPLK,GMIK,SKORD,FK,DELTA,DELTL,TL,GNU,
     2EPSI,E,FLAMDA,TTOTAL,DELP,FLEX,FLEY,DELOLD,U,V,PX,PY,FX,FY,FXY,
     3SQRT2,UOLD,VOLD,N,M,NLEFT,NRIGHT,NTOP,NBOT,MM1,MM1,NNYT,NALPHA,
     4NIN,NOUT,MUGA,MUM,ENDT
 1001 FORMAT (22HOMASS POINT MATRIX HAS I3, 6H ROWS, I3, 8H COLUMNS //
     1 24H MODULUS OF ELASTICITY = 1PE11.3, 15X 16HPOISSONS RATIO = 1PE1
     21.3 / 31H YIELD STRESS IN SIMPLE SHEAR = 1PE11.3, 8X 20HSHORTEST D
     3ISTANCE BETWEEN MASS POINTS = 1PE11.3 / 24H CONVERGENCE CRITERION
     4= 1PE11.3, 15X 20HMAXIMUM TOTAL LOAD = 1PE11.3 / 26H STANDARD LOAD
     5 INCREMENT = 1PE11.3 // 18H LEFT BOUNDARY IS A6, 16X 18HRIGHT BOUN
     6DARY IS A6 / 17H TOP BOUNDARY IS A6, 17X 19HBOTTOM BOUNDARY IS A6)
 1004 FORMAT (I3, I5, 2X, 1P7E12.4, I7)
 1006 FORMAT (17H1LOAD INCREMENT = 1PE12.4, 5X 12HTOTAL LOAD = 1PE12.4//
     1/47H ***** STRESS CONDITIONS AT STRESS POINTS ***** //10H  I     J
     2    VERT STRSS  HOR STRSS   SHR STRSS      FX           FY
     3FXY       YIELD RATIO  YIELD CODE //)
 1010 FORMAT (51HO***** LOADS AND DISPLACEMENTS AT MASS POINTS ***** //
     1 78H  I     J         FX           PY       VERT DISPL  HOR DISPL
     2   U            V  //)
 2005 FORMAT (52HOSTANDARD LOAD INCREMENT IS USED WITH NO ADJUSTMENTS )
 2006 FORMAT (54HOSTANDARD LOAD INCREMENT IS USED WITH DOWNGRADE OPTION)
      GO TO (10, 13), NSW4
C-----EDIT AND WRITE OUT INPUT DATA.
   10 CONTINUE
```

```
8      BDY(1)=265125256060
8      BDY(2)=263167252460
8      BDY(3)=512526433360
8      BDY(4)=314526336060
       WRITE OUTPUT TAPE NOUT, 1001, N, M, E, GNU, FK, FLAMDA, EPSI,
      1       TTOTAL, DELP, BDY(NLEFT), BDY(NRIGHT), BDY(NTOP), BDY(NBOT)
       IF (NALPHA - 1) 2, 3, 2
     3 WRITE OUTPUT TAPE NOUT, 2005
       RETURN
     2 WRITE OUTPUT TAPE NOUT, 2006
       RETURN
C-----WRITE OUT RESULTS.
    13 WRITE OUTPUT TAPE NOUT, 1006, DELOLD, TL
C-----OUTPUT STRESS CONDITIONS AT STRESS POINTS
       DO 30 I = 1, NM1
       DO 30 J = 1, NM1
       VS = (FX(I,J) + FY(I,J) + 2.0*FXY(I,J)) / DELTA
       HS = (FX(I,J) + FY(I,J) - 2.0*FXY(I,J)) / DELTA
       SS = (FX(I,J) - FY(I,J)) / DELTA
       YR = ((FX(I,J) - FY(I,J))*(FX(I,J) - FY(I,J)) + FXY(I,J)*FXY(I,J)*
      1      4.0) / (DELTA*DELTA)
       YR = SQRTF(YR) / FK
       WRITE OUTPUT TAPE NOUT, 1004, I, J, VS, HS, SS, FX(I,J), FY(I,J),
      1       FXY(I,J), YR, NNYT(I,J)
    30 CONTINUE
C-----OUTPUT THE YIELD MATRIX
       WRITE OUTPUT TAPE 6,3000
 3000 FORMAT(1H1 9X1H1 9X1H2 9X1H3/1H )
       DO 36 I=1,NM1
       MM=MUM(I)-1
```

```
     36 WRITE OUTPUT TAPE 6,2000,(NMYT(I,J), J=1,MM)
   2000 FORMAT(1H ,3512)
        WRITE OUTPUT TAPE NOUT, 1010
C-----OUTPUT LOADS AND DISPLACEMENTS AT MASS POINT
        DO 35 I = 1, N
        DO 35 J = 1, M
        VD = (U(I,J) + V(I,J)) / SQRT2
        HD = (U(I,J) - V(I,J)) / SQRT2
        WRITE OUTPUT TAPE NOUT, 1004, I, J, PX(I,J), PY(I,J), VD, HD,
       1      U(I,J), V(I,J)
     35 CONTINUE
        RETURN
        END
*       DATA
1 PERFPLAS II - 7/17/68 - PROB NR-1, 6 IN. EMBEDMENT
    9   18    4    3    1    4    1   11
       74.        .4        .6         3.  10.0E-05  -1.7675    -.3535  -7.07
    1   10   -.88375  -.88375      3
    2   10  -1.7675  -1.7675       4
    3   10  -1.7675  -1.7675       1
    3   11  -1.7675  -1.7675       2
    3   12  -1.7675  -1.7675       2
    3   13  -1.7675  -1.7675       2
    3   14  -1.7675  -1.7675       2
    3   15  -1.7675  -1.7675       2
    3   16  -1.7675  -1.7675       2
    3   17  -1.7675  -1.7675       2
    3   18   -.88375  -.88375      5
```

Appendix H

PHOTOELASTIC STUDY OF THE DISTRIBUTION OF MAXIMUM SHEAR STRESS IN AN ELASTIC MEDIUM

by C. L. Liu

Photoelastic methods of determining the maximum shear stress distribution offer a convenient and inexpensive means of supporting the numerical results obtained from the computer program and the measurements of the field test program. The circular polariscope permits a visualization of the shear stress patterns which develop as loads are applied to a notched two-dimensional model.

Test Specimen and Apparatus

The photoelastic medium used in these tests is urethane rubber having a modulus of elasticity of 500 psi and a Poisson's ratio of 0.48. This is equivalent to a value of 74 psi for the modulus of elasticity as measured by performing triaxial tests on some selected clay sediment cores obtained from San Francisco Bay.

Loads were applied to the urethane rubber via relatively rigid plexiglass (Lucite) forms which were machined to precisely fit the notched area of the urethane rubber. The materials were bonded by an epoxy cement. Difficulties in machining the urethane rubber and in bonding the two materials resulted in the development of residual stresses especially noticeable at the internal corners. Aluminum templates were found to be well suited for making the models. See Figure H-1 for the general specimen dimensions.

The test apparatus used in the experiment is shown schematically in Figure H-2. Briefly, the isochromatic pattern of a specimen strained in the steel angle frame is viewed through the polariscope analyzer, and the image is recorded by the Sinar camera. A simple mechanical jack is used to position the specimen. Figure H-3 illustrates how the tension force on the specimen is controlled by a wing nut. The tensile force on the model was estimated by reproducing the stress pattern with a known force applied by a simple lever balance system, as shown in Figure H-4.

Procedure

The calibration constant C is the ratio of the maximum shear stress, τ_{max}, to the order of birefringence $\bar{N}$ of the isochromatic pattern. A 2-inch circular urethane rubber disc was used for calibration. A photograph of the

disc loaded in pure compression by 4.5 pounds is shown in Figure H-5. The center of the disc is the reference point. The birefringence order at this point is 6.0. The value of τ_{mm} at the center was calculated analytically: $\tau_{mm} = 4F/\pi t D$. The compression force is 4.5 pounds, the model thickness, t, is 0.25 inch, and the model diameter, D, is 2 inches. The value of τ_{mm} at the reference point is found to be 11.5 psi. Thus, the value of C is equal to 1.91 psi. To aid in data reduction, the linear shear-birefringence relation is shown in Figure H-6.

Photographs of unloaded specimens revealed internal stresses which were found to exist near the notched internal corners. These specimens were then tested with loads sufficient to produce clear, distinctive birefringences of a reasonable quantity. A half-embedded circular cylindrical specimen was subjected to approximately equal load increments until failure, and sequential photographs were taken. The force levels in each case were estimated by reloading the specimen with the lever balance system so that the isochromatic pattern in the photographs was reproduced.

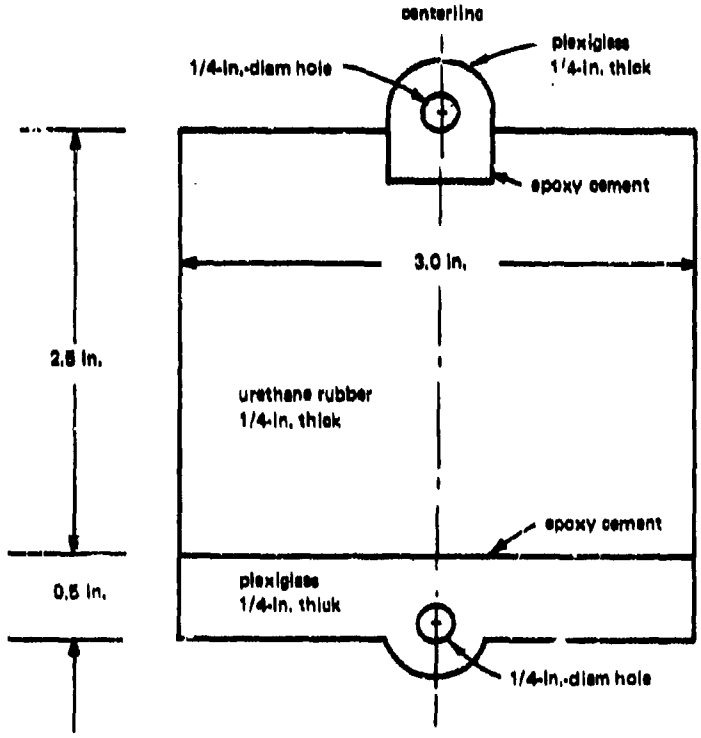

Figure H-1. Typical dimensions of soil models.

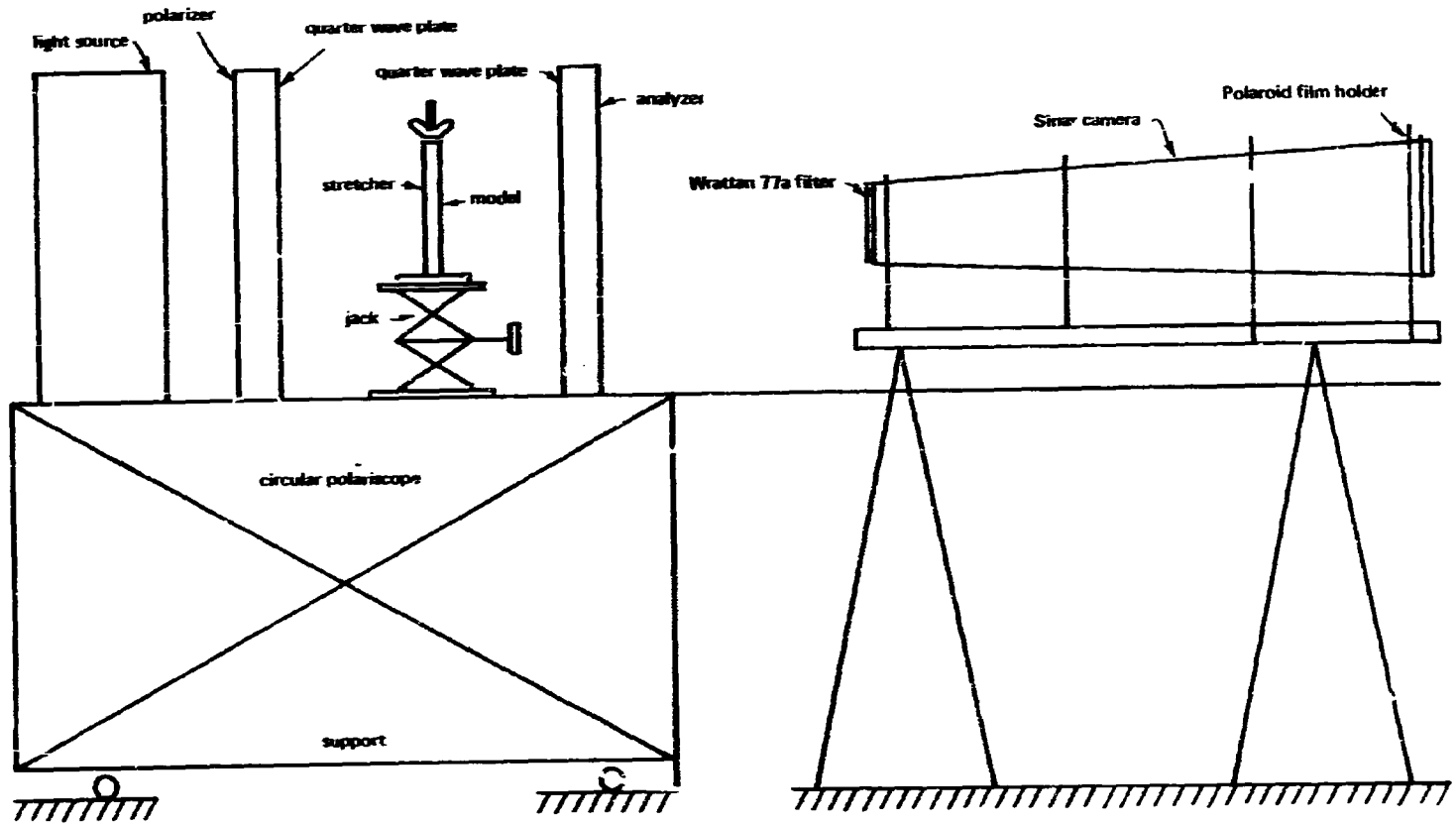

Figure H-2. Test apparatus.

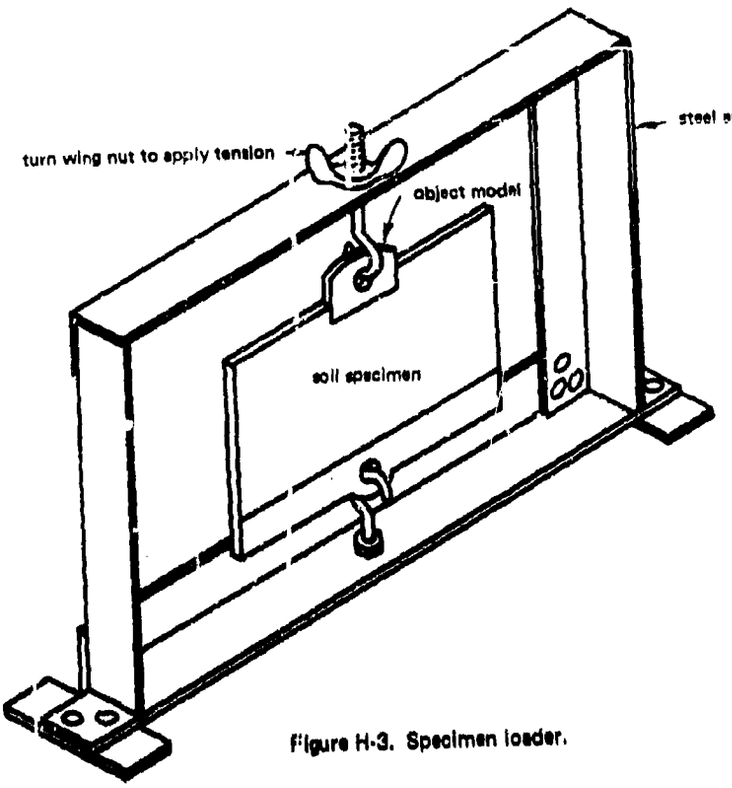

Figure H-3. Specimen loader.

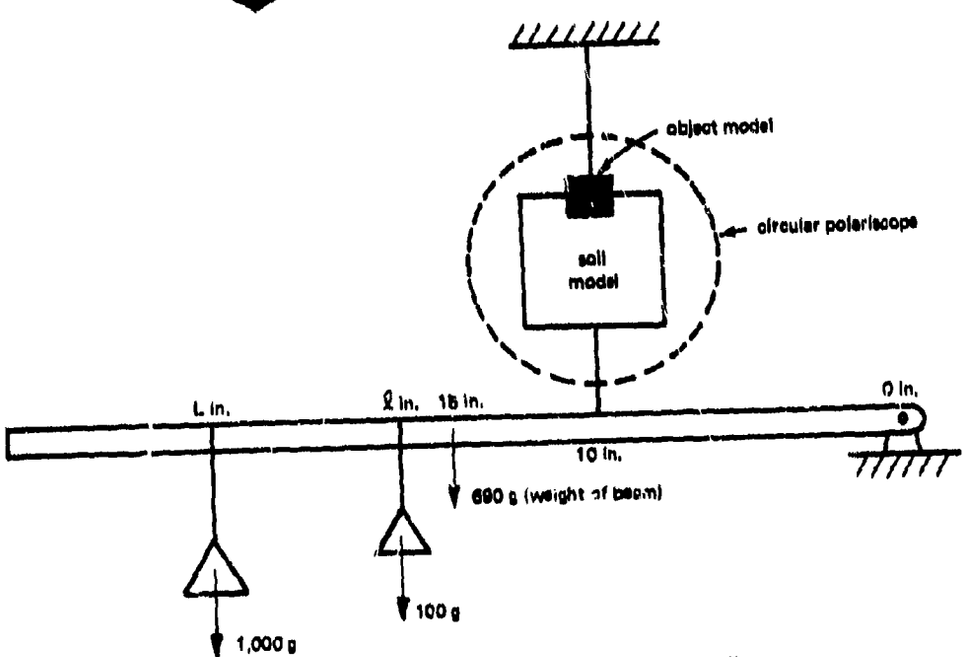

Figure H-4. Force measurement detail.

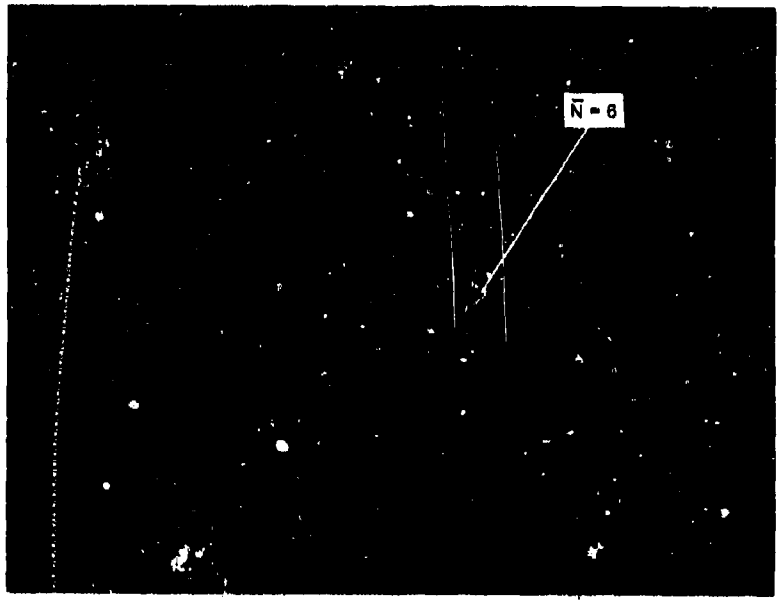

Figure H-5. Calibration disc under compression.

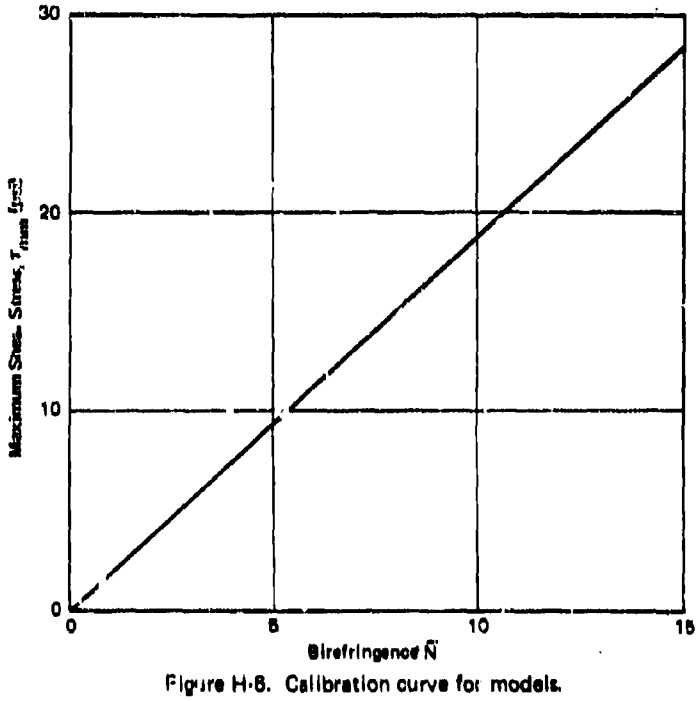

Figure H-6. Calibration curve for models.

All of the photographs were taken with black and white Polaroid Land type 57 films and a Wrattan 77a yellow filter. It was found that the best dark-field polariscope picture was made by using 3000 ASA film with an f32 opening and an exposure of 7 seconds. A blue monochromatic light source was used since it gave more distinctive black and white photographs. In all of the photographs, a transparent scale was used as a length reference.

Results

A summary of model dimensions is shown in Figure H-7. Figures H-8 to H-15 shows a group of models under tensile loadings. Sequential photographs of model F under stepwise load increments are shown in Figures H-16 to H-18. Each loading is given in Table H-1.

Interpretation and Application

Based on the photoelastic principle, the maximum shear stress, τ_{mm}, is proportional to the birefringence order $\bar{N}$. The τ_{mm} distribution is clearly shown in each of the isochromatic photographs. Each black curve may be assigned a birefringence order along which the value of τ_{mm} is constant. Qualitative conclusions can be inferred directly from the photographs; however, quantitative conclusions require a determination of the proportional or calibration constant.

By observing the growth of the birefringence pattern during the test, one may determine the direction of the birefringence variation. Referring to Figure H-9, the curved arrows indicate the directions of increasing birefringence. For example, the value of τ_{mm} is zero at the free corner, is low at the center of the interface, and is highest at the lower corners of the joint. Consequently, failure is initiated at the internal corners and would extend downward and inward following the "ridge" of the τ_{mm} contour to form a failure arc, which is indicated with a dashed line.

Failure curves for the other boundary geometrics are also indicated in the pertinent photographs. As shown in the sequential photographs, Figures H-16 to H-18, the failure curve is independent of the external loading for a given boundary geometry. Behavior in the plastic range cannot be simulated with the urethane rubber models.

In order to make some quantitative estimates of maximum shear stress under a given loading, the following formula is useful:

$$\tau_{mm} = C\bar{N} \qquad \text{(H-1)}$$

where τ_{mm} is the maximum shear stress in the model at a point corresponding to the birefringence order $\bar{N}$ and C is the calibration constant. Thus, for any point in the medium, the maximum shear stress may be calculated. To extrapolate the results to field conditions, the following formula is given:

$$\tau = \frac{F L_m t_m}{F_m L t} \tau_{mm} \qquad \text{(H-2)}$$

where m = model

F = applied force

L = length

t = thickness

τ = maximum shear stress in prototype

In order to compute the breakout force, rearrange Equation H-2 into the following form:

$$F = \frac{F_m L t}{L_m t_m} \left(\frac{\tau}{\tau_{mm}} \right) \qquad \text{(H-3)}$$

The procedure requires (1) selection of a critical point in the medium and (2) determination of the level of loading F_m at which the maximum shear stress reaches the yield stress at the critical point. The critical point is located at the center of the failure ridge. The breakout force is easily calculated from Equation H-3.

As an example, suppose it is desired to find the maximum shear stress at a point 36 inches left of the centerline and 24 inches below the sediment surface of a 4 x 4 x 15-foot parallelepiped which is embedded 6 inches in the soil under an applied load of 10,000 pounds. This embedment condition corresponds to the boundary geometry of Figure H-9, where the equivalent point is designated as point A. The birefringence order $\bar{N}$ at A is 4.5. From Figure H-6, τ_{mm} = 8.6 psi, and from Table H-1, F = 6.14 pounds, so that from Equation H-2

$$\tau = \frac{10{,}000(0.75)(0.25)(8.6)}{(6.14)(48)(15)(12)} = 0.303 \text{ psi}$$

which is the predicted maximum shear stress. As another example, suppose we are interested in determining the breakout force of a 4 x 4 x 15-foot parallelepiped embedded 6 inches in a soil having a shear yielding stress of

0.6 psi. First, the critical point, which is point B in Figure H-9, must be found. With a birefringence order of 6, the value of τ_{mm} is found from Figure H-6 to be equal to 11.5 psi. Using Equation H-3, we have

$$F = \frac{0.6(6.14)(48)(150)(12)}{(0.75)(0.25)(11.5)} = 14{,}750 \text{ pounds}$$

This value will be higher than the actual force since failure does not occur simultaneously at all points along the failure arc. During the failure process, the transfer of load along the failure ridge causes the stress at the critical point to attain the yield point much earlier than predicted. However, the omission of the plastic consideration does not detract from the value of the study reported on herein. It is useful to (1) support the numerical technique given in Appendixes C through G, (2) visualize the mode of failure, and (3) present approximate engineering estimates of the breakout force.

Table H-1. Calculation of Forces on Models

Model	L (in.)	ℓ (in.)	F (lb)	Figure Number
A	29.0	0	8.67	H-8
B	17.5	0	6.14	H-9
C	19.5	0	6.58	H-10
D	19.0	0	6.47	H-11
E	30.0	19.0	9.31	H-12
G	18.0	0	6.25	H-13
H	16.0	0	5.81	H-14
I	17.0	0	6.03	H-15
F	13.5	0	5.26	H-16
F	30.0	0	8.90	H-17

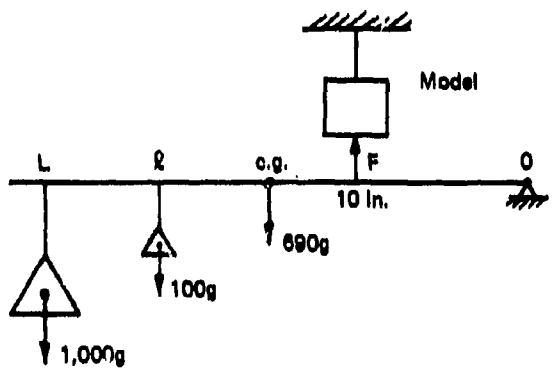

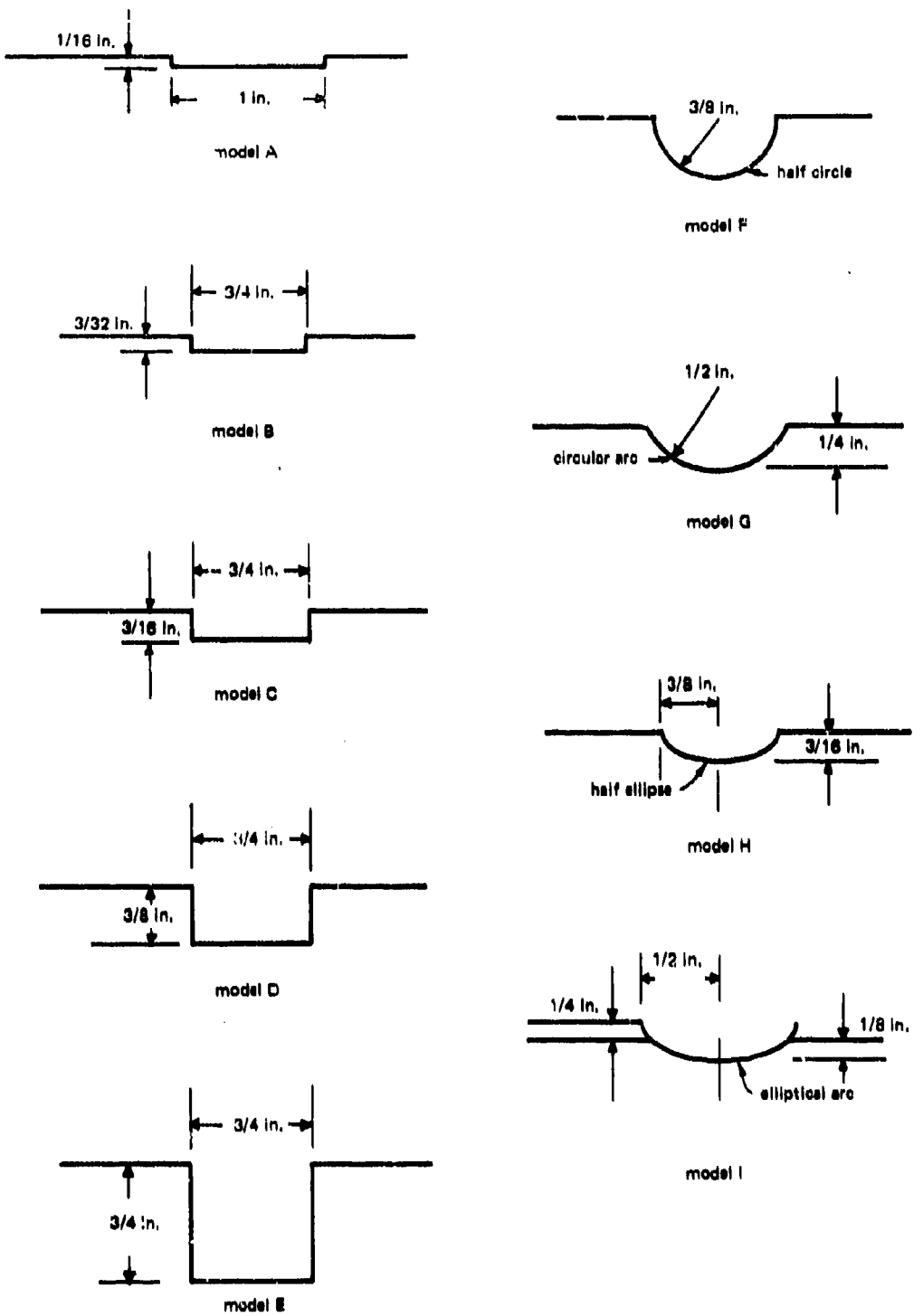

Figure H-7. Geometries of models.

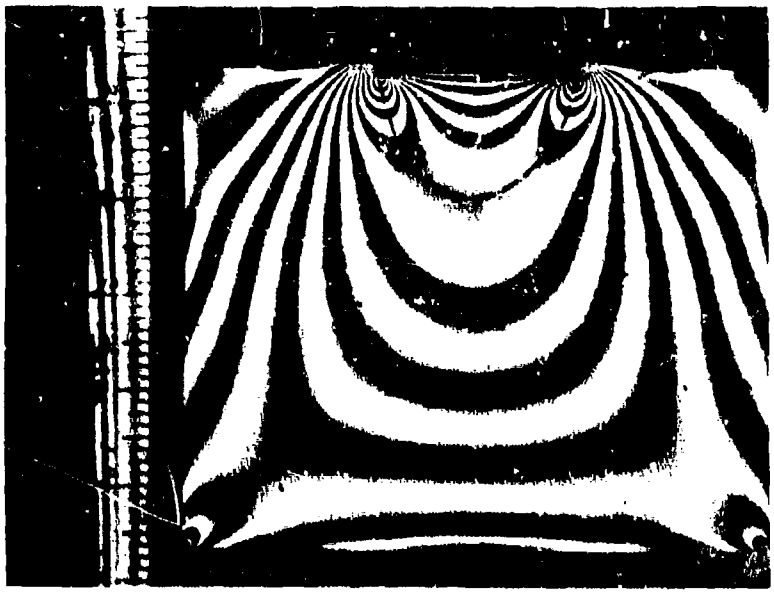

Figure H-8. Model A, vertically loaded.

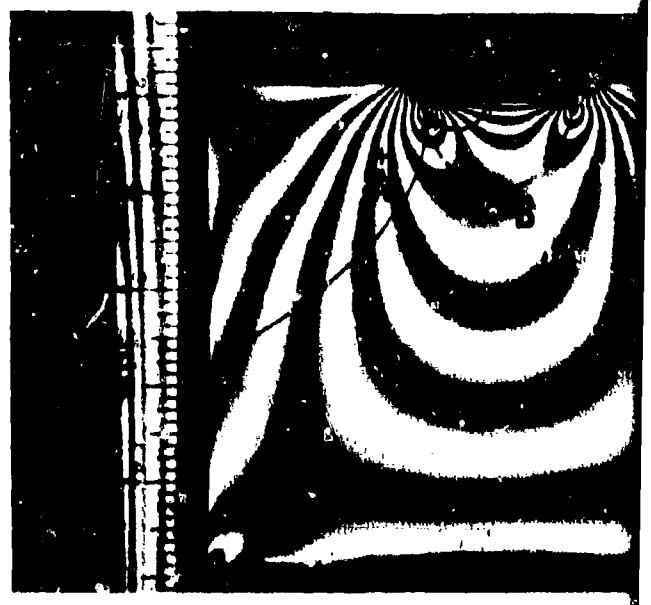

Figure H-9. Model B, vertically loaded.

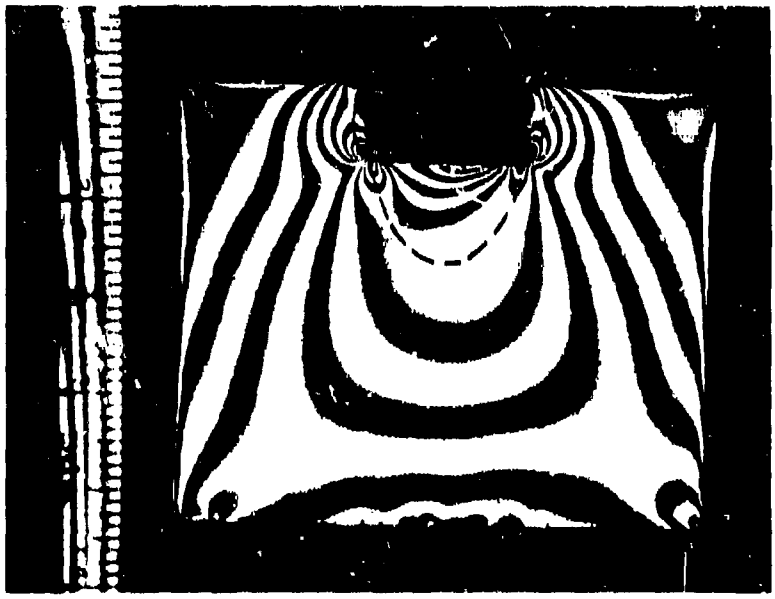

Figure H-11. Model D, vertically loaded.

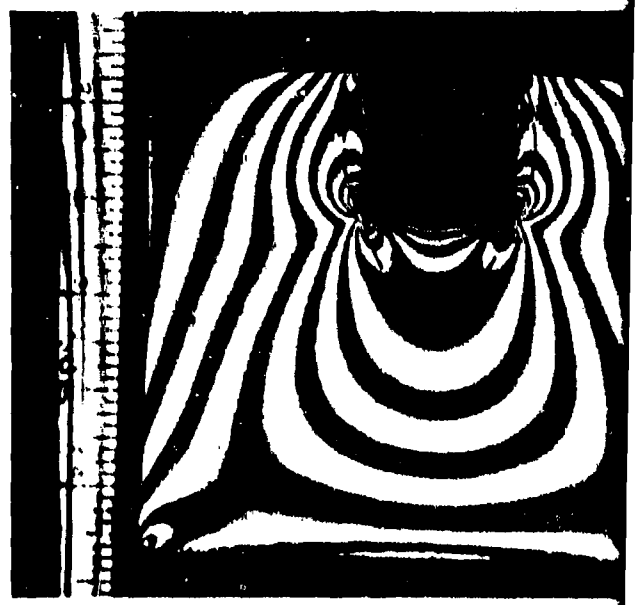

Figure H-12. Model E, vertically loaded.

A

gure H-9. Model B, vertically loaded.

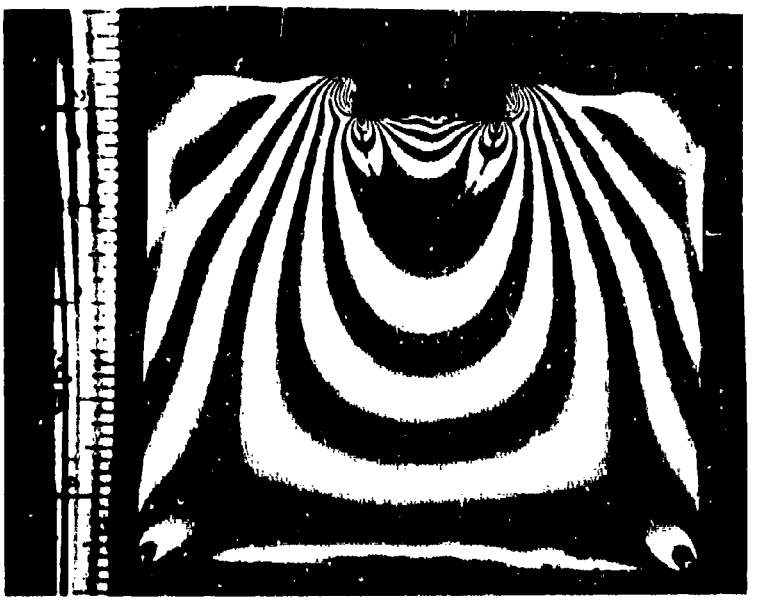

Figure H-10. Model C, vertically loaded.

re H-12. Model E, vertically loaded.

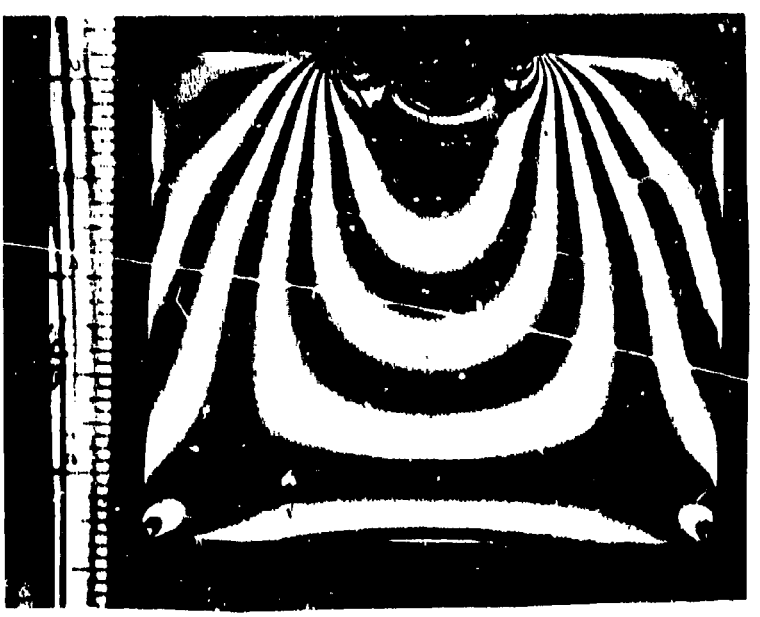

Figure H-13. Model G, vertically loaded.

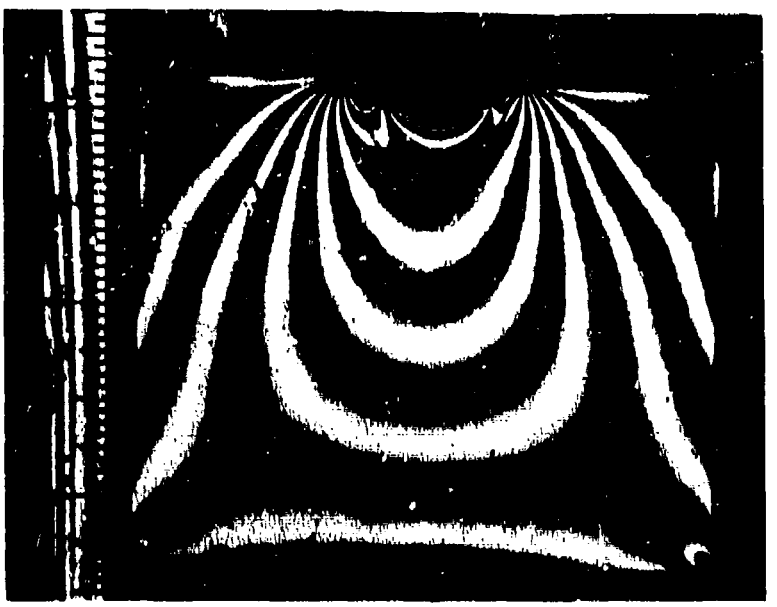

Figure H-14. Model H, vertically loaded.

Figure H-15. Model I, vertically

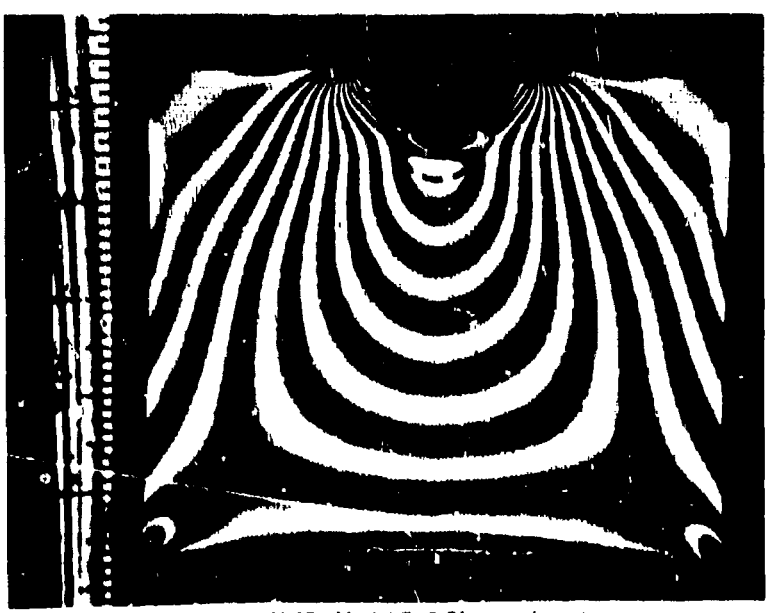

Figure H-17. Model F, 8.00-pound tension.

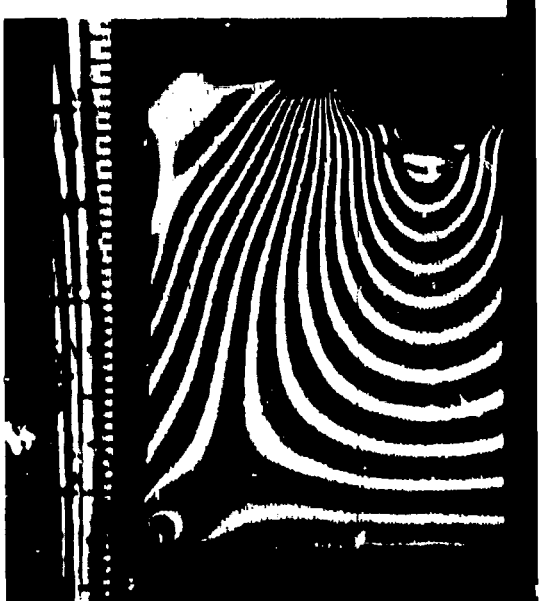

Figure H-18. Model F, 14.60-pou

A

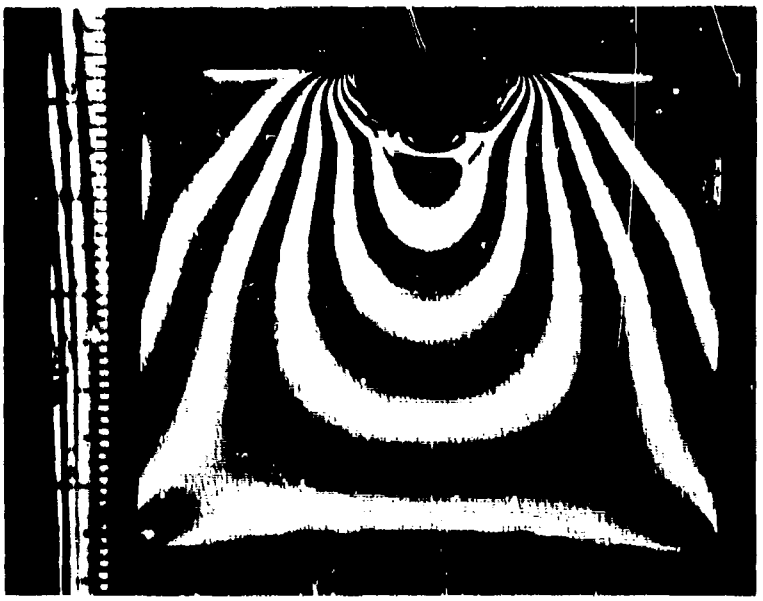

Figure H-16. Model F, 5 26-pound tension.

REFERENCES

Anonymous. "The impossible has been done before. Will it be done now?" Marine Engineering/Log, vol. 61, no. 13, Dec. 1956, pp. 85, 147.

Bowman, G. The man who bought a navy. London, G. Harrap, 1964.

Christian, J. T. Two-dimensional analysis of stress and strain in soils, Report 1. Iteration procedure for saturated elastic porous material. U. S. Army Engineer Waterways Experiment Station, Contract Report no. 3-129. Vicksburg, Miss., June 1965. (Contract DA-22-079-eng-427) (AD 632354) (Massachusetts Institute of Technology, Department of Civil Engineering, Research Report no. R65-64; Soils Publication no. 184)

Crapaud, J. "Compressed air aids in refloating Liberté," Compressed Air Magazine, Sept. 1925, p. 1373.

Ellsberg, E. The far shore. New York, Dodd, Mead, 1960.

Harper, G. N. and Ang, A. A numerical procedure for the analysis of contained plastic flow problems. University of Illinois, Department of Civil Engineering, Civil Engineering Studies, Structural Research Series no. 266. Urbana, Ill., June 1963. (Contract DA-49-146-XZ-104)

Letter of 23 September 1949, with enclosures, from Commander Task unit 49.4.3 to Chief of Naval Operations.

Masters, D. Epics of salvage. Boston, Little, Brown, 1954, pp. 12, 16, and 19.

Momsen, C. E. "Rescue and salvage of U.S.S. Squalus," in U. S. Navy. Bureau of Ships, NAVSHIPS 250-631-2: Submarine salvage; pontoons and related equipment, by B. C. Webb. Boston Naval Shipyard, Mass., Nov. 1964, Appendix, pp. 1-11.

Prager, W. and Hodge, P. G. Theory of perfectly plastic solids. New York, Wiley, 1951.

Schmid, W. E., and Kitago, S. "Shear strength of clays and safety factors as a function of time," in Proceedings of the Sixth International Conference on Soil Mechanics and Foundation Engineering, vol. 1. Toronto, Canada, University of Toronto Press, 1965, pp. 345-349.

Tusler, F. A. "The salvage of the U.S.S. Squalus," American Society of Naval Engineers, Journal, vol. 52, no. 2, May 1940, pp. 157-187.

U. S. Navy. Bureau of Construction and Repair. Technical Bulletin no. 2-27: Report on salvage operations, submarine S-51, by E. Ellsberg. Washington, D. C., 1927.

U. S. Navy. Bureau of Construction and Repair. Technical Bulletin, 1928: Salvage report of the U.S.S. S-1, by H. E. Saunders. Washington, D. C., 1929.

U. S. Navy. Bureau of Ships. NAVSHIPS 250-880-21: Report of the salvage of the U.S.S. Lafayette. Washington, D. C., 1946.

Whitman, R. V. Multidimensional analysis of stress and strain in soils. Stanford Research Institute, Final Report on Contract DA-49-146-XZ-219. Menlo Park, Calif., June 1964. (DASA 1558) (AD 608874)

Whitman, R. V., and Hoeg, K. Two-dimensional analysis of stress and strain in soils, Report 2. Development of plastic zone beneath a footing. U. S. Army Engineer Waterways Experiment Station, Contract Report no. 3-129. Vicksburg, Miss., Dec. 1965. (Contract DA-22-079-eng-427) (AD 633740) (Massachusetts Institute of Technology, Department of Civil Engineering, Research Report no. R65-61; Soils Publication no. 187)

Unclassified
Security Classification

DOCUMENT CONTROL DATA - R & D

(Security classification of title, body of abstract and indexing annotation must be entered when the overall report is classified)

1. ORIGINATING ACTIVITY (Corporate author)
Naval Civil Engineering Laboratory
Port Hueneme, Calif. 93041

2a. REPORT SECURITY CLASSIFICATION
Unclassified

2b. GROUP

3. REPORT TITLE
OCEAN BOTTOM BREAKOUT FORCES
Including Field Test Data and the Development of an Analytical Method

4. DESCRIPTIVE NOTES (Type of report and inclusive dates)
Not final; July 1965—June 1967

5. AUTHOR(S) (First name, middle initial, last name)
Bruce J. Muga

6. REPORT DATE	7a. TOTAL NO. OF PAGES	7b. NO. OF REFS
June 1968	140	17

8a. CONTRACT OR GRANT NO.	9a. ORIGINATOR'S REPORT NUMBER(S)
b. PROJECT NO.	TR-591
c.	9b. OTHER REPORT NO(S) (Any other numbers that may be assigned this report)
d.	

10. DISTRIBUTION STATEMENT
Each transmittal of this document outside the agencies of the U. S. Government must have prior approval of the Naval Civil Engineering Laboratory.

11. SUPPLEMENTARY NOTES	12. SPONSORING MILITARY ACTIVITY
	Naval Facilities Engineering Command Washington, D. C.

13. ABSTRACT

Theoretical and experimental studies were conducted in order to arrive at some appropriate engineering estimates of the force required to extract bodies of various sizes and shapes from the ocean bottom sediments. A review of the literature concerned with breakout forces is presented.

From tests conducted in San Francisco Bay on variously shaped objects having submerged weights of up to 22,200 pounds, it was found that the following empirical formula described well the breakout force requirement:

$$F = 0.20\, A_{max}\, q_d\, e^{-0.00540\,(t\,-\,260)}$$

where F = breakout force, lb

A_{max} = horizontal projection of the maximum contact area, $in.^2$

q_d = average supporting pressure provided by the soil to maintain the embedded object in static equilibrium, $lb/in.^2$

t = time allowed for breakout, min

Results yielded by the empirical formula agreed very well with a complicated theoretical procedure based on an iterative solution of a lumped parameter model of the ocean bottom. Solutions were obtained for various load conditions and bottom (object) geometries.

DD FORM 1 NOV 65 1473 (PAGE 1)
S/N 0101-807-6801

Unclassified
Security Classification

14 KEY WORDS	LINK A		LINK B		LINK C	
	ROLE	WT	ROLE	WT	ROLE	WT
Breakout forces						
Salvage						
Ocean bottom						
Mathematical soil model						
Continuum mechanics						
Field tests						